NAGI-36

Institute for Computational and Applied Mechanics (ICAM)

RADIATIVE INTERACTIONS IN LAMINAR DUCT FLOWS

by

P. A. Trivedi and S. N. Tiwari

ICAM

ODU/ICAM Report 90-101
December 1990

Old Dominion University
Norfolk, Virginia 23529-0247

RADIATIVE INTERACTIONS IN LAMINAR DUCT FLOWS
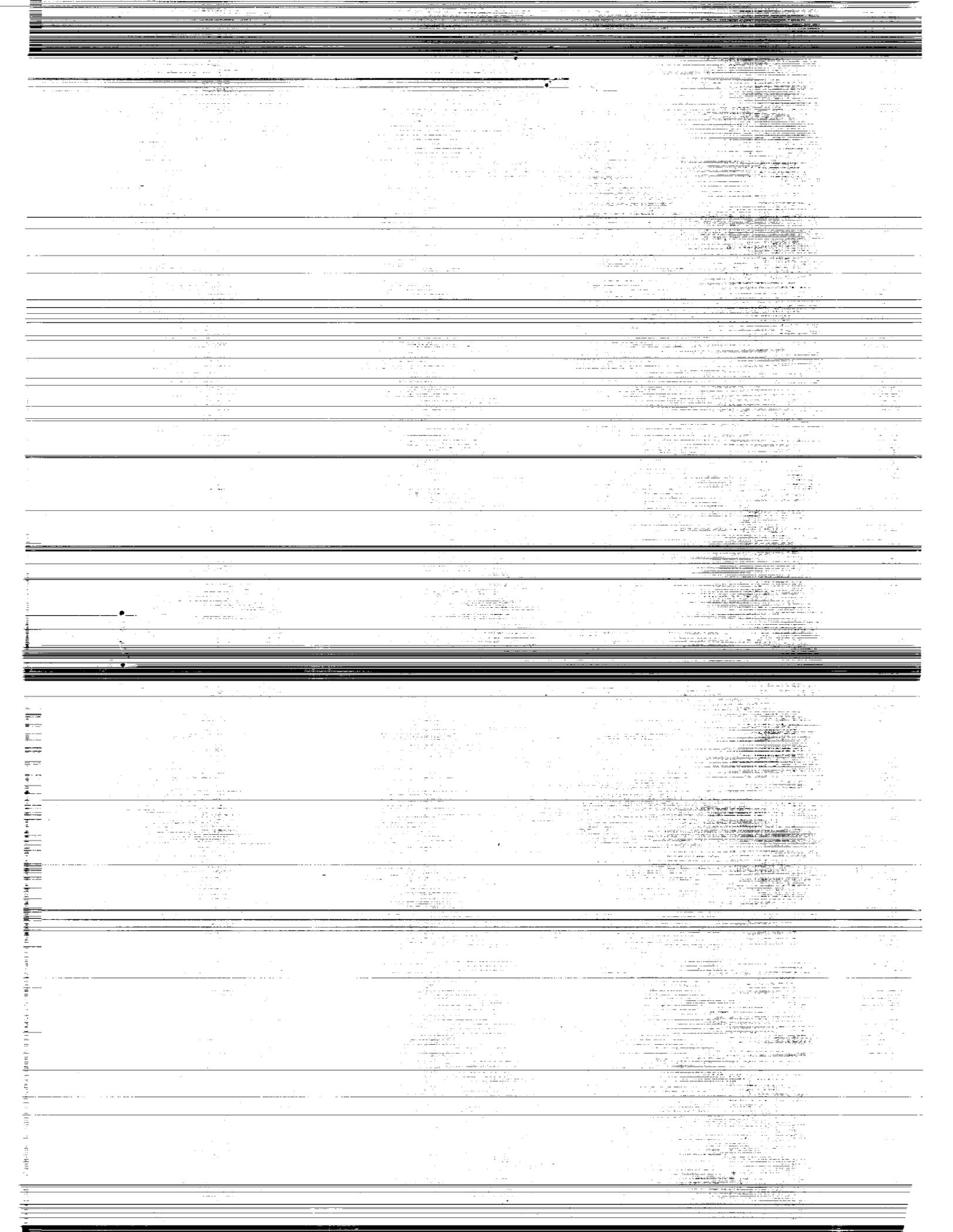
P. A. TRIVEDI* and S. N. Tiwari†
Department of Mechanical Engineering and Mechanics
Old Dominion University, Norfolk, VA 23529-0247

ABSTRACT

Analyses and numerical procedures are presented for infrared radiative energy transfer in gases when other modes of energy transfer occur simultaneously. Two types of geometries are considered, a Parallel Plate Duct and a Circular Duct. Fully developed laminar incompressible flows of absorbing-emitting species in black surfaced ducts are considered under the conditions of uniform wall heat flux. The participating species considered are OH, CO, CO_2, and H_2O. Nongray as well as gray formulations are developed for both geometries. Appropriate limiting solutions of the governing equations are obtained and conduction-radiation interaction parameters are evaluated. Tien and Lowder's wide band model correlation has been used in nongray formulation. Numerical procedures are presented to solve the integro-differential equations for both geometries. The range of physical variables considered are Temperature 300 K- 2000 K, Pressure 0.1 atm- 100.0 atm, and Spacing between Plates/Radius of the Tube 0.1 cm- 100 cm. An extensive parametric study based on nongray formulation is presented. Results obtained for different flow conditions indicate that the radiative interactions can be quite significant in fully developed incompressible flows.

---

*Graduate Research Assistant, ICAM Fellow
†Eminent Professor, ICAM Director

FOREWORD

TABLE OF CONTENTS

iv

NOMENCLATURE

A	band absorptance = $A(u,\beta)$, cm^{-1}
A_o	band width parameter, cm^{-1}
C_o	correlation parameter, atm^{-1} - cm^{-1}
C_p	specific heat at constant pressure kJ/Kg-K = erg/gm-K
e_ω	Planck's function, (W-cm^2)/cm^{-1}
$e_{\omega o}$	Planck's function evaluated at wave number ω_o
e_1, e_2	emissive power of surfaces with temperature T_1 and T_2, W-cm^{-2}
k	thermal conductivity, erg/cm-sec-K
L	distance between the plates, cm.
P	pressure, atm
P_i	partial pressure
q_R	total radiative heat flux, J/m^2-s
$q_{R\omega}$	spectral radiative heat flux, (W-cm^{-2})/cm^{-1}
r	physical coordinate for circular duct
r_o	radius of circular duct, cm
S	integrated intensity of a wide band, atm^{-1}-cm^{-2}
T	temperature, K
T_1, T_2	wall temperature K; $T_1 = T_w$
T_b	bulk temperature, K
u	nondimensional coordinate = SPy/A_o
u_o	nondimensional path length = SPL/A_o
x,y	physical coordinates
θ	nondimensional temperature
θ_b	nondimensional bulk temperature
κ_ω	spectral absorption coefficient, cm^{-1}
κ_p	Planck mean absorption coefficient, cm^{-1}
ξ, η	computational coordinates

ρ	density, kg/m^3
σ	Stefan-Boltzman constant, erg/(sec-cm-K^4)
τ	optical coordinate
τ_o	optical path length
ω	wave number, cm^{-1}
ω_o, ω_i	wave number at the band center, cm^{-1}

LIST OF FIGURES

Chapter 1

INTRODUCTION

There is renewed interest in investigating various aspects of radiative energy transfer in participating mediums. Radiative interactions become important in many engineering problems involving high temperature gases. Recent interest lies in the areas of design of high pressure combustion chambers and high enthalpy nozzles, entry and reentry phenomena, hypersonic propulsion, and defence oriented research.

Basic formulations on radiative energy transfer in participating mediums are available in standard references [1–8]. The review articles presented in [9–24] are useful in understanding the radiative properties of participating species and the nature of nongray radiation. The validity of radiative transfer analyses depends upon the accuracy with which absorption-emission and scattering characteristics of molecular species are modeled and these are reviewed in [12,13].

For gray participating mediums between parallel plates and in a cylinder, the exact formulations are available in the literature for different physical conditions. Ussikin and sparrow [25] studied thermal radiation between parallel plates separated by an absorbing-emitting, nonisothermal gray gas. Sparrow, Ussikin, and Hubbard [26] investigated radiative transfer in a nonisothermal gray spherical medium. Viskanta [27] studied the interaction of conduction, laminar convection, and radiation in a plane layer of a radiating fluid. Cess and Tiwari [28] investigated heat transfer to laminar flow of an absorbing-emitting gas between parallel plates. Tiwari [29] studied radiative interaction in transient energy transfer in gaseous systems. Tiwari and Singh [30] extended Tiwari's work [29] for fully developed laminar flows. The studies presented in [27–29] have

reviewed other available literature on gray as well as nongray radiative transfer between planar geometries.

Einstein [31] considered radiant energy transfer in an absorbing-emitting gray gas flowing within a black walled cylindrical pipe. Nichols [32] studied the influence of the absorption of radiation on the temperature profile and heat transfer to an absorbing medium flowing turbulently in an annulus. deSoto and Edwards [33] predicted the radiative interchange between a black tube and a nonisothermal nongray gas within the tube. deSoto [34] investigated the coupling of radiation with convection and conduction in a nonisothermal nongray gas flowing in the entrance region of a black walled tube. Pearce and Emery [35] treated the thermal entry region for laminar flow of a gray gas or a gas with gray bands. Kesten [36] presented the equation for the spectral radiant heat flux distribution in an absorbing-emitting gas contained in a long cylinder. Landram, Greif, and Habib [37] studied heat transfer in turbulent pipe flows with optically thin radiation. Habib and Greif [38] investigated nongray radiative transport in a cylindrical medium. Tiwari and Cess [39] studied heat transfer to laminar flow of nongray gases through a circular tube. Wassel and Edwards [40] investigated molecular gas band radiation in cylinders for the axial band absorptance, mean beam length, absorptivity and emissivity for a nongray gas.

As mentioned earlier, in case of combustion chambers and industrial furnaces, heat transfer takes place by simultaneous convection and radiation. Also, in some postulated nuclear reactor loss-of-coolant accident scenarios, it is important to predict heat transfer from heated walls to flowing water vapor, which is capable of absorbing and emitting thermal radiation. The main emphasis of this study is to present basic formulations and solution procedure, to calculate the radiative interaction in an absorbing-emitting medium in a laminar flow through parallel plates and a circular duct while other modes of heat transfer occur simultaneously. To accomplish this it is essential to review different band absorption models available in the literature and incorporate the most suitable model

in the governing equations. For certain applications, it is desirable to provide limiting forms of the basic governing equations and, if possible, obtain closed form solutions. These solutions are very useful in estimating the extent of radiative interaction for a given physical problem.

A review of different absorption models is presented in Chap. 2. The general problem of radiative interaction is formulated for flow between black parallel plates in Chap. 3 for both gray and nongray mediums. A similar formulation is presented for the flow through a black circular duct in Chap. 4. The numerical procedure for both cases is presented in Chap. 5. Typical results for both geometries are presented and discussed in Chap. 6. Finally, the results and conclusions reached from this study are summarized in Chap. 7.

Chapter 2

BAND ABSORPTION AND CORRELATIONS

The study of radiative transmission in nonhomogeneous gaseous systems requires a detailed knowledge of the absorption, emission, and scattering characteristics of the specific species under investigation. In absorbing and emitting mediums, an accurate model for the spectral absorption coefficient is of vital importance in the correct formulation of the radiative flux equations. A systematic representation of the absorption by a gas, in the infrared part of spectrum, requires the identification of the major infrared bands and the evaluation of the line parameters (line intensity, line half-width, and spacing between the lines) of these bands. The line parameters depend upon the temperature, pressure and concentration of the absorbing molecules and, in general, these quantities vary continuously along a nonhomogeneous path in the medium. In recent years, considerable efforts have been expended in obtaining the line parameters and absorption coefficients of important atomic and molecular species.

For an accurate evaluation of the transmittance (or absorptance) of a molecular band, a convenient line model is used to represent the variation of the spectral absorption coefficient. The line models usually employed are Lorentz, Doppler, and Voight line profiles. A complete formulation (and comparison) of the transmittance and absorption by these line profiles is given in [9–13]. In a particular band consisting of many lines, the absorption coefficient varies very rapidly with frequency. Thus, it becomes very difficult and time-consuming task to evaluate the total band absorption over the actual band contour by employing an appropriate line profile model. Consequently, several approximate band models (narrow as well as wide) have been proposed which represent absorption from an actual band with reasonable accuracy [6–13] and [14–24]. Several

4

continuous correlations for the total band absorption are available in literature [9–13] and [19–23]. These have been employed in many nongray radiative transfer analyses with varying degree of success [9–13] and [14–23]. A brief discussion is presented here on the total band absorption, band models, and band absorptance correlations.

The absorption within a narrow spectral interval of a vibration rotation band can quite accurately be represented by the so-called "narrow band models." For a homogeneous path, the total absorptance of a narrow band is given by

$$A_N = \int\limits_{\Delta\omega} [1 - \exp(-k_\omega X)]\, d\omega \tag{2.1}$$

where k_ω is the volumetric absorption coefficient, ω is the wave number, and $X = py$ is the pressure path length. The limits of integration in Eq.(2.1.1) are over the narrow band pass considered. The total band absorption of the so-called "wide band models" is given by

$$A = \int\limits_{-\infty}^{\infty} [1 - \exp(-k_\omega X)]\, d(\omega - \omega_o) \tag{2.2}$$

where the limits of integration are over the entire band pass and ω_o is the wave number at the center of the wide band. In actual radiative transfer analyses, the quantity of frequent interest is the derivative of Eqs.(2.1.1) and (2.1.2).

Four commonly used narrow band models are Elsasser, Statistical, Random Elsasser, and Quasi-Random. The application of a model to a particular case depends upon the nature of absorbing-emitting molecule. Complete discussions on narrow band models, and expressions for transmittance and integrated absorptance are available in the literature [9–13] and [14–16]. Detailed discussions on the wide band models are given in [9–13] and [17–23]. The relations for total absorptance of a wide band are obtained from the absorptance formulations of narrow band models by employing the relations for the variation of line intensity as [9–13] and [20–23]

$$\frac{S_j}{d} = \left(\frac{S}{A_o}\right) \exp\left\{ -\frac{b_o\, |\omega - \omega_o|}{A_o} \right\} \tag{2.3}$$

where S_j is the intensity of the jth spectral line, d is the line spacing, S is the integrated intensity of a wide band, A_o is the band width parameter, and $b_o = 2$ for a symmetrical band and $b_o = 1$ for bands with upper and lower wave number heads at ω_o. The total absorptance of an exponential wide band, in turn, may be expressed by

$$\bar{A}(u,\beta) \equiv \frac{A(u,\beta)}{A_o} = \frac{1}{A_o} \int\limits_{wide\,band} [\bar{A}_N(u,\beta)]\, d(\omega - \omega_o) \qquad (2.4)$$

where $u = \frac{SX}{A_o}$ is the nondimensional path length, $\beta = \frac{2\pi\gamma_L}{d}$ is the line structure parameter, γ_L is the Lorentz line half-width, and $\bar{A}_N(u,\beta)$ represents the mean absorptance of a narrow band.

By employing the Elsasser narrow band absorptance relation and Eq.(2.1.3) the expression for the exponential wide band absorptance is obtained as [12]

$$\bar{A}(u,\beta) = \gamma + \left(\frac{1}{\pi}\right) \int\limits_{0}^{\pi} [\ln\psi + E_1(\psi)]\, dz \qquad (2.5)$$

where $\psi = \frac{u\sinh\beta}{(\cosh\beta - \cos z)}$, $\gamma = 0.5772156$ is the Euler's constant, and $E_1(\psi)$ is the exponential integral of the first order. Analytic solution of Eq.(2.1.5) can be obtained in a series form as [12,13]

$$\bar{A}(u,\beta) = \sum_{n=1}^{\infty} -\frac{A^n SUM(mn)}{n(B+1)^n n!(n-1)!} \qquad (2.6)$$

where

$$SUM(mn) = \sum_{m=0}^{\infty} \frac{(n+m-1)!(2m-1)!C^m}{2^m(m!)^2}$$

$$A = -u\tanh\beta, \; B = \frac{1}{\cosh\beta}$$

$$C = \frac{2}{(1+\cosh\beta)} = \frac{2B}{(B+1)} \qquad (2.7)$$

The series in Eq.(2.1.6) converges rapidly. When the weak line approximation for the Elsasser model is valid (i.e. β is large), then Eq.(2.1.5) reduces to

$$\bar{A}(u) = \gamma + \ln(u) + E_1(u) \qquad (2.8)$$

In the linear limit, Eqs.(2.1.5) and (2.1.6) reduce to $\bar{A} = u$, and in the logarithmic limit they reduce to $\bar{A} = \gamma + \ln(u)$. It can be shown that Eq.(2.1.5) reduces to the correct limiting form in square-root limit. Results of Eqs.(2.1.5) and (2.1.6) are found to be identical for all pressures and pathlengths. For p > 1 atm., results of Eqs.(2.1.5)-(2.1.7) are in good agreement for all pathlengths.

By employing the uniform statistical, general statistical, and random Elsasser narrow band models absorptance relations and Eq.(2.1.3), three additional expressions for the exponential wide band absorptance were obtained in [12,13]. The absorptance results of the four wide band models are discussed in detail in [13]. The expression obtained by employing the uniform statistical model also reduces to the relation given by Eq.(2.1.7) for large β.

Several continuous correlations for the total absorptance of a wide band, which are valid over different values of path length and line structure parameter, are available in literature. These are discussed, in detail, in [9–13] and [20–23] and are presented here in the sequence that they became available in the literature. Most of these correlations are developed to satisfy at least some of the limiting conditions (nonoverlapping line, linear, weak line, and strong line approximations and square-root, large pressure, and large path length limits) for the total band absorptance [10–13]. Some of the correlations even have experimental justification [9–18].

The first correlation for the exponential wide band absorptance (a three piece correlation) was proposed by Edwards et al. [17,18]. The first continuous correlation was proposed by Tien and Lowder [9], and this is of the form

$$\bar{A}(u, \beta) = \ln\left[u f(t) \frac{(u+2)}{(u+2f(t))} + 1\right] \tag{2.9}$$

where

$$f(t) = 2.94\left[1 - \exp(-2.60t)\right] \ , \ t = \frac{\beta}{2}$$

This correlation does not reduce to the correct limiting form in the square-root limit [10,13], and its use should be made for $\beta \geq 0.1$. Another continuous correlation was proposed by Goody and Belton [22], and in terms of the present nomenclature, this is given by

$$\bar{A}(u,\beta) = 2\ln\left[1 + \frac{u}{\sqrt{4 + \left(\frac{\pi u}{4t}\right)}}\right] \ , \ \beta = 2t \tag{2.11}$$

Use of this correlation is restricted to relatively small β values [10–13]. Tien and Ling [23] have proposed a simple two parameter correlation for $\bar{A}(u,\beta)$ as

$$\bar{A}(u) = \sinh^{-1}(u) \tag{2.12}$$

which is valid only for the limit of large β. A relatively simple continuous correlation was introduced by Cess and Tiwari [12,13], and this is of the form

$$\bar{A}(u,\beta) = 2\ln\left[1 + \frac{u}{2 + \sqrt{u\left(1 + \frac{1}{\bar{\beta}}\right)}}\right] \tag{2.13}$$

where $\bar{\beta} = \frac{4t}{\pi} = \frac{2\beta}{\pi}$. By slightly modifying Eq.(2.1.13), another form of the wide band absorptance is obtained as [29]

$$\bar{A}(u,\beta) = 2\ln\left[1 + \frac{u}{2 + \sqrt{u\left(c + \frac{\pi}{2\beta}\right)}}\right] \tag{2.14}$$

where
$$0.1, \quad \beta \leq 1 \, and \, all \, u \, values$$
$$c = 0.1, \quad \beta > 1 \, and \, u \leq 1$$
$$0.25, \beta > 1 \, and \, u > 1.$$

Equations.(2.1.11) and (2.1.14) reduce to all the limiting forms [10]. Based on the formulations of slab band absorptance, Edwards and Balakrishnan [20] have proposed the correlation

$$\bar{A}(u) = \ln(u) + E_1(u) + \gamma + \frac{1}{2} - E_3(u) \tag{2.16}$$

which is valid for large β. For present application, this correlation should be modified by using the technique discussed in [12,13]. Based upon the formulation of the total band absorptance from the general statistical model, Felske and Tien [21] have proposed a continuous correlation for $\bar{A}(u,\beta)$ as

$$\bar{A}(u,\beta) = 2E_1(t\rho_u) + E_1\left(\frac{\rho_u}{2}\right) - E_1\left[\left(\frac{\rho_u}{2}\right)(1+2t)\right]$$
$$+ \ln\left[\frac{(t\rho_u)^2}{(1+2t)}\right] + 2\gamma \tag{2.17}$$

where

$$\rho_u = \sqrt{\left(\frac{t}{u}\right)\left[1+\left(\frac{t}{u}\right)\right]} \tag{2.18}$$

The absorptance relation given by Eq.(2.1.17) is another simple correlation which is valid for all path lengths and for $t = (\beta/2) \geq 1$. The relation of Eq.(2.1.16) can be treated as another correlation applicable to gases whose spectral behavior can be described by the Elsasser model. In ref. 13, Tiwari has shown that Elsasser as well as random model formulations for the total band absorptance reduce to Eq.(2.1.17) for $t \geq 1$.

Band absorptance results of various correlations are compared and discussed in some detail in [12,13] and [24]. It was found that results of these correlations could be in error by as much as 40 % when compared with the exact solutions based on different models. Felske and Tien's correlation was found to give the least error when compared with the exact solution based on Elsasser model. The results of Cess and Tiwari's correlations followed the trend of general statistical model. Tiwari and Batki's correlation [Eq.(21.16) or (2.1.17)] was found to provide a uniformly better approximation for the total band absorptance at relatively high pressures. The sole motivation in presenting the various correlations here is to see if their use in actual radiative processes made any significant difference in the final results.

In Ref. 24, use of several continuous correlations for total band absorptance was made to two problems to investigate their influence on the final results of actual radiative processes. For the case of radiative transfer in a gas with internal heat source, it

was found that actual center-line temperature results obtained by using the different correlations follow the same general trend as the results of total band absorptance by these correlations. From these results, it may be concluded that use of the Tien and Lowder's correlation should be avoided at lower pressures, but its use is justified (at moderate and high pressures) to gases whose spectral behavior can be described by the regular Elsasser band model. For all pressures and path length conditions, use of the Cess and Tiwari's correlations could be made to gases with bands of highly overlapping lines. In a more realistic problem involving flow of absorbing emitting gas, results of different correlations (except the Tien and Lowder's correlation) differ from each other by less than 6% for all pressures and path lengths. Use of Tien and Lowder's correlations is justified for gases like CO at moderate and high pressures. For gases like CO_2, use of any other correlation is recommended. While Felske and Tien's correlation is useful for all pressures and path lengths to gases having random band structure, Tiwari and Batki's simple correlation could be employed to gases with regular or random band structure but for $p \geq 1.0$ atm.

Chapter 3

LAMINAR FLOW BETWEEN PARALLEL PLATES

This chapter covers the development of different types of formulation for steady laminar flow of absorbing-emitting, constant property, incompressible gas through two parallel black plates. Basic formulation for such a flow is given in Sec. 3.1. Gray gas formulation is developed with limiting cases in Sec. 3.2 and Nongray formulation is given in Sec. 3.3.

3.1 Basic Formulation

The physical model for the parallel plate geometry is shown in (Fig. 3.1.1). For radiation participating medium, the equations expressing conservation of mass and momentum remain unaltered, while the conservation of energy for such a flow is given as[1]

$$\rho C_p \frac{DT}{Dt} = div\,(k\nabla T) + \beta T \frac{DP}{Dt} + \mu \Phi - div\, q_R \qquad (3.1)$$

where μ is the dynamic viscosity, β is the coefficient of thermal expansion of the fluid and Φ is the Rayleigh dissipation function.

The Condition of uniform surface heat flux for each plate is assumed such that the temperature of the plates varies in the axial direction. Fully developed heat transfer is considered and axial conduction and radiation is assumed to be negligible as compared with the normal components. In other words, this represents physical conditions of a large value of Peclet number[1]. Consequently Eq.(3.1.1) can be expressed as

$$\rho C_p \left[u \frac{\partial T}{\partial x} + v \frac{\partial T}{\partial y} \right] = k \frac{\partial^2 T}{\partial y^2} + \beta T u \frac{dp}{dx} + \mu \left[\frac{\partial u}{\partial y} \right]^2 - div\, q_R \qquad (3.2)$$

11

If in addition, it is assumed that the Eckert number of the flow is small, then Eq.(3.1.2) simplifies to

$$u\frac{\partial T}{\partial x} + v\frac{\partial T}{\partial y} = \alpha\frac{\partial^2 T}{\partial y^2} - \frac{1}{\rho C_p}\frac{\partial q_R}{\partial y} \qquad (3.3)$$

where $\alpha = (k / \rho C_p)$ represents the thermal diffusivity of the fluid.

For a steady fully developed flow, $v = 0$ and u is given by the parabolic velocity profile as

$$u = 6u_m\left(\xi - \xi^2\right) \quad ; \quad \xi = \frac{y}{l} \qquad (3.4)$$

where u_m represents the mean velocity. Also for the flow of a perfect gas with uniform wall heat flux, $\frac{\partial T}{\partial x}$ is constant and is given by

$$\frac{\partial T}{\partial x} = \frac{2\alpha q_w}{u_m L/k} \qquad (3.5)$$

Now, by combining Eqs.(3.1.3–3.1.5), the energy equation is expressed as

$$\frac{\partial^2 T}{\partial y^2} - \frac{12q_w}{L/k}\left(\xi - \xi^2\right) = \frac{1}{k}\frac{\partial q_R}{\partial y} \qquad (3.6)$$

Upon defining nondimensional temperature as

$$\theta = \frac{(T - T_1)}{(q_w L/k)} \qquad (3.7)$$

the energy equation, Eq.(3.1.6), is expressed as

$$\frac{\partial^2 \theta}{\partial \xi^2} - 12\left(\xi - \xi^2\right) = \frac{1}{q_w}\frac{\partial q_R}{\partial \xi} \qquad (3.8)$$

The boundary conditions for this problem can be expressed as

$$At\ the\ surface\ ;\ \theta\left(0\right) = \theta\left(1\right) = 0 \qquad (3.9a)$$

$$At\ \xi = \frac{1}{2} \quad ; \quad \frac{d\theta}{d\xi} = \theta_\xi = 0\ and\ q_R = 0 \qquad (3.9b)$$

$$\left(\frac{d\theta}{d\xi}\right)_{\xi=0} = -\left(\frac{d\theta}{d\xi}\right)_{\xi=1} \qquad (3.9c)$$

It should be noted that all the boundary conditions given in Eqs. (3.1.9) are not independent and any two conditions can be used to obtain solutions.

Equation. (3.1.8) can be integrated once and using the boundary condition, one can obtain another form of the energy equation as

$$\theta_\xi - 2\left(3\xi^2 - 2\xi^3\right) + 1 = \frac{q_R\left(\xi\right)}{q_w} \qquad (3.10)$$

For flow problems, the quantity of primary interest is the bulk temperature of the gas, which may be expressed as [11]

$$\theta_b = \frac{\left(T_b - T_1\right)}{q_w L/k} = 6\int_0^1 \theta\left(\xi\right)\left(\xi - \xi^2\right) d\xi \qquad (3.11)$$

The heat transfer q_w is given by the expression, $q_w = h_c\left(T_1 - T_b\right)$, where h_c is the effective heat transfer coefficient (W/cm^2—K). In general, the heat transfer results are expressed in terms of the Nusselt number, $Nu = h_c D_h/k$. Here, D_h represents the hydraulic diameter, and for the parallel plate geometry it equals twice the plate separation, i.e., $D_h = 2L$. Upon eliminating the heat transfer coefficient h_c from expression for q_w and Nu, a relation between the Nusselt number and the bulk temperature is obtained as

$$Nu = \frac{2L q_w}{k\left(T_1 - T_b\right)} = -\frac{2}{\theta_b} \qquad (3.12)$$

The heat transfer results, therefore, can be expressed either in terms of Nu or θ_b. In order to accomplish this, a proper formulation for the radiative flux appearing in Eqs. (3.1.8) and (3.1.10) must be provided.

As discussed in Chap. 2, the expression for the radiative flux is formulated in terms of the absorption coefficient, which in turn is a strong function of frequency. Probably the greatest simplification in formulating the radiative flux model is the gray medium approximation. This is discussed in the following section. The gray medium approximation also serves as an initial step toward nongray analyses.

3.2 Gray Gas Formulation

In gray gas formulation (gray-medium approximation), the absorption and the scattering coefficients are assumed to be independent of the wavelength. For a gray non-scattering medium with black bounding surfaces the equation for radiation flux can be given as [1]

$$q_R = 2\sigma T_1^4 E_3(\tau) - 2\sigma T_2^4 E_3(t - \tau)$$
$$+ 2\sigma \int_0^\tau T^4(t) E_2(\tau - t)\, dt - 2\sigma \int_\tau^{\tau_o} T^4(t) E_2(t - \tau)\, dt \qquad (3.13)$$

where

$$\tau = \int_0^y \kappa(y)\, dy \ , \quad \tau_o = \int_0^L \kappa(y)\, dy \ , \quad E_n(t) = \int_0^1 \mu^{n-2} e^{-\frac{t}{\mu}}\, d\mu$$

In the preceding equations, $E_n(t)$ are the exponential integral functions, and τ and τ_o represent the optical coordinate and optical path, respectively. For exponential kernal approximation,

$$E_2(t) \simeq \frac{3}{4} e^{-\frac{3}{2}t} \ ; \quad E_3(t) \simeq \frac{1}{2} e^{-\frac{3}{2}t} \qquad (3.14)$$

Consequently, Eq. (3.2.13) is written as

$$q_R = \sigma T_1^4 e^{-\frac{3}{2}\tau} - \sigma T_2^4 e^{-\frac{3}{2}(\tau_o - \tau)}$$
$$+ \frac{3}{2}\sigma e^{-\frac{3}{2}\tau} \int_0^\tau T^4(t) e^{\frac{3}{2}t} dt - \frac{3}{2}\sigma e^{\frac{3}{2}\tau} \int_\tau^{\tau_o} T^4(t) e^{-\frac{3}{2}t} dt \qquad (3.15)$$

Upon differentiating Eq. (3.15) twice, the integrals can be eliminated and the following expression is obtained

$$\frac{d^2 q_R}{d\tau^2} - \frac{9}{4} q_R = 3\sigma \frac{dT^4}{d\tau} \qquad (3.16)$$

For linerized radiation Eq.(3.16) becomes

$$\frac{d^2 q_R}{d\tau^2} - \frac{9}{4} q_R = 12\sigma T_w^3 \frac{dT}{d\tau} \qquad (3.17)$$

By defining dimensionless quantities

$$\theta = \frac{T - T_w}{q_w L / k} \quad ; \quad \tau_o = \kappa_p L$$

$$\xi = \frac{y}{L} = \frac{\tau}{\tau_o} \tag{3.18}$$

where κ_p is the Planck mean absorption coefficient, Eq. (3.17) can now be written as

$$\frac{d^2 q_R}{d\xi^2} - \frac{9}{4} \tau_o^2 q_R = \left[\frac{12\sigma T_w^3 \tau_o^2}{k \kappa_p} \right] q \frac{d\theta}{d\xi} \tag{3.19}$$

In obtaining Eq.(3.19), it has been assumed that the absorption coefficient (not the Planck mean absorption coefficient) is not a function of temperature. This is consistent with the assumption of constant fluid properties in the medium. The boundary conditions for Eq.(3.19) are found to be

$$q_R \left(\frac{1}{2} \right) = 0$$

$$\frac{3}{2} q_R (0) = \frac{1}{\tau_o} \left(\frac{dq_R}{d\xi} \right)_{\xi=0} \tag{3.20}$$

Using the dimensionless quantities defined by Eq. (3.18) the energy equation given by Eq. (3.8) is expressed as

$$12 \left(\xi - \xi^2 \right) = \frac{d^2 \theta}{d\xi^2} - \frac{1}{q} \frac{dq_R}{d\xi} \tag{3.21}$$

For this case, the boundary conditions become

$$\theta (0) = 0 \quad ; \quad \frac{d\theta}{d\xi} \left(\frac{1}{2} \right) = 0 \tag{3.22}$$

Equations (3.19) and (3.21) can now be solved simultaneously and the following result is obtained for the bulk temperature

$$\theta_b = C_1 \left[24 - 12M_1 + M_1^3 + \left(M_1^3 - 12M_1 - 24 \right) e^{-M_1} \right] \tag{3.23}$$

$$- \frac{12\gamma_1}{5M_1^4} + \frac{17\gamma_1}{70M_1^2} - \frac{17}{70}$$

where

$$M_1^2 = \frac{9}{4}\tau_o^2 + \gamma_1$$

$$\gamma_1 = \frac{12\sigma T_w^3 \tau_o^2}{k\kappa_p}$$

$$C_1 = \frac{\gamma_1}{M_1^8} \left[\frac{48 - 3\tau_o M_1^2 + 36\tau_o}{3\tau_o(1 - e^{-M_1}) + 2M_1(1 + e^{-M_1})} \right] \qquad (3.24)$$

The bulk temperature can be easily calculated from Eq.(3.23) for any gas once the Planck's mean absorption coefficient κ_p is known.

Two limiting solutions can also be found for large and small optical thicknesses. These are called optically thin limit and optically thick limit solutions.

3.2.1 Optically Thin Limit

The solution in the optically thin limit is obtained by making use of the parameter M_1 defined in Eq. (3.24) as

$$M_1^2 = \frac{9}{4}\tau_o^2 + \gamma_1 \qquad (3.25)$$

In the optically thin limit $\tau_o \longrightarrow 0$ and, therefore,

$$\lim_{\tau_o \to 0} (M_1^2) -> \gamma_1 \quad , \quad \lim_{\tau_o \to 0} (M_1) = \sqrt{\gamma_1} \qquad (3.26)$$

Consequently,

$$\lim_{\tau_o \to 0} (C_1) = \frac{24}{\gamma_1^{\frac{7}{2}} \left(1 + e^{-\sqrt{\gamma_1}}\right)} \qquad (3.27)$$

The expression for the bulk temperature in thin limit, therefore, is obtained as,

$$(\theta_b)_{thin} = \frac{24}{\gamma_1^{\frac{7}{2}} \left(1 + e^{-\sqrt{\gamma_1}}\right)} \left[24 - 12\sqrt{\gamma_1} + \left(\gamma_1^{\frac{3}{2}} - 12\sqrt{\gamma_1} - 24\right) e^{-\sqrt{\gamma_1}}\right] - \frac{12}{5\gamma_1}$$

$$(\theta_b)_{thin} = \frac{1}{\gamma_1^3} \left\{ \frac{576}{\sqrt{\gamma_1}} \left[\frac{1 - e^{-\sqrt{\gamma_1}}}{1 + e^{-\sqrt{\gamma_1}}}\right] - 288 + 24\gamma_1 - 2.4\gamma_1^2 \right\}$$

$$(3.28)$$

3.2.2 Optically Thick Limit

In the optically thick limit $\tau_o - > \infty$. From the definitions of γ_1 and M_1 given in Eq. (3.24), it is obvious therefore $\tau_o >> 1$, $M_1 >> 1$. Equation (3.23), therefore, reduces to

$$(\theta_b)_{thick} = -\frac{17}{70} + \frac{17}{70}\left[\frac{4}{N\left(3 + \frac{4}{N}\right)}\right] \tag{3.29}$$

and rearranging the terms, a simpler form is obtained as

$$(\theta_b)_{thick} = -\frac{17}{70}\left[\frac{1}{1 + \left(\frac{4}{3N}\right)}\right] \tag{3.30}$$

where,

$$N = \frac{k\kappa_p}{4\sigma T_w^3}$$

3.3 Nongray Formulation

In this section, formulation of the problem under realistic conditions is tried. Under realistic conditions the gas is not gray, that is the band parameters are functions of wavelength. Now, for solving Eq.(3.1.10), first we need to get equation for radiative flux. The radiative transfer equations are formulated for one-dimensional planar systems. For diffuse boundaries and in the absence of scattering, the expression for the radiative flux is given as [1]

$$
\begin{aligned}
q_{R\lambda}(\tau_\lambda) =\ & 2B_{1\lambda}E_3(\tau_\lambda) - 2B_{2\lambda}E_3(\tau_{o\lambda} - \tau_\lambda) \\
& + 2\left[\int_0^{\tau_\lambda} e_{b\lambda}(t)\,E_2(\tau_\lambda - t)\,dt - \int_{\tau_\lambda}^{\tau_{o\lambda}} e_{b\lambda}(t)\,E_2(t - \tau_\lambda)\,dt\right]
\end{aligned} \tag{3.31}
$$

where

$$\tau_\lambda = \int_0^y k_\lambda dy \quad ; \quad \tau_{o\lambda} = \int_0^L k_\lambda dy \tag{3.32a}$$

$$E_n(t) = \int_0^1 \mu^{n-2} e^{-\frac{t}{\mu}} d\mu \tag{3.32b}$$

In the preceding equations, $E_n(t)$ are the exponential functions, and τ_λ and $\tau_{o\lambda}$ represent the optical coordinate and optical path, respectively. The quantities $B_{1\lambda}$ and $B_{2\lambda}$ represent the spectral surface radiosities, and for nonreflecting boundaries, Eq.(3.31) is expressed in terms of the wave number as [35]

$$q_{R\omega}\left(\tau_\omega\right) = e_{1\omega} - e_{2\omega}$$
$$+ 2\left[\int_0^{\tau_\omega} F_{1\omega}\left(t\right)E_2\left(\tau_\omega - t\right)dt - \int_{\tau_\omega}^{\tau_{o\omega}} F_{2\omega}\left(t\right)E_2\left(t - \tau_\omega\right)dt\right] \quad (3.33)$$

where

$$F_{1\omega}\left(t\right) = e_\omega\left(t\right) - e_{1\omega} \ ; \ F_{2\omega}\left(t\right) = e_\omega\left(t\right) - e_{2\omega}$$

Equation (3.33) is the general equation for one-dimensional absorbing-emitting medium with diffuse non-reflecting boundaries. For nongray analyses, it is often convenient to replace the exponential integrals by appropriate exponential functions. Upon employing the exponential kernal approximation

$$E_2\left(t\right) = \tfrac{3}{4}exp\left(-\tfrac{3}{2}t\right) \ , \ E_1\left(t\right) = \tfrac{9}{8}exp\left(-\tfrac{3}{2}t\right)$$

Equation (3.33) is expressed in physical coordinates as

$$q_{R\omega}\left(y\right) = e_{1\omega} - e_{2\omega}$$
$$+ \frac{3}{2}\int_0^y F_{1\omega}\left(z\right)k_\omega exp\left[-\frac{3}{2}k_\omega\left(y - z\right)\right]dz$$
$$- \frac{3}{2}\int_y^L F_{2\omega}\left(z\right)k_\omega exp\left[-\frac{3}{2}k_\omega\left(z - y\right)\right]dz \quad (3.34)$$

where z is a dummy variable for y. In obtaining Eq. (3.34) it has been assumed that temperature differences in the medium are small and κ_ω is independent of temperature. This is consistent with the assumption of constant properties within the medium.

As discussed in Chap. 2, the total band absorptance can be expressed as

$$A\left(y\right) = \int\limits_0^\infty \left[1 - exp\left(-k_\omega y\right)\right] d\omega \quad \sim cm^{-1} \tag{3.35}$$

where both k_ω and ω have units of cm^{-1}. Differentiation of Eq.(3.35) gives

$$A'\left(y\right) = \int\limits_0^\infty k_\omega exp\left(-k_\omega y\right) d\omega \quad \sim cm^{-2} \tag{3.36}$$

and

$$A''\left(y\right) = \int\limits_0^\infty -k_\omega^2 exp\left(-k_\omega y\right) d\omega \quad \sim cm^{-3} \tag{3.37}$$

Equations (3.35)–(3.37) are employed to express Eq.(3.34) in terms of the band absorptance.

The total radiative flux is given by

$$q_R\left(y\right) = \int\limits_0^\infty q_{R\omega}\left(y\right) d\omega \tag{3.38}$$

such that

$$\frac{dq_R\left(y\right)}{dy} = \int\limits_0^\infty \frac{dq_{R\omega}}{dy} d\omega = \frac{d}{dy} \int\limits_0^\infty q_{R\omega} d\omega \tag{3.39}$$

Upon substituting Eq.(3.34) in Eq.(3.38) there is obtained for a multiband gaseous system

$$q_R\left(y\right) = e_1 - e_2 + \frac{3}{2} \sum_{i=1}^n \int\limits_{\Delta\omega_i}$$

$$\left\{ \int\limits_0^y F_{1\omega_i}\left(z\right) k_{\omega_i} exp\left[-\frac{3}{2}k_{\omega_i}\left(y - z\right)\right] dz \right.$$

$$\left. - \int\limits_y^L F_{2\omega_i}\left(z\right) k_{\omega_i} exp\left[-\frac{3}{2}k_{\omega_i}\left(z - y\right)\right] dz \right\} d\omega_i \tag{3.40}$$

It should be noted that the following relations have been used in obtaining Eq.(3.40)

$$\int\limits_0^\infty e_{1\omega} d\omega = e_1 \; ; \; \int\limits_0^\infty e_{2\omega} d\omega = e_2$$

$$\int\limits_{0}^{\infty}\left\{\int\limits_{0}^{y} F_{1\omega}(z)\,k_{\omega}\,exp\left[-\frac{3}{2}k_{\omega}(y-z)\right]dz\right\}d\omega =$$

$$\sum_{i=1}^{n}\int\limits_{\Delta\omega_i}\left\{\int\limits_{0}^{y} F_{1\omega_i}(z)\,k_{\omega_i}\,exp\left[-\frac{3}{2}k_{\omega_i}(y-z)\,dz\right]\right\}d\omega_i$$

where n represents the number of bands in a multiband system.

By utilizing the definition of the band absorptance and its derivatives as given by Eqs.(3.35)–(3.37) and evaluating the value of the Planck function at the center of each band, Eq.(3.40) is expressed as

$$q_R(y) = e_1 - e_2 + \frac{3}{2}\sum_{i=1}^{n}\left\{\int\limits_{0}^{y} F_{1\omega_{oi}}(z)\,A_i'\left[\frac{3}{2}(y-z)\right]dz\right.$$

$$\left. - \int\limits_{y}^{L} F_{2\omega_{oi}}(z)\,A_i'\left[\frac{3}{2}(z-y)\right]dz\right\} \qquad (3.41)$$

where ω_{oi} represents the center of the ith band.

Equation (3.41) is in proper form for obtaining the nongray solutions of molecular species. However, in order to be able to use the band model correlations, this equation must be transformed in terms of the correlation quantities defined in Chap. 2. The following quantities, therefore, are needed for the transformation

$$u = \left(\frac{S}{A_o}\right)py \ ; \ u_o = \left(\frac{S}{A_o}\right)PL \ ; \ PS = \int\limits_{\Delta\omega} k_{\omega}d\omega \qquad (3.42)$$

Now, by using the definition $\bar{A} = \frac{A}{A_o}$, Eq.(3.36)-(3.37) are written as,

$$\bar{A}'(y) = \frac{d}{dy}\left[\bar{A}(y)\right] = \frac{1}{A_o}\frac{dA(y)}{dy} = \frac{A'(y)}{A_o} \ \sim cm^{-1} \qquad (3.43a)$$

$$A'(y) = A_o\frac{d\bar{A}(y)}{dy} = A_o\left[\frac{d\bar{A}(u)}{du}\frac{du}{dy}\right] = PS(T)\,\bar{A}'(u) \qquad (3.43b)$$

$$A''(y) = [PS(T)]^2\left(\frac{1}{A_o}\right)\bar{A}'' \qquad (3.43c)$$

The dimensions of both sides in Eq.(3.43b) and (3.43c) agree with the dimensions given in Eqs.(3.36) and (3.37). By employing the definitions of Eqs.(3.42) and (3.43),

Eq.(3.41) is expressed as

$$q_R(u) = e_1 - e_2 + \frac{3}{2}\sum_{i=1}^{n} A_{oi}\left\{ \int_0^{u_i} F_{1\omega_i}(u_i')\, \bar{A}_i'\left[\frac{3}{2}(u_i - u_i')\right] du_i' \right.$$

$$\left. - \int_{u_i}^{u_{oi}} F_{2\omega_i}(u_i')\, \bar{A}_i'\left[\frac{3}{2}(u_i' - u_i)\right] du_i' \right\} \quad (3.44)$$

where u' is the dummy variable for u and $\bar{A}'(u) = \frac{d\bar{A}}{du}$. It should be noted that $F_{1\omega i}$ and $F_{2\omega i}$ in Eq.(3.44) represent the values of $F_{1\omega}$ and $F_{2\omega}$ at the center of the ith band, and $\frac{dq_R}{dy} = \left(\frac{dq_R}{du}\right)\left(\frac{du}{dy}\right) = \left[\frac{PS(T)}{A_o}\right]\left(\frac{dq_R}{du}\right)$.

By defining the new independent variables as

$$\xi = \frac{u}{u_o} = \frac{y}{L} \quad ; \quad \xi' = \frac{u'}{u_o} = \frac{z}{L} \quad (3.45)$$

Eq.(3.44) can be expressed as

$$q_R(\xi) = e_1 - e_2 + \frac{3}{2}\sum_{i=1}^{n} A_{oi}u_{oi}\left\{ \int_0^{\xi} F_{1\omega_i}(\xi')\, \bar{A}_i'\left[\frac{3}{2}u_{oi}(\xi - \xi')\right] d\xi' \right.$$

$$\left. - \int_{\xi}^{1} F_{2\omega_i}(\xi')\, \bar{A}_i'\left[\frac{3}{2}u_{oi}(\xi' - \xi)\right] d\xi' \right\} \quad (3.46)$$

where again $\bar{A}'(u)$ denotes the derivative of A(u) with respect to u, and $\frac{dq_R}{du} = \left(\frac{dq_R}{d\xi}\right)\left(\frac{d\xi}{du}\right) = \left(\frac{1}{u_o}\right)\left(\frac{dq_R}{d\xi}\right)$.

Equations (3.44) and (3.46) allow us to make use of the band model correlations for the wide-band absorptance because these correlations are expressed in terms of u and β. However, it is often desirable and convenient to express the relations for q_R and div q_R which only involve $\bar{A}(u)$ and $\bar{A}'(u)$ but not $\bar{A}''(u)$. This is accomplished by integrating the integrals in the above equation by parts. This results in simpler integrals. Upon performing the integration, Eq. (3.46) is expressed as

$$q_R(\xi) = e_1 - e_2 + \frac{3}{2}\sum_{i=1}^{n} A_{oi}\left\{ \int_0^{\xi} \left[\frac{de_{\omega_i}(\xi')}{d\xi'}\right] \bar{A}_i\left[\frac{3}{2}u_{oi}(\xi - \xi')\right] d\xi' \right.$$

$$\left. - \int_{\xi}^{1} \left[\frac{de_{\omega_i}(\xi')}{d\xi'}\right] \bar{A}_i\left[\frac{3}{2}u_{oi}(\xi' - \xi)\right] d\xi' \right\} \quad (3.47)$$

By differentiating Eq. (3.47) using the Leibinitz formula, there is obtained

$$
\frac{dq_{R(\xi)}}{d\xi} = \frac{3}{2} \sum_{i=1}^{n} A_{oi} u_{oi} \left\{ \int_{0}^{\xi} \left[\frac{de_{\omega_i}(\xi')}{d\xi'} \right] \bar{A}'_i \left[\frac{3}{2} u_{oi} (\xi - \xi') \right] d\xi' \right.
$$
$$
\left. - \int_{\xi}^{1} \left[\frac{de_{\omega_i}(\xi')}{d\xi'} \right] \bar{A}'_i \left[\frac{3}{2} u_{oi} (\xi' - \xi) \right] d\xi' \right\} \qquad (3.48)
$$

Equations (3.47) and (3.48) are the most convenient equations to use when employing the band-model correlations in radiative transfer analyses.

For the present physical problem, $e_1 = e_2$ and $F_{1\omega i} = F_{2\omega i}$. Thus, for the case of linearized radiation, a combination of Eqs.(3.10) and (3.46) results in [29]

$$
\theta' - 2 \left(3\xi^2 - 2\xi^3 \right) + 1 = \frac{3}{2} \left(\frac{L}{k} \right) \sum_{i=1}^{n} H_{1i} u_{oi}
$$
$$
\left\{ \int_{0}^{\xi} \theta (\xi') \bar{A}'_i \left[\frac{3}{2} u_{oi} (\xi - \xi') \right] d\xi' \right.
$$
$$
\left. - \int_{\xi}^{1} \theta (\xi') \bar{A}'_i \left[\frac{3}{2} u_{oi} (\xi' - \xi) \right] d\xi' \right\} \qquad (3.49)
$$

where $H_{1i} = A_{oi} (T) \left(\frac{de_{\omega i}}{dT} \right)_{T_1}$; $H_1 = \sum_{i=1}^{n} H_{1i}$

A combination of Eqs.(3.10) and (3.48) gives an alternate form of the energy equation for the steady case as

$$
\theta' - 2 \left(3\xi^2 - 2\xi^3 \right) + 1 = \left(\frac{L}{k} \right) \sum_{i=1}^{n} H_{1i}
$$
$$
\left\{ \int_{0}^{\xi} \left(\frac{d\theta}{d\xi'} \right) \bar{A}_i \left[\frac{3}{2} u_{oi} (\xi - \xi') \right] d\xi' \right.
$$
$$
\left. + \int_{\xi}^{1} \left(\frac{d\theta}{d\xi'} \right) \bar{A}_i \left[\frac{3}{2} u_{oi} (\xi' - \xi) \right] d\xi' \right\} \qquad (3.50)
$$

Note that this equation can also be obtained directly by integrating the left hand side of Eq. (3.49) by parts. Equations (3.49) and (3.50) provide two forms of the energy equation for the steady-state conditions.

For the case of negligible radiation, Eqs. (3.49) and (3.50) reduce to

$$\theta' = 2\left(3\xi^2 - 2\xi^3\right) - 1 \tag{3.51}$$

The solution of Eq.(3.51) is found to be

$$\theta(\xi) = \xi\left(2\xi^2 - \xi^3 - 1\right) \tag{3.52}$$

Thus, a combination of Eqs. (3.11) and (3.52) gives the result for the bulk temperature for the steady case with no radiation as

$$\theta_b = -\frac{17}{70} = -0.24286 \tag{3.53}$$

This result is useful in determining the extent of radiative contributions.

3.3.1 Optically Thin Limit

In the optically thin limit [1], $\bar{A}(u) = u$, $\bar{A}'(u) = 1$, and $\bar{A}''(u) = 0$. In this limit, therefore, Eqs.(3.49) and (3.50), reduce to

$$\theta' - 2\left(3\xi^2 - 2\xi^3\right) + 1 = \frac{3}{2}N\left[\int_0^\xi \theta(\xi')\,d\xi' - \int_0^1 \theta(\xi')\,d\xi'\right] \tag{3.54}$$

$$\theta' - 2\left(3\xi^2 - 2\xi^3\right) + 1 = \frac{3}{2}N\left[\int_0^\xi (\xi - \xi')\left(\frac{d\theta}{d\xi'}\right)d\xi' + \int_\xi^1 (\xi' - \xi)\left(\frac{d\theta}{d\xi'}\right)d\xi'\right] \tag{3.55}$$

where $N = \left(\frac{PL^2}{k}\right)K_1 = \left(\frac{PL^2}{k}\right)\sum_{i=1}^n S_i(T)\left(\frac{de_{\omega_i}}{dT}\right)_{T_1}$

$H_{1i} = A_{oi}(T)\left(\frac{de_{\omega_i}}{dT}\right)_{T_1}$; $H_1 = \sum_{i=1}^n H_{1i}$

The differentiation of Eqs.(3.54) and (3.55) yields the same energy equation for the optically thin limit as

$$\theta'' - 3N\theta = 12\left(\xi - \xi^2\right) \tag{3.56}$$

The solution of Eq.(3.56) satisfying the boundary conditions $\theta(0) = 0$ and $\theta(1) = 0$ is found to be

$$\theta(\xi) = \left(\frac{16}{3N^2}\right)\left[\frac{\sinh\left(-\frac{\sqrt{3N}}{2}\right)}{\sinh\left(\sqrt{3N}\right)}\right]\cosh\left[\sqrt{3N}\left(\xi - \frac{1}{2}\right)\right]$$
$$+ \left(\frac{4}{N}\right)\left(\xi^2 - \xi + \frac{2}{3N}\right) \tag{3.57}$$

Alternatively, the solution of Eq.(3.57) is written as

$$\theta(\xi) = C_1\exp\left(\sqrt{m}\xi\right) + C_2\exp\left(-\sqrt{m}\xi\right)$$
$$+ \left(\frac{1}{m^2}\right)\left(24 - 12m\xi + 12m\xi^2\right) \quad ; \quad m = 3N \tag{3.58}$$

The constants C_1 and C_2 are obtained by using the boundary conditions $\theta(0) = 0$ and $\theta'(1/2) = 0$, and the solution for $\theta(\xi)$ is found to be

$$\theta(\xi) = \left(\frac{1}{m^2}\right)\left\{ \begin{array}{l} \left(-\frac{24}{1 + e^{-\sqrt{m}}}\right)\left(e^{-\sqrt{m}}e^{\sqrt{m}\xi} + e^{-\sqrt{m}\xi}\right) \\ + 24 - 12m\xi + 12m\xi^2 \end{array} \right\} \tag{3.59}$$

Equations (3.59) and (3.3.60) should produce identical results. The expression for the bulk temperature, in this case, is obtained by combining Eqs.(3.11) and (3.59) as

$$\theta_b = \frac{576}{m^{\frac{7}{2}}}\left[\frac{1 - e^{-\sqrt{m}}}{1 + e^{-\sqrt{m}}}\right] - \frac{288}{m^3} + \frac{24}{m^2} - \frac{12}{5m} \tag{3.60a}$$

$$\theta_b = \left[\frac{1}{(3N)^3}\right]\left\{\frac{576}{\sqrt{3N}}NEXP - 21.6N^2 + 72N - 288\right\} \tag{3.60b}$$

where

$$NEXP = \frac{1 - e^{-\sqrt{3N}}}{1 + e^{-\sqrt{3N}}}$$

3.3.2 Large Path Length Limit

In the large path length limit, $u_{oi} \gg 1$ for each band of interest and $\bar{A}(u) = \ln(u)$, $\bar{A}'(u) = \frac{1}{u}$, and $\bar{A}''(u) = -\frac{1}{u^2}$ [29]. Thus, in this limit Eqs. (3.49) and (3.50) reduce to

$$\theta' - 2\left(3\xi^2 - 2\xi^3\right) + 1 = M \int_0^1 \frac{\theta(\xi')}{(\xi - \xi')} d\xi' \tag{3.61}$$

$$\theta' - 2\left(3\xi^2 - 2\xi^3\right) + 1 = \left(\frac{L}{k}\right) \sum_{i=1}^n H_{1i}$$
$$\left\{ \int_0^\xi \left(\frac{d\theta}{d\xi'}\right) \ln\left[\frac{3}{2}u_{oi}(\xi - \xi')\right] d\xi' \right.$$
$$\left. + \int_\xi^1 \left(\frac{d\theta}{d\xi'}\right) \ln\left[\frac{3}{2}u_{oi}(\xi' - \xi)\right] d\xi' \right\} \tag{3.62}$$

where $M = \frac{H_1 L}{k} = \left(\frac{L}{k}\right) \sum_{i=1}^n A_{oi} \left(\frac{de_{oi}}{dT}\right)_{T_1}$

Through integration by parts, it can be shown that Eq.(3.62) reduces to Eq.(3.61). The non-dimensional parameter M constitutes the radiation-conduction interaction parameter for the large path length limit. Equation (3.61) does not appear to possess a closed form solution; a numerical solution, however, can be obtained easily.

Chapter 4

LAMINAR FLOW THROUGH CIRCULAR DUCT

This chapter covers the development of different types of formulation for steady laminar fully developed flow of absorbing-emitting, constant property, incompressible gas in a circular duct. Basic formulation for such a flow is given in Sec. 4.1. Gray gas formulation is developed in Sec. 4.2 and nongray formulation is given in Sec. 4.3.

4.1 Basic Formulation

The physical model for the circular duct geometry is shown in (Fig.4.1). For radiation participating medium, the equations expressing conservation of mass and momentum remain unaltered, while conservation of energy for such a flow is given by the same expression as Eq.(3.1), i.e.,

$$\rho C_p \frac{DT}{Dt} = div\,(k\nabla T) + \beta T \frac{DP}{Dt} + \mu \Phi - div\,q_R \tag{4.1}$$

Under similar conditions as mentioned in Sec. 3.1, Eq.(4.1) can be written in circular coordinates as

$$u \frac{\partial T}{\partial x} = \frac{\alpha}{r} \frac{\partial}{\partial r} \left(r \frac{\partial T}{\partial r} \right) - \frac{1}{\rho C_p} \frac{1}{r} \frac{\partial}{\partial r} (r q_R) \tag{4.2}$$

By noting that for a uniform wall heat flux and fully developed heat transfer

$$\frac{\partial T}{\partial x} = \frac{2\alpha q_w}{u_m r_o k} \tag{4.3}$$

and by employing the parabolic laminar velocity profile for u given by

$$u = 2u_m \left[1 - \left(\frac{r}{r_o} \right)^2 \right] \tag{4.4}$$

27

Eq. (4.2) can be written as

$$4\left[1 - \left(\frac{r}{r_o}\right)^2\right]\left(\frac{r}{r_o}\right) = \frac{k}{q_w}\frac{\partial}{\partial r}\left(r\frac{\partial T}{\partial r}\right) - \frac{1}{q_w}\frac{\partial}{\partial r}(rq_R) \tag{4.5}$$

By noticing that for the case of a circular duct $u = C_o^2 Pr$ and $u_o = C_o^2 Pr_o$, Eq. (4.5) is expressed as

$$4\left[1 - \left(\frac{u}{u_o}\right)^2\right]\left(\frac{u}{u_o}\right) = \frac{k}{q_w}C_o^2 P\frac{\partial}{\partial u}\left(u\frac{\partial T}{\partial u}\right) - \frac{1}{q_w}\frac{\partial}{\partial u}(uq_R) \tag{4.6}$$

Defining non-dimensional quantities

$$\xi = \frac{r}{r_o} = \frac{u}{u_o}$$

$$\theta = \frac{T - T_w}{q_w r_o/k} = \frac{kC_o^2 P}{u_o q_w}(T - T_w) \tag{4.7}$$

Eq.(4.6) can be rewritten as

$$4\left(\xi - \xi^2\right) = \frac{\partial}{\partial \xi}\left(\xi\frac{\partial\theta}{\partial\xi}\right) - \frac{1}{q_w}\frac{\partial}{\partial\xi}(\xi q_R) \tag{4.8}$$

The boundary conditions for this case are given as

$$\theta'(0) = 0$$

$$\theta(1) = 0 \tag{4.9}$$

Integrating Eq.(4.8) once and by noting that at $\xi = 0$, $(\partial\theta/\partial\xi) = 0$ and $q_R = 0$, we get

$$\theta_\xi + \xi^3 - 2\xi = \frac{q_R(\xi)}{q_w} \tag{4.10}$$

For the circular geometry, the bulk temperature is defined as

$$\theta_b = \frac{1}{u_m\pi r_o^2}\int_0^{2\pi}\int_0^{r_o} u(r)\,\theta(r)\,r\,dr\,d\theta \tag{4.11}$$

A combination of Eqs. (4.4) and (4.11a) results in

$$\theta_b = 4\int_0^1 \left(\xi - \xi^3\right)\theta(\xi)\,d\xi \tag{4.12}$$

The Nusselt number based on the hydraulic diameter $D_h = 2r_o$ is given as

$$N_u = \frac{2r_o q_w}{k(T - T_b)} = -\frac{2}{\theta_b} \tag{4.13}$$

4.2 Gray Gas Formulation

For a gray non-scattering medium within a black bounding surface, the equation for radiative flux can be written using the exponential approximation as [29]

$$\frac{d}{dr}\left[\frac{1}{r}\frac{d}{dr}(rq_R)\right] - \frac{9}{4}\kappa_p^2 q_R = 3\sigma\kappa_p\frac{dT^4}{dr} \tag{4.14}$$

For linearized radiation Eq.(4.13) can be written in dimensionless form as

$$\frac{d}{d\xi}\left[\frac{1}{\xi}\frac{d}{d\xi}(\xi q_R)\right] - \frac{9}{4}\tau_o^2 q_R = \gamma_2 q_w\frac{d\theta}{d\xi} \tag{4.15}$$

where

$$\gamma_2 = \frac{12\sigma\kappa_p T_w^3 r_o^2}{k} = \frac{12\sigma T_w^3\tau_o^2}{k\kappa_p}, \quad \tau_o = \kappa_p r_o \tag{4.16}$$

Boundary conditions for Eq.(4.14) are

$$\text{At} \quad \xi = 1, \frac{3}{2}q_R = -\frac{1}{\tau_o}\left[\frac{1}{\xi}\frac{d}{d\xi}(\xi q_R)\right]$$

$$q_R(0) = 0 \tag{4.17}$$

Equation (4.8) can be integrated once to give

$$\frac{d\theta}{d\xi} = \frac{q_R(\xi)}{q_w} + 2\xi - \xi^3 - \frac{C_1}{\xi} \tag{4.18}$$

Equation (4.14) and (4.16) are combined to give

$$\xi^2\frac{d^2q_R}{d\xi^2} + \xi\frac{dq_R}{d\xi} - (M_2^2\xi^2 + 1)q_R = \gamma_2 q_w(2\xi^3 - \xi^5 - C_1\xi) \tag{4.19}$$

where

$$M_2^2 = \frac{9}{4}\tau_o^2 + \gamma_2$$

The solution of Eq.(4.18) is found to be

$$q_R = C_2 I_1(M_2\xi) + C_3 K_1(M_2\xi) + \frac{\gamma_2 q_w}{M_2^4}(M_2^2\xi^3 + 8\xi - 2M_2^2\xi) \tag{4.20}$$

For a finite solution as $\xi \longrightarrow 0$, C_3 must be taken to be zero and

$$q_R = C_2 I_1(M_2\xi) + \frac{\gamma_2 q_w}{M_2^4}(M_2^2\xi^3 + 8\xi - 2M_2^2\xi) \tag{4.21}$$

From Eqs.(4.16) and (4.20), there is obtained

$$C_2 I_1(M_2) + \frac{\gamma_2 q_w}{M_2^4}(8 - M_2^2)$$

$$= -\frac{2}{3\tau_o}\left\{C_2\left[I_1(M_2) + \left(\frac{d}{d\xi}I_1(M_2\xi)\right)_{\xi=1}\right] + \frac{16\gamma_2 q_w}{M_2^4}\right\} \quad (4.22)$$

or

$$3\tau_o C_2 I_1(M_2) + \frac{\gamma_2 q_w}{M_2^4}(24\tau_o - 3\tau_o M_2^2)$$

$$= -2C_2\left[I_1(M_2) + \left(M_2 I_o(M_2\xi) - \frac{I_1(M_2\xi)}{\xi}\right)_{\xi=1}\right] - \frac{32\gamma_2 q_w}{M_2^4} \quad (4.23)$$

$$C_2\left[3\tau_o I_1(M_2) + 2M_2 I_o(M_2)\right] = \frac{\gamma_2 q_w}{M_2^4}\left[3\tau_o M_2^2 - 24\tau_o - 32\right] \quad (4.24)$$

and

$$C_2 = \left[\frac{3\tau_o M_2^2 - 24\tau_o - 32}{2M_2 I_o(M_2) + 3\tau_o I_1(M_2)}\right]\left(\frac{\gamma_2 q_w}{M_2^4}\right)$$

From Eq.(4.2.17) and (4.2.20) one finds

$$\frac{d\theta}{d\xi} = \frac{C_2}{q_w}I_1(M_2\xi) + \frac{\gamma_2}{M_2^4}(M_2^2\xi^3 + 8\xi - 2M_2^2\xi) + 2\xi - \xi^3 - \frac{C_1}{\xi} \quad (4.25)$$

where from the boundary condition $\theta'(0) = 0$, $C_1 = 0$

Equation (4.24) is integrated once to give

$$\theta = \frac{C_2}{q_w M_2}I_o(M_2\xi) + \frac{\gamma_2}{M_2^4}\left(\frac{M_2^2\xi^4}{4} + 4\xi^2 - M_2^2\xi^2\right) + \xi^2 - \frac{1}{4}\xi^4 - C_4 \quad (4.26)$$

From the boundary condition $\theta(1) = 0$, one finds

$$C_4 = \frac{C_2}{q_w M_2}I_o(M_2) + \frac{\gamma_2}{M_2^4}\left(\frac{16 - 3M_2^2}{4}\right) + \frac{3}{4}$$

Consequently, Eq.(4.25) becomes

$$\theta = \frac{C_2}{q_w M_2}\left[I_o(M_2\xi) - I_o(M_2)\right]$$

$$+ \frac{\gamma_2}{4M_2^4}(M_2^2\xi^4 + 16\xi^2 - 4M_2^2\xi^2 + 3M_2^2 - 16) + \xi^2 - \frac{1}{4}\xi^4 - \frac{3}{4} \quad (4.27)$$

The expression for the bulk temperature can be easily obtained as

$$\theta_b = C \left[\left(\frac{8 - M_2^2}{M_2^2} \right) I_o(M_2) - \frac{16 I_1(M_2)}{M_2^3} \right]$$
$$+ \frac{11}{24} \frac{\gamma_2}{M_2^2} - \frac{8}{3} \frac{\gamma_2}{M_2^4} - \frac{11}{24}$$

(4.28)

where

$$C = \frac{\gamma_2}{M_2^5} \left[\frac{3\tau_o M_2^2 - 24\tau_o - 32}{2 M_2 I_o(M_2) + 3\tau_o I_1(M_2)} \right]$$

$$M_2^2 = \frac{9}{4}\tau_o^2 + \gamma_2$$

$$\gamma_2 = \frac{12\sigma\kappa_p T_w^3 r_o^2}{k} = \frac{12\sigma T_w^3 r_o^2}{k\kappa_p}$$

$$\tau_o = \kappa_p r_o$$

4.2.1 Optically Thin Limit

Recall the definition of M_2 as

$$M_2^2 = \frac{9}{4}\tau_o^2 + \gamma_2$$

For optically thin conditions $\tau_o \longrightarrow 0$ and, therefore,

$$\lim \tau_o - > 0 \left(M_2^2 \right) = \gamma_2 \quad , \quad \lim \tau_o - > 0 \left(M_2 \right) = \gamma_2^{\frac{1}{2}}$$

$$\lim \tau_o - > 0 \left(C \right) = -\frac{32}{2\sqrt{\gamma_2} I_o \left(\sqrt{\gamma_2} \right)} = -\frac{16}{\sqrt{\gamma_2} I_o \left(\sqrt{\gamma_2} \right)}$$

The expression for the bulk temperature in the optically thin limit, therefore, becomes

$$(\theta_b)_{thin} = \frac{1}{\gamma_2^3} \left[\frac{256}{\sqrt{\gamma_2}} \frac{I_1 \left(\sqrt{\gamma_2} \right)}{I_o \left(\sqrt{\gamma_2} \right)} - 128 + 16\gamma_2 - \frac{8\gamma_2^2}{3} \right]$$

(4.29)

By employing the series expansion of the modified Bessel functions for small values of the argument γ_2, Eq. (4.29) can be written in an alternate form, and by letting $\gamma_2 - > 0$ in that form there is obtained the result in the transparent limit $(\theta_b)_{thin} = -\frac{11}{24}$.

4.2.2 Optically Thick Limit

The asymptotic series for modified Bessel's functions for large value of M_2 are

$$I_o(M_2) \simeq \frac{e^{M_2}}{\sqrt{2\pi M_2}}\left[1 + \frac{1}{8M_2} + \frac{9}{128M_2^2} + ...\right] \qquad (4.30a)$$

$$I_1(M_2) \simeq \frac{e^{M_2}}{\sqrt{2\pi M_2}}\left[1 - \frac{3}{8M_2} - \frac{15}{128M_2^2} + ...\right] \qquad (4.30b)$$

Substituting for $I_o(M_2)$ and $I_1(M_2)$ from Eq. (4.30) into Eq. (4.27) and taking the limit as $\tau_o \longrightarrow \alpha$, we get

$$(\theta_b)_{thick} = \frac{11}{24}\frac{\gamma_2}{M_2^2} - \frac{8}{3}\frac{\gamma_2}{M_2^4} - \frac{11}{24} \qquad (4.31)$$

Defining

$$N = \frac{k\kappa_p}{4\sigma T_w^3}$$

$$\gamma_2 = \frac{3\tau_o^2}{N} \quad and \quad M_2^2 = \frac{3}{4}\left(3 + \frac{4}{N}\right)\tau_o^2$$

Eq. (4.31) is expressed in an alternate form as

$$(\theta_b)_{thick} = -\frac{11}{24}\left[\frac{1}{1 + (\frac{4}{3N})}\right] \qquad (4.32)$$

Equation (4.32) also reduces to the correct form for the case of no radiative interaction.

4.3 Nongray Formulation

In this section, formulation of the problem under realistic conditions is presented. Under such conditions the gas is nongray, that is the band parameters are functions of the wavelength. For solution of Eq.(4.10), an appropriate equation for radiative flux is needed. For a circular geometry, the expression for the radiative heat flux in terms of

non-dimensional path length is given as [39]

$$
q_R(u) = 4a \int\limits_0^{\frac{\pi}{2}} \Bigg\{ \int\limits_{u \sin \gamma}^{u} \Big\{ [B_{\omega c}(u') - B_{\omega c}(T_w)] \, \bar{A}' \left(\frac{b}{\cos \gamma} (u + u' - 2u \sin \gamma) \right)
$$

$$
+ \bar{A}' \left(\frac{b}{\cos \gamma} (u - u') \right) \Big\} du'
$$

$$
- \int\limits_u^{u_o} [B_{\omega c}(u') - B_{\omega c}(T_w)] \, \bar{A}' \left(\frac{b}{\cos \gamma} (u + u' - 2u \sin \gamma) \right)
$$

$$
+ \bar{A}' \left(\frac{b}{\cos \gamma} (u' - u) \right) \Big\} du' \Bigg\} d\gamma \tag{4.33}
$$

where a = 1 and b = 5/4. Equation (4.33) is expressed in an alternate form as

$$
q_R(\xi) = 4au_o \int\limits_0^{\frac{\pi}{2}} \Bigg\{ \int\limits_{\xi \sin \gamma}^{\xi} \Big\{ [B_{\omega c}(\xi') - B_{\omega c}(T_w)] \, \bar{A}' \left(\frac{bu_o}{\cos \gamma} (\xi + \xi' - 2\xi \sin \gamma) \right)
$$

$$
+ \bar{A}' \left(\frac{bu_o}{\cos \gamma} (\xi - \xi') \right) \Big\} d\xi'
$$

$$
- \int\limits_\xi^1 [B_{\omega c}(\xi') - B_{\omega c}(T_w)] \, \bar{A}' \left(\frac{bu_o}{\cos \gamma} (\xi + \xi' - 2\xi \sin \gamma) \right)
$$

$$
+ \bar{A}' \left(\frac{bu_o}{\cos \gamma} (\xi' - \xi) \right) \Big\} d\xi' \Bigg\} d\gamma \tag{4.34}
$$

In order to combine Eq.(4.10) and (4.34), the Planck's function is linearized as,

$$
B_{\omega c}(\xi) - B_{\omega c}(T_w) = \frac{1}{\pi} [e_\omega(\xi) - e_{\omega c}(T_w)]
$$

$$
\simeq \frac{1}{\pi} \left(\frac{de_{\omega c}}{dT} \right)_{T_w} (T - T_w) \tag{4.35}
$$

Now, a combination of Eqs.(4.10), (4.34) and (4.35) yields

$$
\frac{d\theta}{d\xi} + \xi^3 - 2\xi = \frac{4ar_o}{\pi k} u_o \left(\frac{de_{\omega c}}{dT} \right)_{T_w} \int\limits_0^{\frac{\pi}{2}} \Bigg\{
$$

$$
\int\limits_{\xi \sin \gamma}^{\xi} \theta(\xi') \, \bar{A}_i' \left[\frac{bu_o}{\cos \gamma} (\xi - \xi') \right] d\xi'
$$

$$-\int\limits_{\xi}^{1}\theta\left(\xi'\right)\bar{A}_i{}'\left[\frac{bu_o}{\cos\gamma}\left(\xi'-\xi\right)\right]d\xi'$$

$$\left.+\int\limits_{\xi\sin\gamma}^{1}\theta\left(\xi'\right)\bar{A}_i{}'\left[\frac{bu_o}{\cos\gamma}\left(\xi+\xi'-2\xi\sin\gamma\right)\right]d\xi'\right\}\ d\gamma \quad (4.36)$$

For nongray gases with n-bands, Eq.(4.36) is written in the following form,

$$\frac{d\theta}{d\xi}+\xi^3-2\xi=\frac{4r_o}{\pi k}\sum_{i=1}^{n}H_i u_{oi}\int\limits_{0}^{\frac{\pi}{2}}\Bigg\{$$

$$\int\limits_{\xi\sin\gamma}^{\xi}\theta\left(\xi'\right)\bar{A}_i{}'\left[\frac{b_i}{\cos\gamma}\left(\xi-\xi'\right)\right]d\xi'$$

$$-\int\limits_{\xi}^{1}\theta\left(\xi'\right)\bar{A}_i{}'\left[\frac{b_i}{\cos\gamma}\left(\xi'-\xi\right)\right]d\xi'$$

$$\left.+\int\limits_{\xi\sin\gamma}^{1}\theta\left(\xi'\right)\bar{A}_i{}'\left[\frac{b_i}{\cos\gamma}\left(\xi+\xi'-2\xi\sin\gamma\right)\right]d\xi'\right\}\ d\gamma \quad (4.37)$$

where

$$H_i\ =\ A_{oi}\left(\frac{de_{\omega i}}{dT}\right)_{T_w}\ ,\qquad \bar{A}_i'\ =\ \frac{A_i'}{A_{oi}}$$

Combined solutions of Eqs. (4.37) and (4.11) are obtained by numerical procedures.

4.3.1 Large Path Length Limit

As noted earlier, in the large path length limit $u_{oi} \gg 1$ for each band of interest, and $\bar{A}_i'\left(u_i\right)=1/u_i$. In this limit, Eq. (4.37) reduces to

$$\frac{d\theta}{d\xi}+\xi^3-2\xi=\frac{4ar_o}{\pi bk}\sum_{i=1}^{n}H_i\int\limits_{0}^{\frac{\pi}{2}}\Bigg\{\cos\gamma\Bigg[\int\limits_{\xi\sin\gamma}^{1}\theta\left(\xi'\right)\frac{d\xi'}{\left(\xi-\xi'\right)}$$

$$\left.\left.+\int\limits_{\xi\sin\gamma}^{1}\theta\left(\xi'\right)\frac{d\xi'}{\left(\xi+\xi'-2\xi\sin\gamma\right)}\right]\right\}\ d\gamma \quad (4.38)$$

or

$$\frac{1}{\xi}\frac{d\theta}{d\xi} + \xi^2 - 2 = \frac{8ar_o}{\pi bk}H\int\limits_0^{\frac{\pi}{2}}\left\{\cos\gamma\left(1-\sin\gamma\right)\right.$$

$$\left.\left[\int\limits_{\xi\sin\gamma}^1 \theta\left(\xi'\right)\frac{d\xi'}{\left(\xi-\xi'\right)\left(\xi+\xi'-2\xi\sin\gamma\right)}\right]\right\}\ d\gamma \quad (4.39)$$

The solution of Eq.(4.38) or (4.39) can be obtained either numerically or in closed form.

Chapter 5

METHOD OF SOLUTION

The solution procedure for both cases, the parallel plate geometry and the circular duct, are presented in this chapter. In principle, the same numerical procedure applies to both the general and large path length limit cases for both geometries.

5.1 Parallel Plates

The general solution of Eq.(3.49) is obtained numerically by employing the method of variation of parameters. For this, a polynomial form for $\theta(\xi)$ is assumed in powers of ξ as

$$\theta(\xi) = \sum_{m=0}^{n} a_m \xi^m \tag{5.1}$$

By considering a five term series solution (a quartic solution in ξ) and satisfying the boundary conditions $\theta(0) = \theta'(1/2) = 0$ and $\theta'(0) = -\theta'(1)$, one obtains

$$\theta(\xi) = a_1\left(\xi - 2\xi^3 + \xi^4\right) + a_2\left(\xi^2 - 2\xi^3 + \xi^4\right) \tag{5.2}$$

and

$$\theta'(\xi) = a_1\left(1 - 6\xi^2 + 4\xi^3\right) + a_2\left(2\xi - 6\xi^2 + 4\xi^3\right) \tag{5.3}$$

A substitution of Eq.(5.3) in Eq.(3.49) results in

$$a_1\left(1 - 6\xi^2 + 4\xi^3\right) + a_2\left(2\xi - 6\xi^2 + 4\xi^3\right) - 2\left(3\xi^2 - 2\xi^3\right) + 1$$

$$= \frac{3}{2}\left(\frac{L}{k}\right) \sum_{i=1}^{n} H_{1i} u_{oi}$$

$$\left\{\int_0^\xi \theta(\xi') \bar{A}_i'\left[\frac{3}{2} u_{oi}(\xi - \xi')\right] d\xi'\right.$$

37

$$-\int_{\xi}^{1} \theta\left(\xi'\right) \bar{A}_i' \left[\frac{3}{2} u_{oi} \left(\xi' - \xi\right)\right] d\xi' \Bigg\} \tag{5.4}$$

where expressions for $\theta\left(\xi'\right)$ are obtained from Eq.(5.2)

The two unknown constants a_1 and a_2 in Eq.(5.4) are evaluated by satisfying the integral equation at two convenient locations ($\xi = 0$ and $\xi = 1/4$ in the present case). The entire procedure for obtaining a_1 and a_2 is described in [35]. With known values of a_1 and a_2, Eq.(5.2) provides the general solution for $\theta(\xi)$. The expression for the bulk temperature is obtained by combining Eqs.(3.11) and (5.2) as

$$\theta_b = \frac{17a_1 + 3a_2}{70} \tag{5.5}$$

The governing equation for the large path length limit is Eq.(3.61). For this equation also the solution is given by Eqs.(5.2) and (5.5) but the values of a's are different in this case [35].

5.2 Circular Duct

The general solution of Eq.(4.32) is obtained numerically by employing the method of variation of parameter similar to that discussed in Sec. 5.1. For this, a polynomial form for $\theta(\xi)$ is assumed in powers of ξ as given by Eq. (5.1). By considering a five term series solution (a quartic solution in ξ) and satisfying the boundary conditions $\theta\left(1\right) = 0$, $\theta'\left(0\right) = 0$ and $\theta\left(1\right) = \theta\left(-1\right)$, one obtains

$$\theta\left(\xi\right) = a_1 \left(\xi^2 - 1\right) + a_2 \left(\xi^4 - 1\right) \tag{5.6}$$

and

$$\theta'\left(\xi\right) = 2a_1\xi + 4a_2\xi^3 \tag{5.7}$$

A substitution of Eqs.(5.6) and (5.7) in Eq.(4.32) results in

$$\xi^3 (4a_2 + 1) + 2\xi (a_1 - 1) = \frac{4r_o}{\pi k} \sum_{i=1}^{n} H_i u_{oi} \int_0^{\frac{\pi}{2}} \left\{ \right.$$

$$\int_{\xi \sin \gamma}^{\xi} \theta (\xi') \bar{A}_i' \left[\frac{b_i}{\cos \gamma} (\xi - \xi') \right] d\xi'$$

$$- \int_{\xi}^{1} \theta (\xi') \bar{A}_i' \left[\frac{b_i}{\cos \gamma} (\xi' - \xi) \right] d\xi'$$

$$+ \int_{\xi \sin \gamma}^{1} \theta (\xi') \bar{A}_i' \left[\frac{b_i}{\cos \gamma} (\xi + \xi' - 2\xi \sin \gamma) \right] d\xi' \left. \right\} \quad d\xi \quad (5.8)$$

where expression for $\theta (\xi')$ are obtained from Eq.(5.7).

The two unknown constants a_1 and a_2 in Eq.(5.8) are obtained by satisfying the integral equation at any two locations of ξ. The entire procedure is described in Appendix A and relations for the constants are expressed as

$$a_1 = ((zz_1\alpha_4) - (zz_2\alpha_2)) / DEN \qquad (5.9)$$

$$a_2 = ((zz_2\alpha_1) - (zz_1\alpha_3)) / DEN \qquad (5.10)$$

$$DEN = (\alpha_1\alpha_4 - \alpha_2\alpha_3) \qquad (5.11)$$

The quantity appearing in Eqs.(5.9)-(5.11) are defined in Appendix A.

Now, with known values of a_1 and a_2, Eq.(5.6) provides the general solution for $\theta(\xi)$. The expression for the bulk temperature is obtained by combining Eq.(4.11) and (5.6) as

$$\theta_b = -\frac{2}{3}a_1 - \frac{5}{6}a_2 \qquad (5.12)$$

The governing equation for the large path length limit is Eq.(4.34). For this equation also the solution is given by Eq.(5.6) but the values of a_1 and a_2 are different. In large path length limit, the integrals can be evaluated in close forms. Procedure is described briefly

Equation (4.34) is expressed in an alternate form as

$$\frac{d\theta}{d\xi} + \xi^3 - 2\xi = M \int\limits_0^{\frac{\pi}{2}} \cos\gamma \int\limits_{\xi\sin\gamma}^1 \theta\left(\xi'\right) \left[\frac{d\xi'}{(\xi - \xi')} + \frac{d\xi'}{(\xi + \xi' - 2\xi\sin\gamma)}\right] d\gamma \quad (5.13)$$

where

$$M = \frac{4r_\rho a}{\pi b k} \sum_{i=1}^n H_i = \frac{16r_\rho}{5\pi k} \sum_{i=1}^n H_i \text{At } \xi = 1/2, \text{ Eq. (5.13) becomes}$$

$$a_1 + \frac{1}{2}a_2 - \frac{7}{8} = M \int\limits_0^{\frac{\pi}{2}} \cos\gamma \int\limits_{\frac{1}{2}\sin\gamma}^1 \theta\left(\xi'\right) \left[\frac{1}{\frac{1}{2} - \xi'} + \frac{1}{\frac{1}{2} + \xi' - \sin\gamma}\right] d\xi'd\gamma \quad (5.14)$$

Substituting for $\theta\left(\xi'\right)$ in terms of a_1 and a_2 as given by Eq. (5.6), and rearranging Eq.(5.14), one obtains

$$-\frac{7}{8} = a_1 \left\{-1 + M \int\limits_0^{\frac{\pi}{2}} \cos\gamma \int\limits_{\frac{1}{2}\sin\gamma}^1 \left[\frac{\left(\xi'^2 - 1\right)}{\frac{1}{2} + \xi' - \sin\gamma} - \frac{\left(\xi'^2 - 1\right)}{\xi' - \frac{1}{2}}\right] d\xi'd\gamma\right\}$$

$$+ a_2 \left\{-\frac{1}{2} + M \int\limits_0^{\frac{\pi}{2}} \cos\gamma \int\limits_{\frac{1}{2}\sin\gamma}^1 \left[\frac{\left(\xi'^4 - 1\right)}{\frac{1}{2} + \xi' - \sin\gamma} - \frac{\left(\xi'^4 - 1\right)}{\xi' - \frac{1}{2}}\right] d\xi'd\gamma\right\} \quad (5.15)$$

By evaluating the inner integral Eq.(5.15) is expressed as

$$-\frac{7}{8} = a_1 \left\{-1 + M \int\limits_0^{\frac{\pi}{2}} \cos\gamma \left[\left(\sin^2\gamma - \sin\gamma - \frac{3}{4}\right) \ln\left(3 - 2\sin\gamma\right)\right.\right.$$

$$\left.- \left(\sin^2\gamma - \sin\gamma\right) \ln\left(1 - \sin\gamma\right) - \frac{1}{2}\sin^2\gamma + \frac{3}{2}\sin\gamma - 1\right] d\gamma\right\}$$

$$+ a_2 \left\{-\frac{1}{2} + M \int\limits_0^{\frac{\pi}{2}} \cos\gamma \left[\left(\sin^4\gamma - 2\sin^3\gamma + \frac{3}{2}\sin^2\gamma - \frac{1}{2}\sin\gamma - \frac{15}{16}\right)\right.\right.$$

$$\ln\left(3 - 2\sin\gamma\right) - \left(\sin^4\gamma - 2\sin^3\gamma + \frac{3}{2}\sin^2\gamma - \frac{1}{2}\sin\gamma\right) \ln\left(1 - \sin\gamma\right)$$

$$\left.\left.- \frac{7}{12} + \frac{17}{24}\sin\gamma - \frac{11}{18}\sin^2\gamma + \frac{23}{12}\sin^3\gamma - \frac{2}{3}\sin^4\gamma\right] d\gamma\right\} \quad (5.16)$$

Now solving these trigonometric integrals and simplifying, one obtains

$$-\frac{7}{8} = a_1 \left\{ -1 + M \left[\frac{1}{12} - \frac{9}{8} A \log(3) \right] \right\}$$
$$+ a_2 \left\{ -\frac{1}{2} + M \left[\left(-\frac{207}{160} A \log(3) - \frac{121}{400} + \frac{13}{12} \right) + \left(\frac{1}{25} - \frac{1}{12} \right) - \frac{123}{360} \right] \right\} \quad (5.17)$$

Equation (5.2.17) can now be written as

$$-\frac{7}{8} = a_1 \alpha_1 + a_2 \alpha_2 \tag{5.18}$$

where

$$\alpha_1 = -1 + M \left[\frac{1}{12} - \frac{9}{8} A \log(3) \right]$$
$$\alpha_2 = -.5 + M \left[\frac{19}{48} - \frac{207}{160} A \log(3) \right]$$

At $\xi = 1$, a similar solution procedure yields the result

$$-1 = a_1 \alpha_3 + a_2 \alpha_4 \tag{5.19}$$

where

$$\alpha_3 = -2 + M \left[-\frac{2}{3} A \log(2) - \frac{2}{3} \right] \tag{5.20}$$
$$\alpha_4 = -4 + M \left[-\frac{4}{5} A \log(2) - \frac{17}{15} \right]$$

Now, with known values of a_1 and a_2, Eq. (5.6) provides the general solution for $\theta(\xi)$ and the bulk temperature is given by Eq. (5.12).

Chapter 6

RESULTS AND DISCUSSION

Extensive results have been obtained for variation of temperature (θ) and bulk temperature (θ_b) at different conditions for all four species in both the cases, and most of these are available in Appendix B and C. The computer programs used for numerical solution for both geometries are provided in Appendix D and E. Selected results are presented here to compare and illustrate the variation of temperature θ with ξ and of bulk temperature θ_b with plate spacing L or duct radius r_o. Variation of bulk temperature with pressure is also presented to illustrate the effect of large pressure path length and it's approach to limit of large u_{oi} much more clearly.

Although the results are similar in nature for both the geometries, they are presented in seperate sections for clarity.

6.1 Parallel Plates

The results for temperature variations across the duct are presented in Figs. 6.1–6.4. Figure 6.1 shows temperature profile for H_2O at $T_w = 500$ K, P = 1 atm and L = 10 cm with general as well as in the limit of large u_{oi}. This demonstrates that the limit of large u_{oi} overestimates the radiative energy transfer giving a conservative approximation. Thus, for practical and realistic problems, it might be easier to find out the extent of radiative interaction using the limit of large u_{oi} formulation and then use the general formulation which is computationally complex and expensive. Figure 6.2 demonstrates the effect of higher wall temperatures on temperature profiles. As the wall temperature increases temperature profile becomes less and less parabolic. In other words, temperature gets distributed more and more evenly across the duct. The effect of increasing pressure at any

42

temperature shows a similar trend (Fig. 6.3). At high pressures, the results approach the limit of large u_{oi}. The comparison of temperature profiles for the four species presented in Fig. 6.4 demonstrates the relative importance of each species in energy transfer. Water vapor (H_2O) is the most radiation participating species among the four considered here. For the physical conditions of Fig. 6.4, OH is the least radiation participating species.

The bulk temperature results as a function of the distance between the plates are presented in Figs. 6.5–6.9. The limiting value of $\theta_b = -0.243$ corresponds to negligible radiation. For a particular plate spacing L, the large path length results represent the limiting solutions for high pressures. The results, in general, demonstrate that the effect of radiation increases with increasing plate spacing.

General as well as limit of large u_{oi} solutions for the bulk temperature are illustrated in Figs. 6.5–6.7 for H_2O. The results for H_2O at $T_w = 1000$ K are presented for P = 1, 2, 5, 10 atm. It is noted that as pressure increases the ability of gas to transfer radiative energy increases, approaching the correct limiting solution of large u_{oi}. The results shown in Fig. 6.6 for H_2O, demonstrate the effect of increasing wall temperature. It is obvious that the radiative transfer is more pronounced at the higher wall temperature. The results presented in Fig. 6.7 illustrate both effects.

Comparison of bulk temperature results with plate spacing for various species is presented in Figs. 6.8 and 6.9 for a pressure of one atmosphere. The results clearly demonstrate the relative ability of the four species for radiative transfer at different path lengths. For lower plate spacings and relatively higher temperatures, however, CO_2 shows a significantly higher ability than other species. This is a typical distinguishing feature of the CO_2 under optically thin conditions[29].

The trend of the general solution approaching the limit of large u_{oi} (large path length limit) is illustrated in Fig. 6.10. A comparison of results for various species is shown in Fig. 6.11.

Gas : H_2O
$T_w = 500$ K
$L = 10$ cm

$-\theta = \dfrac{(T-T_1)}{(q_w L/k)}$

0.35
0.30
0.25
0.20
0.15
0.10
0.05
0.00

$P = 1$

LLU (Limit of Large u_{oi})

0.00   0.20   0.40   0.60   0.80   1.00

ξ
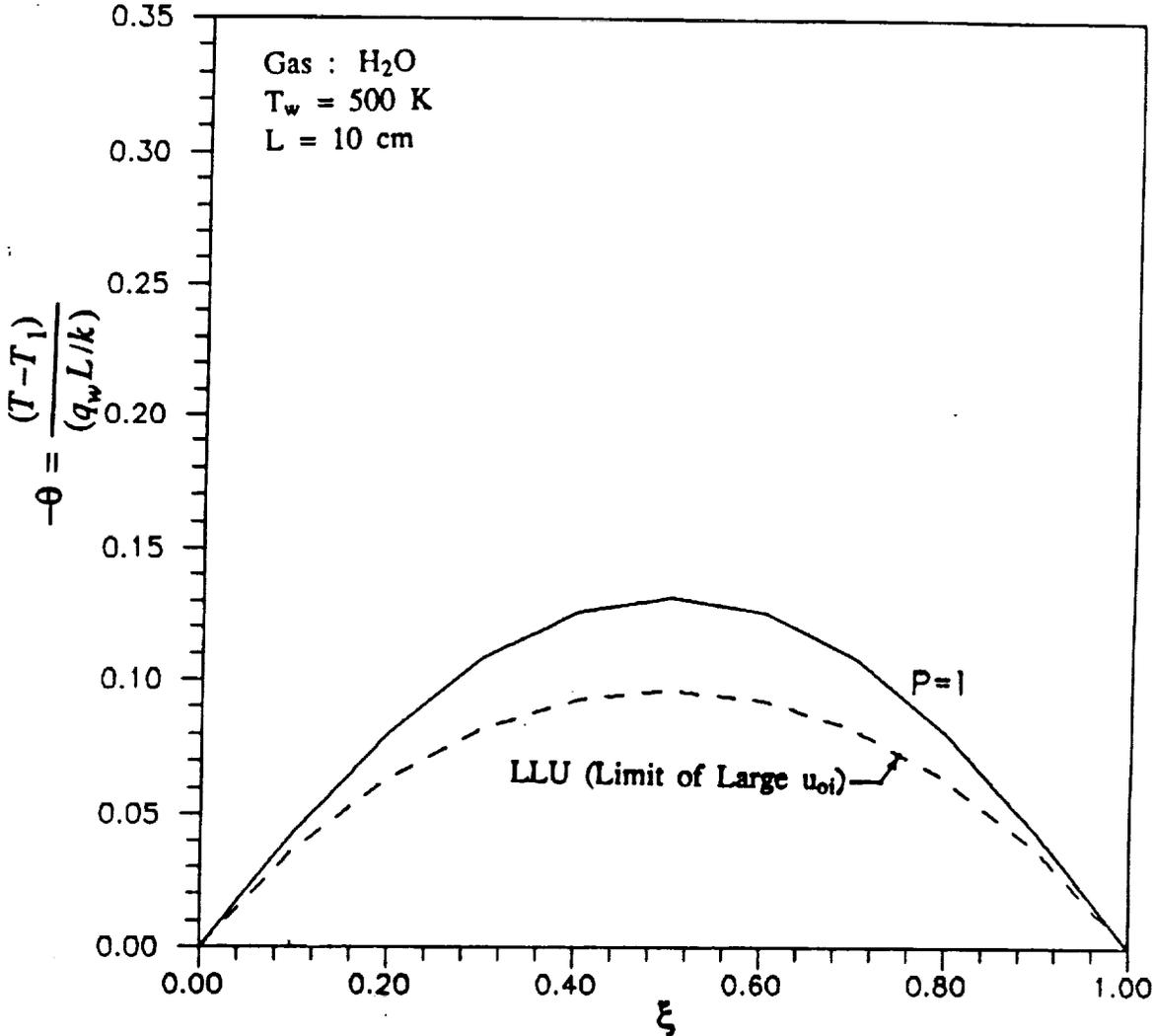
Figure 6.1 Comparison of temperature variations across the duct for H_2O;

$T_w = 500$ K, P = 1 atm and L = 10 cm.
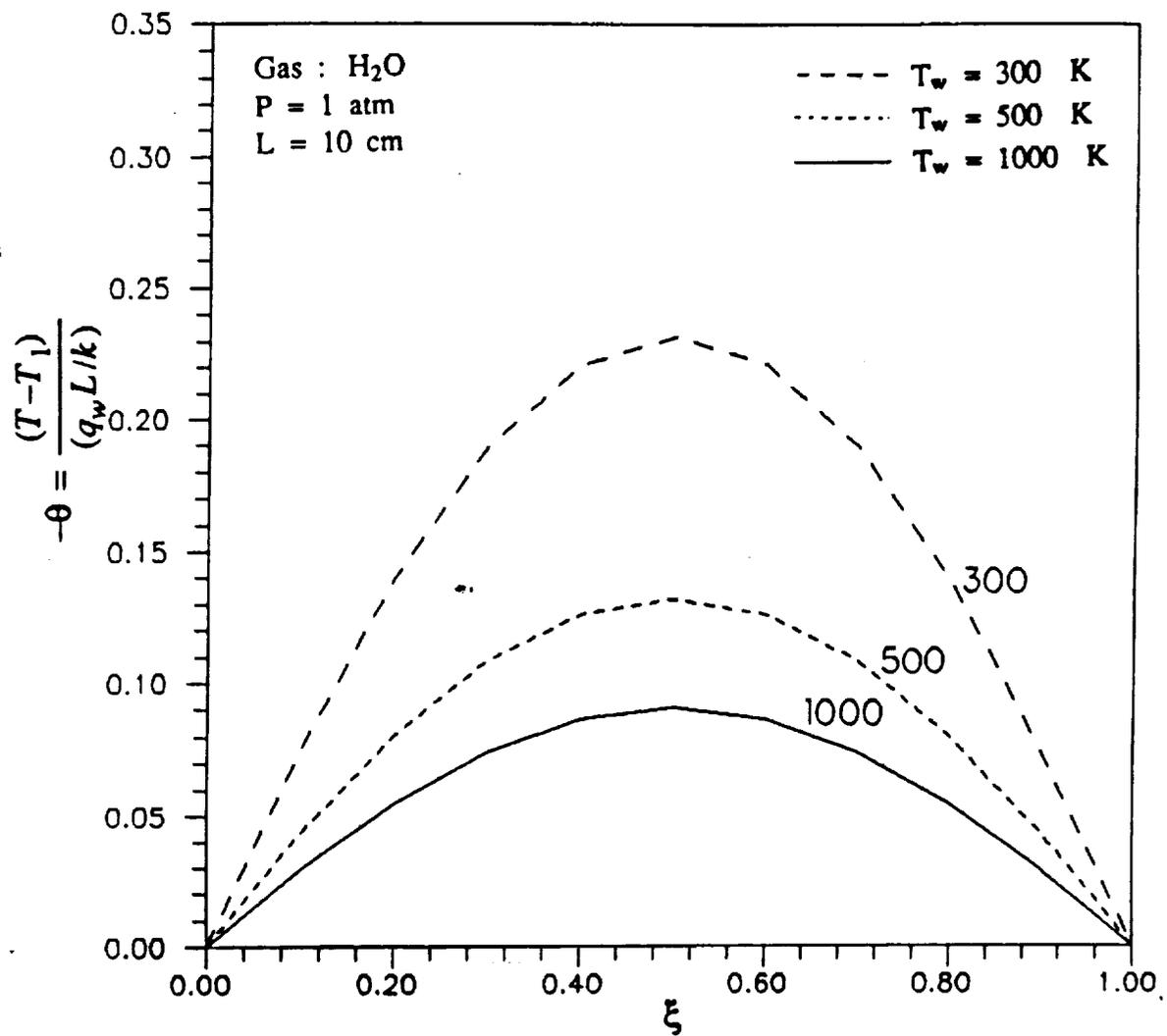
Figure 6.2 Comparison of temperature variations across the duct for H_2O;

T_w = 300, 500, 1000 K, P = 1 atm and L = 10 cm.
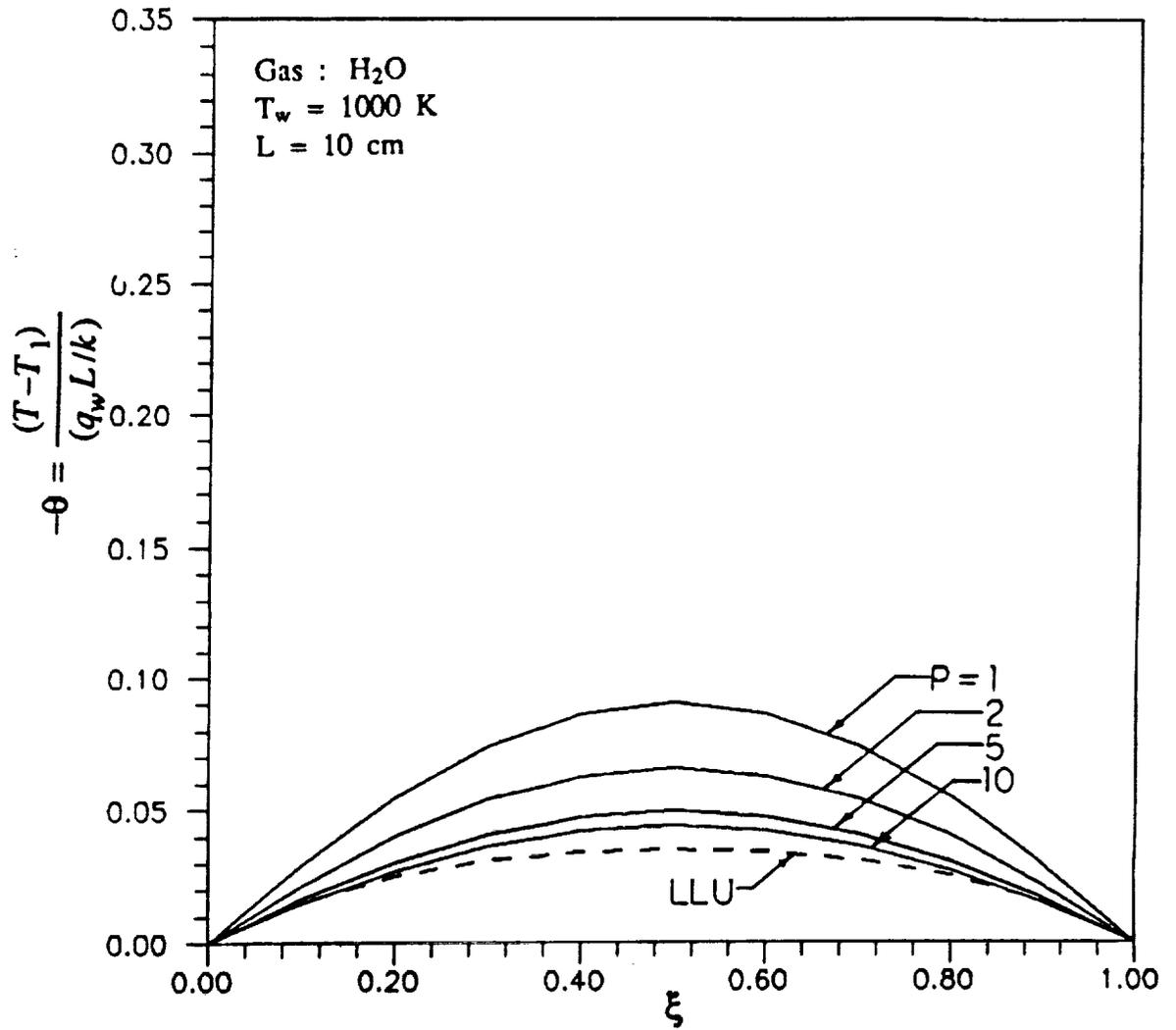
Figure 6.3 Comparison of temperature variations across the duct for H_2O;
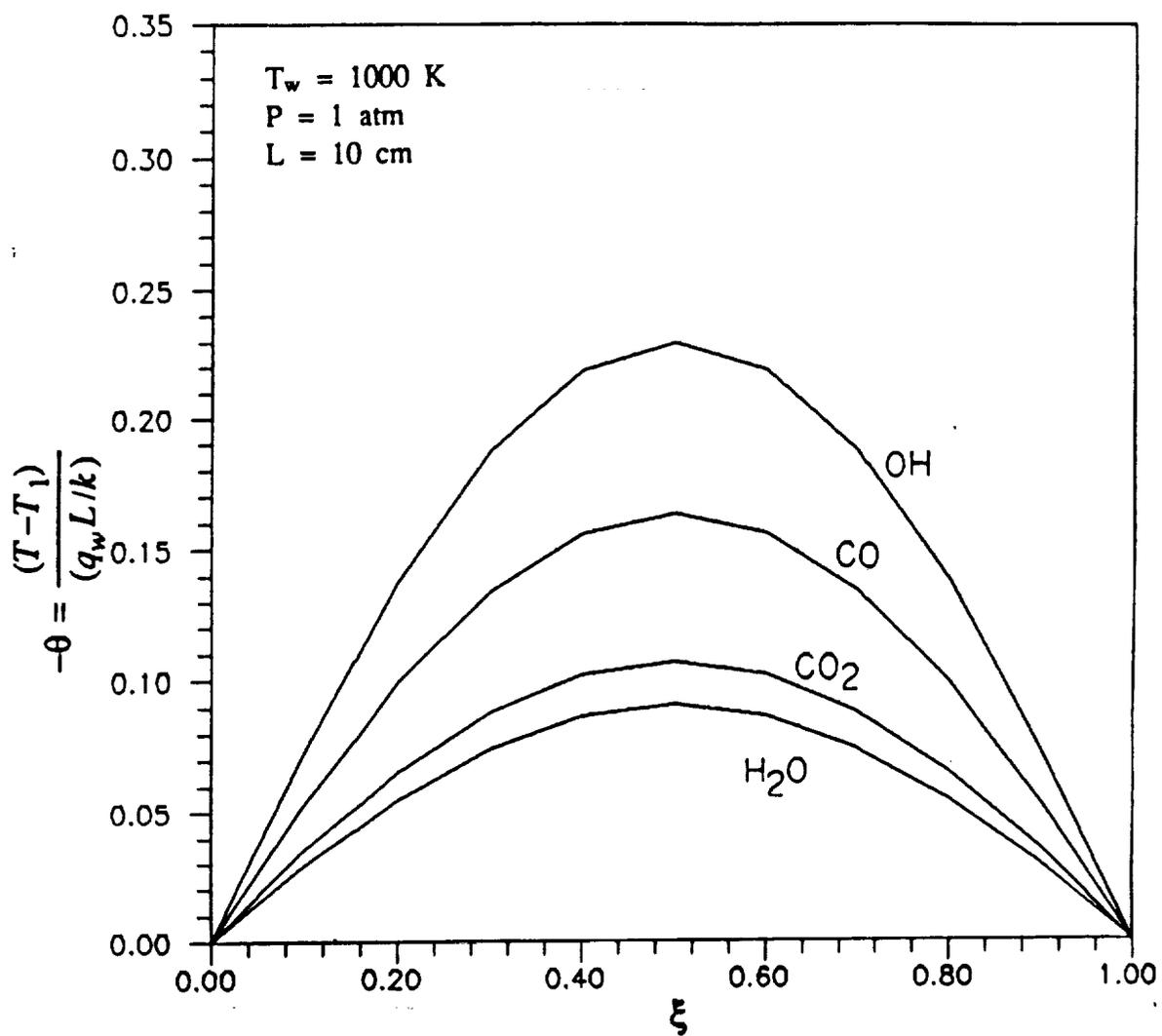
$T_w = 1000$ K and L = 10 cm.

Figure 6.4 Comparison of temperature variations across the duct for various

species; $T_w = 1000$ K, $P = 1$ atm and $L = 10$ cm.
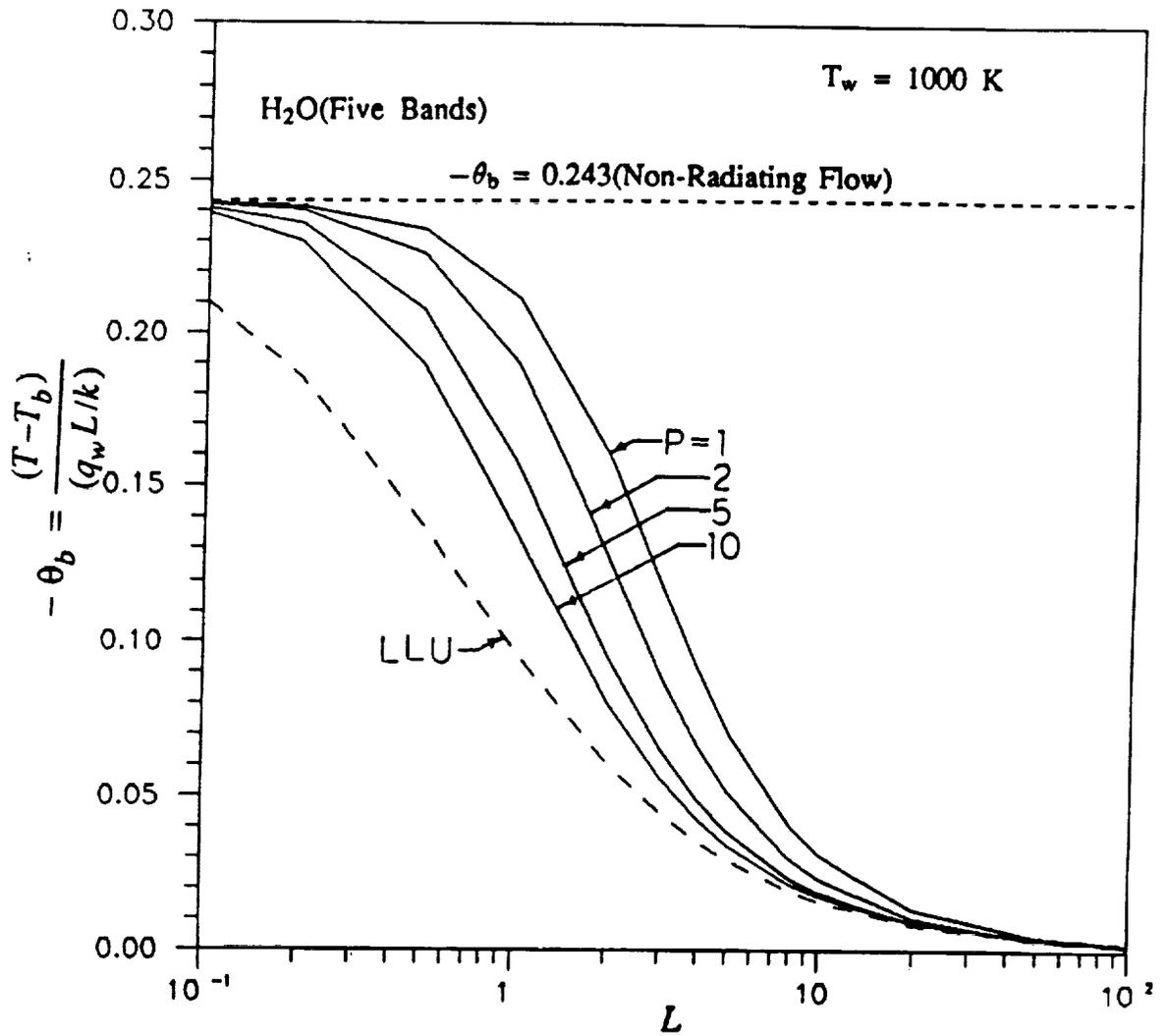
Figure 6.5 Variation of bulk temperature with plate spacing for H_2O;

$T_w = 1000$ K.
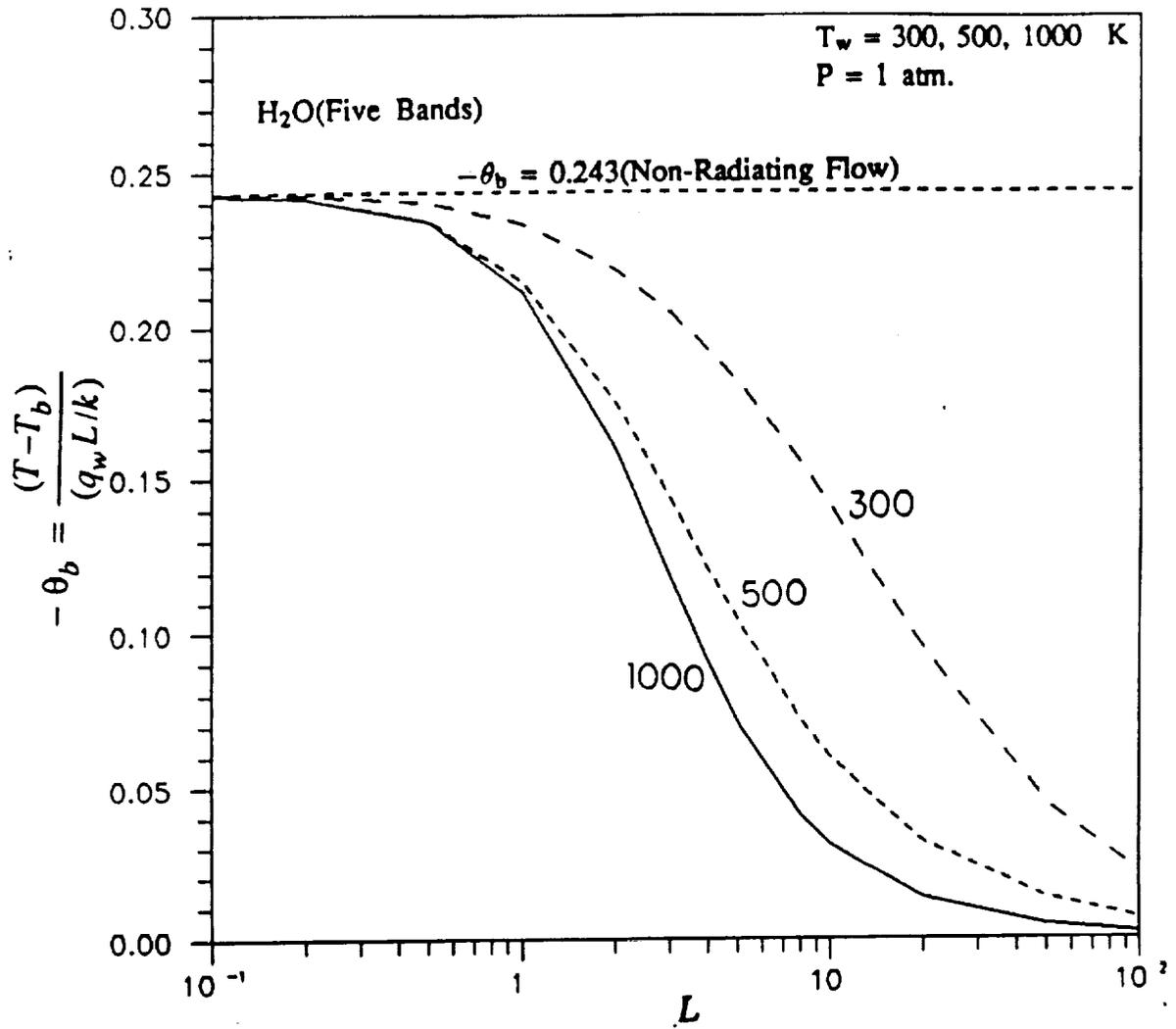
Figure 6.6 Variation of bulk temperature with plate spacing for H_2O;

P = 1 atm.
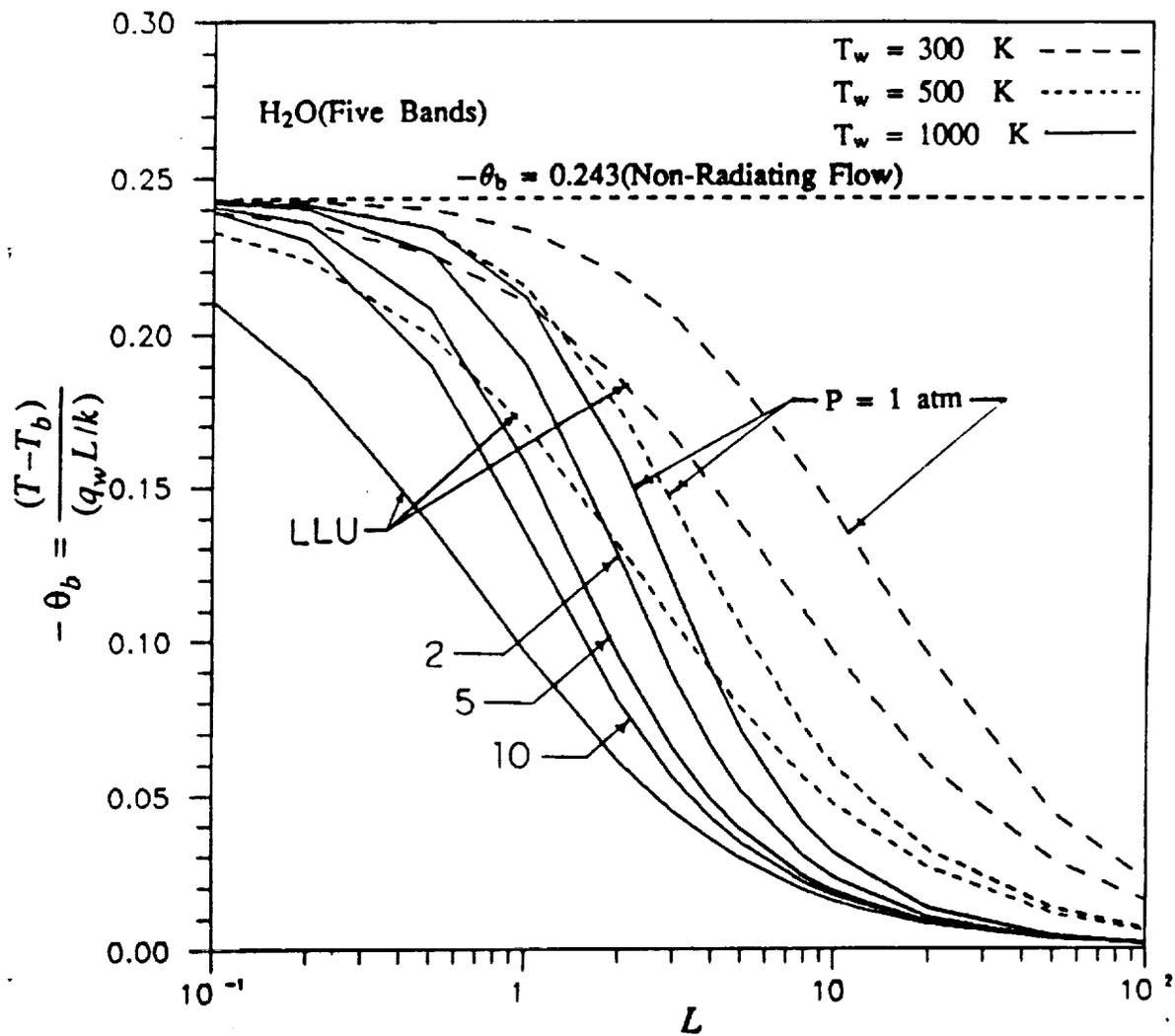
Figure 6.7 Variation of bulk temperature with plate spacing for H_2O.
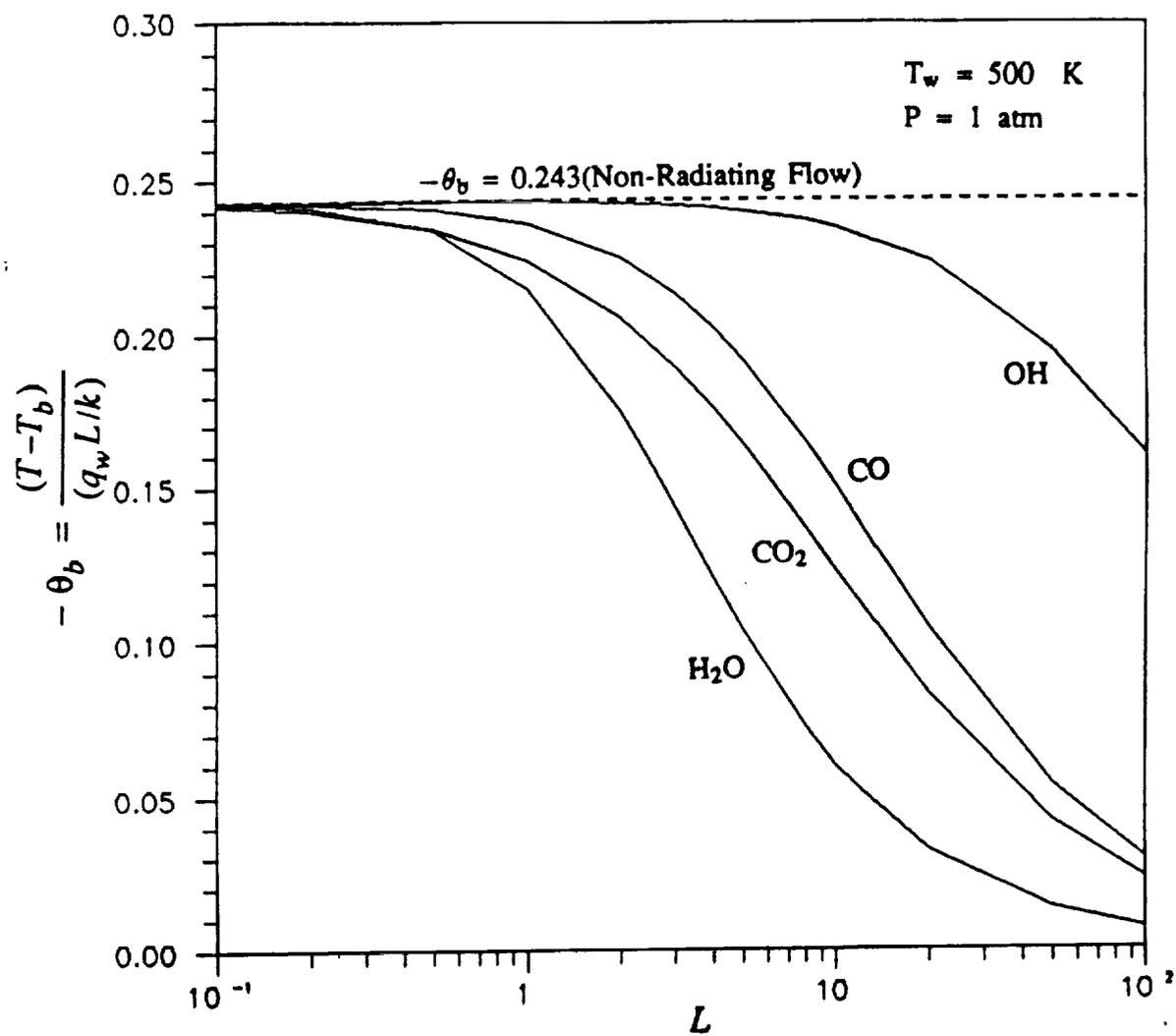
Figure 6.8 Variation of bulk temperature with plate spacing for various species; $T_w = 500$ K and $P = 1$ atm.
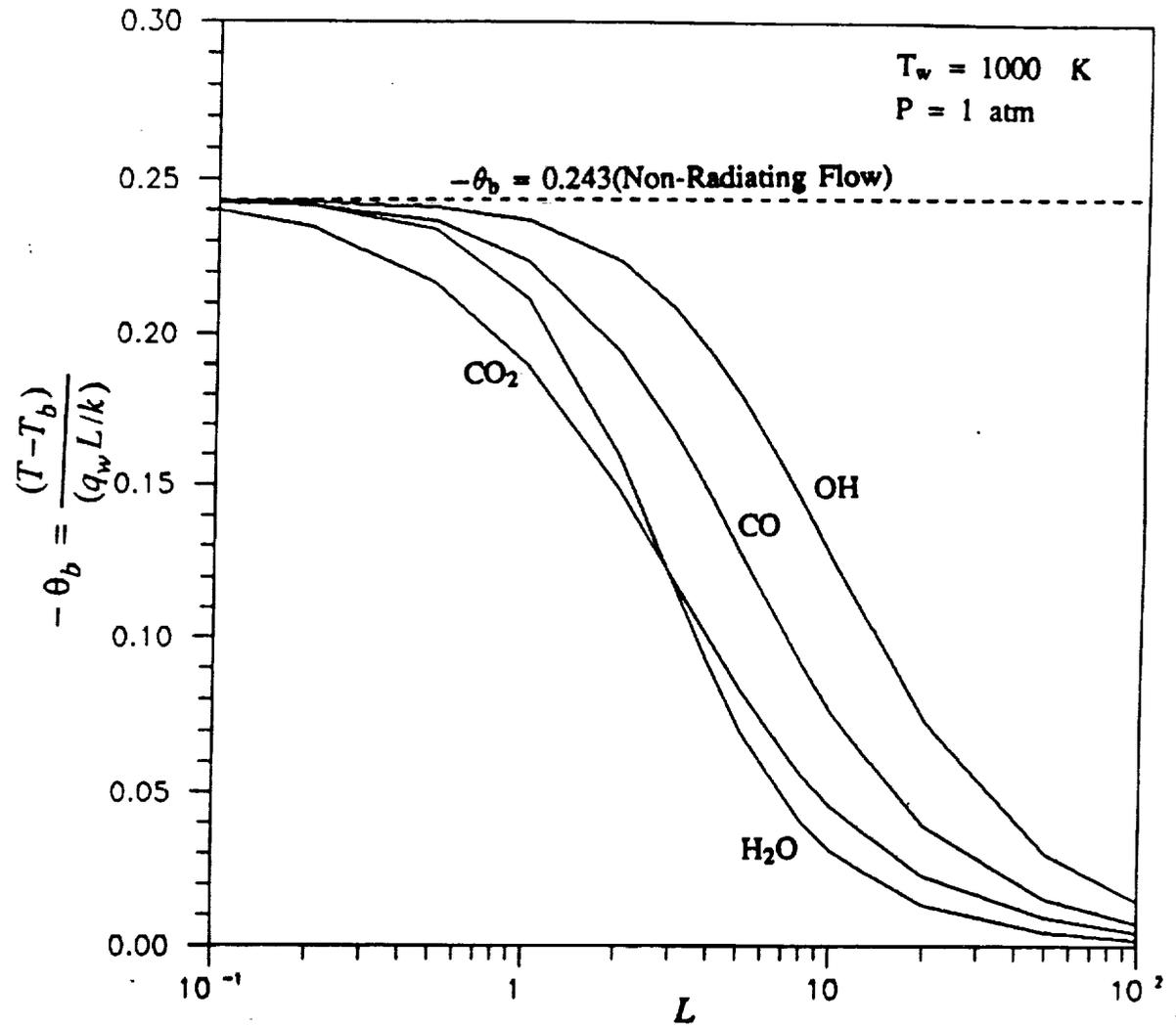
Figure 6.9 Variation of bulk temperature with plate spacing for various

species; T_w = 1000 K and P = 1 atm.
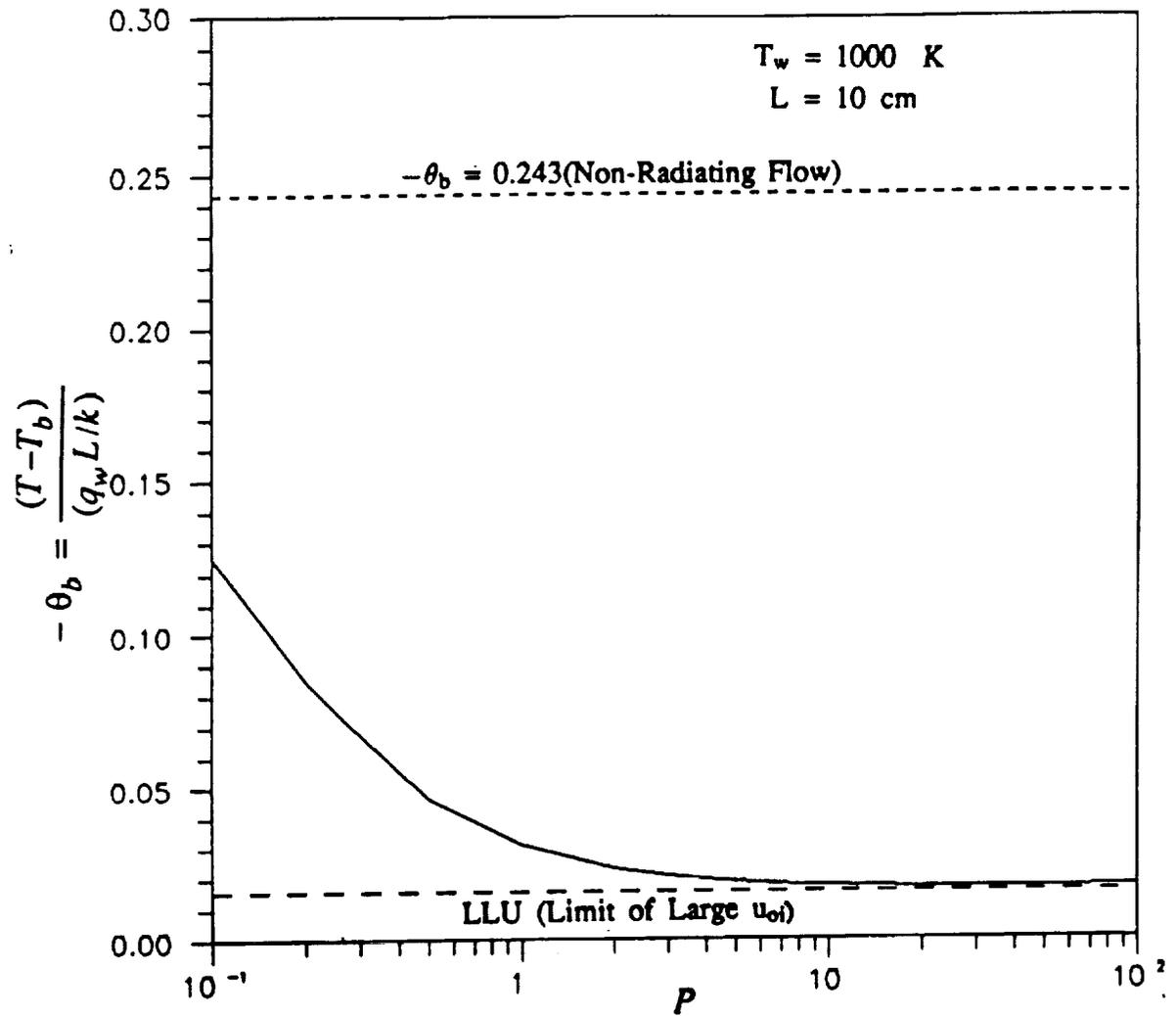
Figure 6.10 Variation of bulk temperature with pressure for H_2O;
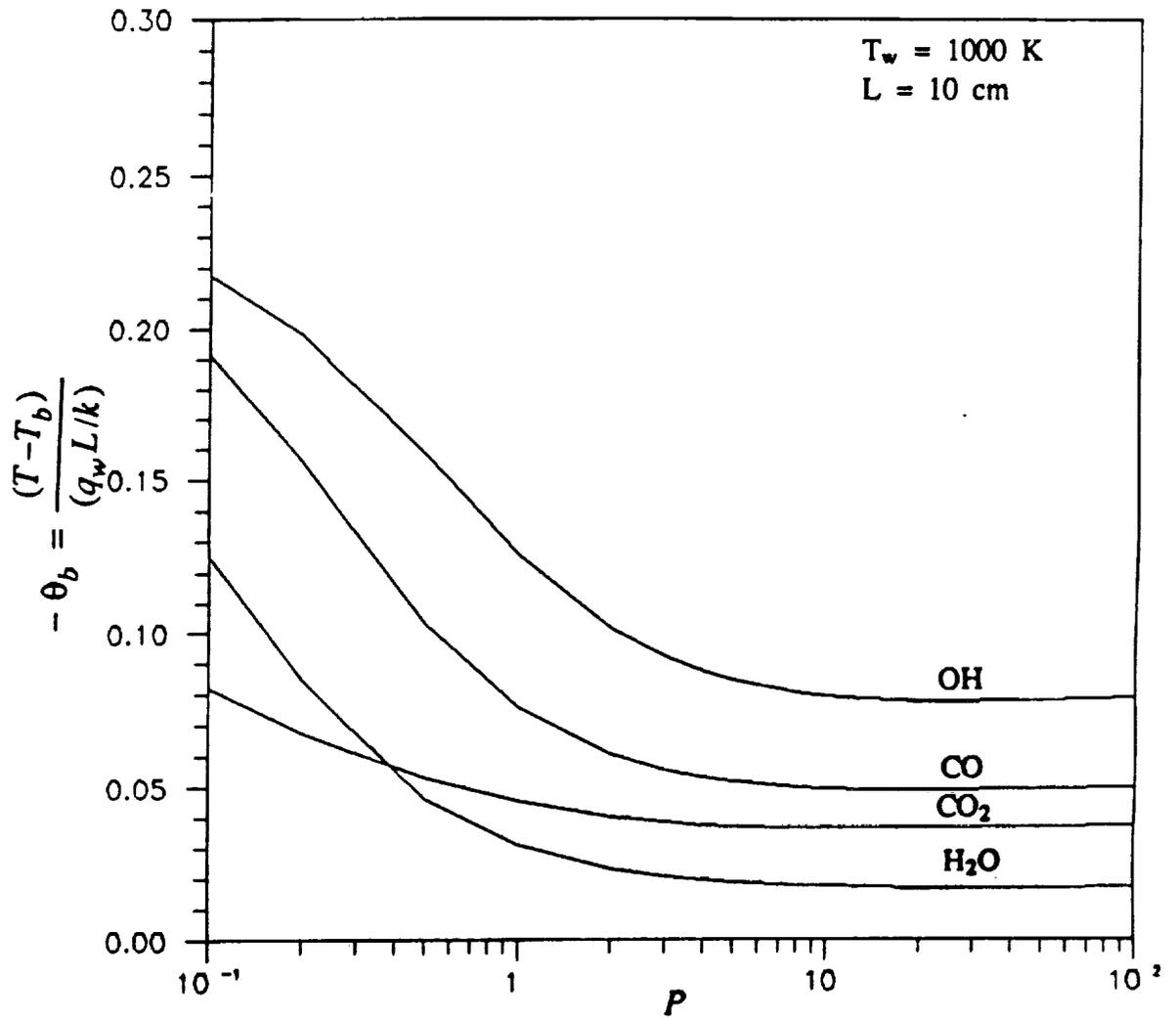
$T_w = 1000$ K and $L = 10$ cm.

Figure 6.11 Variation of bulk temperature with pressure for various species

T_w = 1000 K and L = 10 cm.

6.2 Circular Duct

All results for circular duct are presented in Figs. 6.12–6.22. The results are for the same species at the same conditions as for the parallel plate geometry. The results, in general, exhibit the same trend as presented in Figs. 6.1–6.12 for the parallel plate geometry. However, the extent of radiative interactions is entirely different. This is because the circular geometry provides additional degrees of freedom for radiative interactions[39]. Other basic differences are noted below.

Results of temperature variations across the duct are plotted from $\xi = -1.0$ to 1.0, because of the difference in the location of the coordinate axes as shown in Fig. 4.1. The limiting value of $\theta_b = -0.4583$ corresponds to the case of negligible radiation. Another important point to note is that the general solution approaches the limit of large u_{oi} at lower path lengths than for the parallel plate geometry. Extensive results for circular duct for all species were obtained. Some of these results are included in Appendix C.
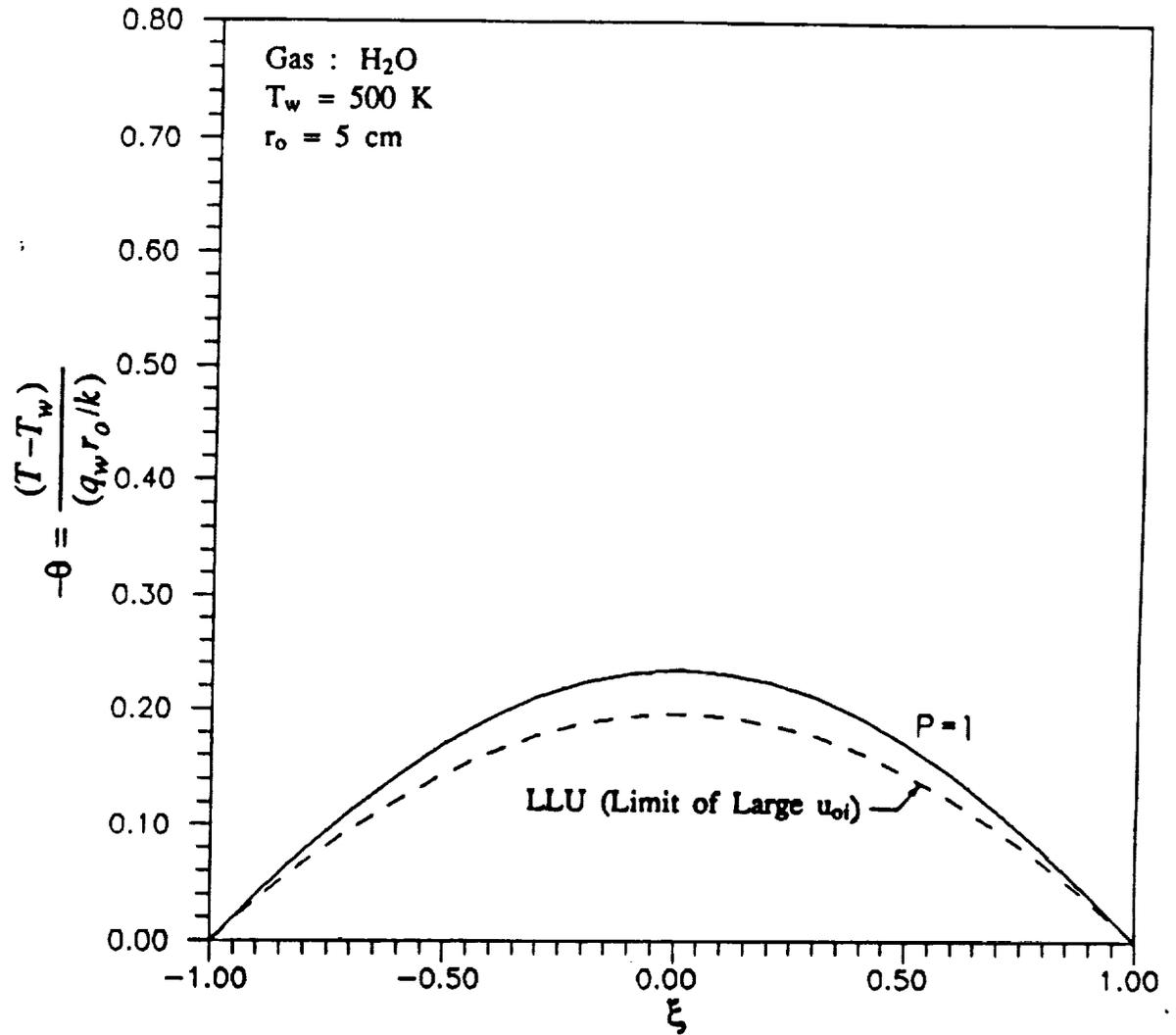
Figure 6.12 Comparison of temperature variations across the duct for H_2O;

$T_w = 500$ K, $P = 1$ atm and $r_o = 5$ cm.
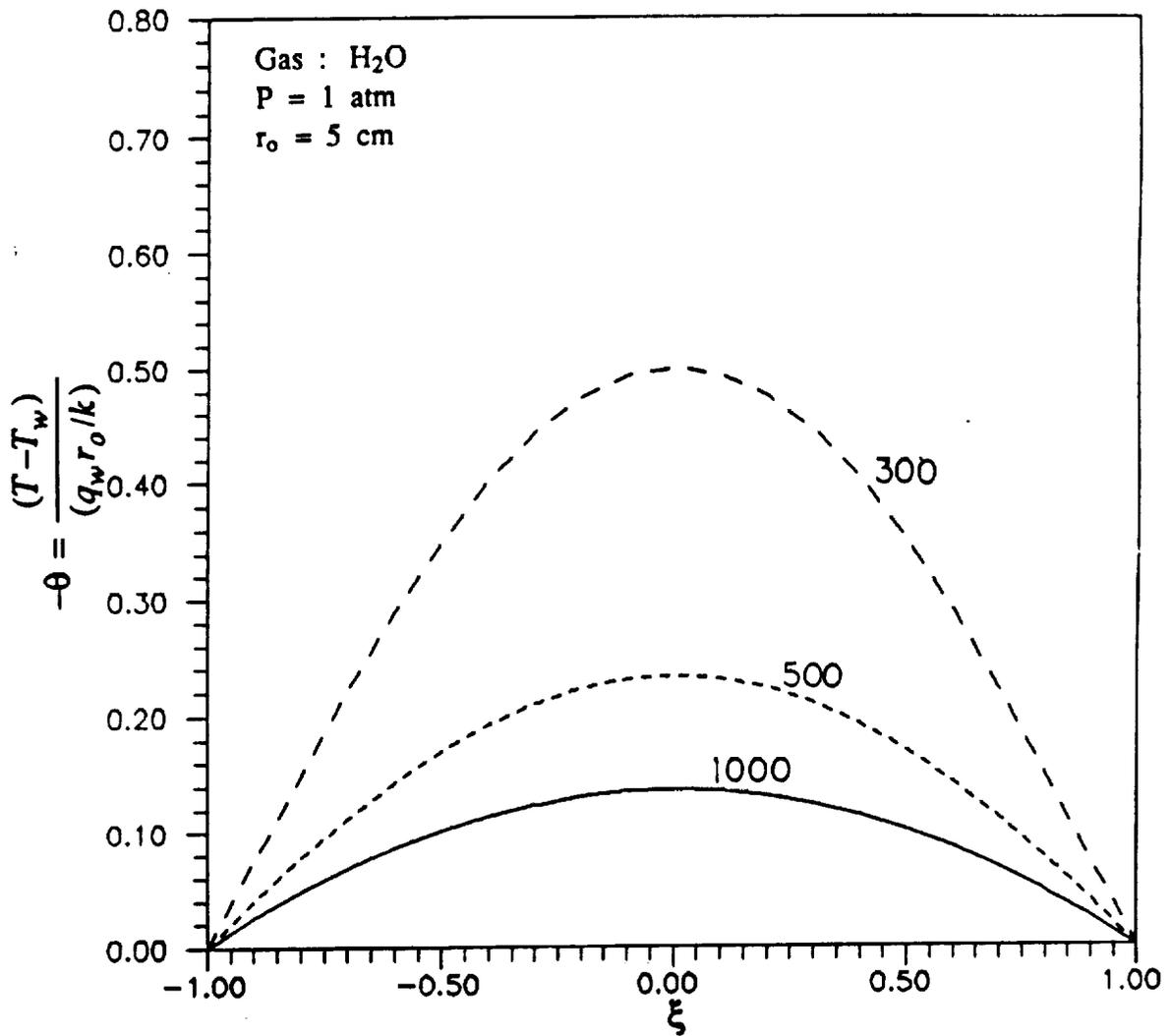
Figure 6.13 Comparison of temperature variations across the duct for H_2O;

$T_w = 300$, 500, 1000 K, $P = 1$ atm and $r_o = 5$ cm.
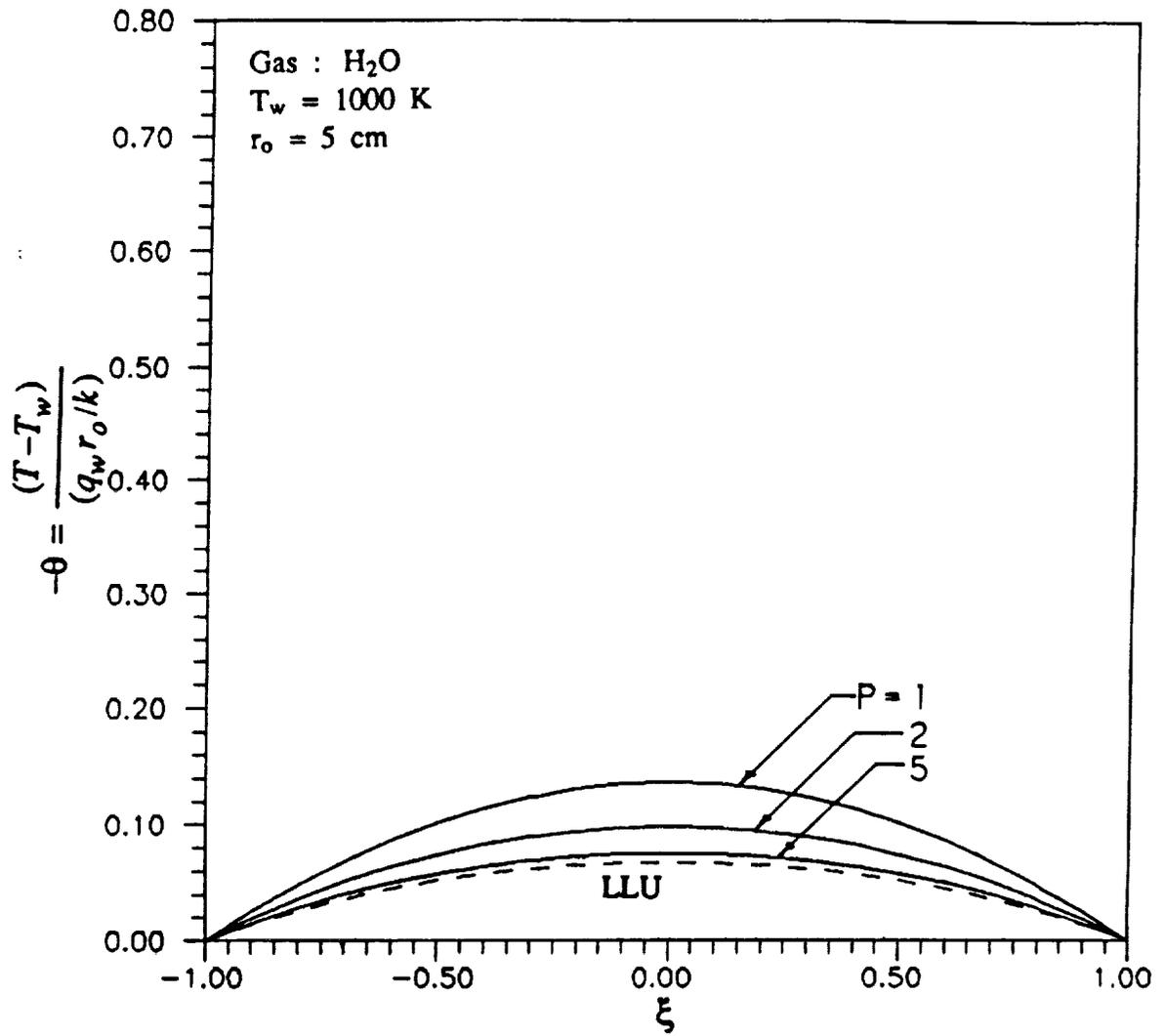
Figure 6.14 Comparison of temperature variations across the duct for H_2O;
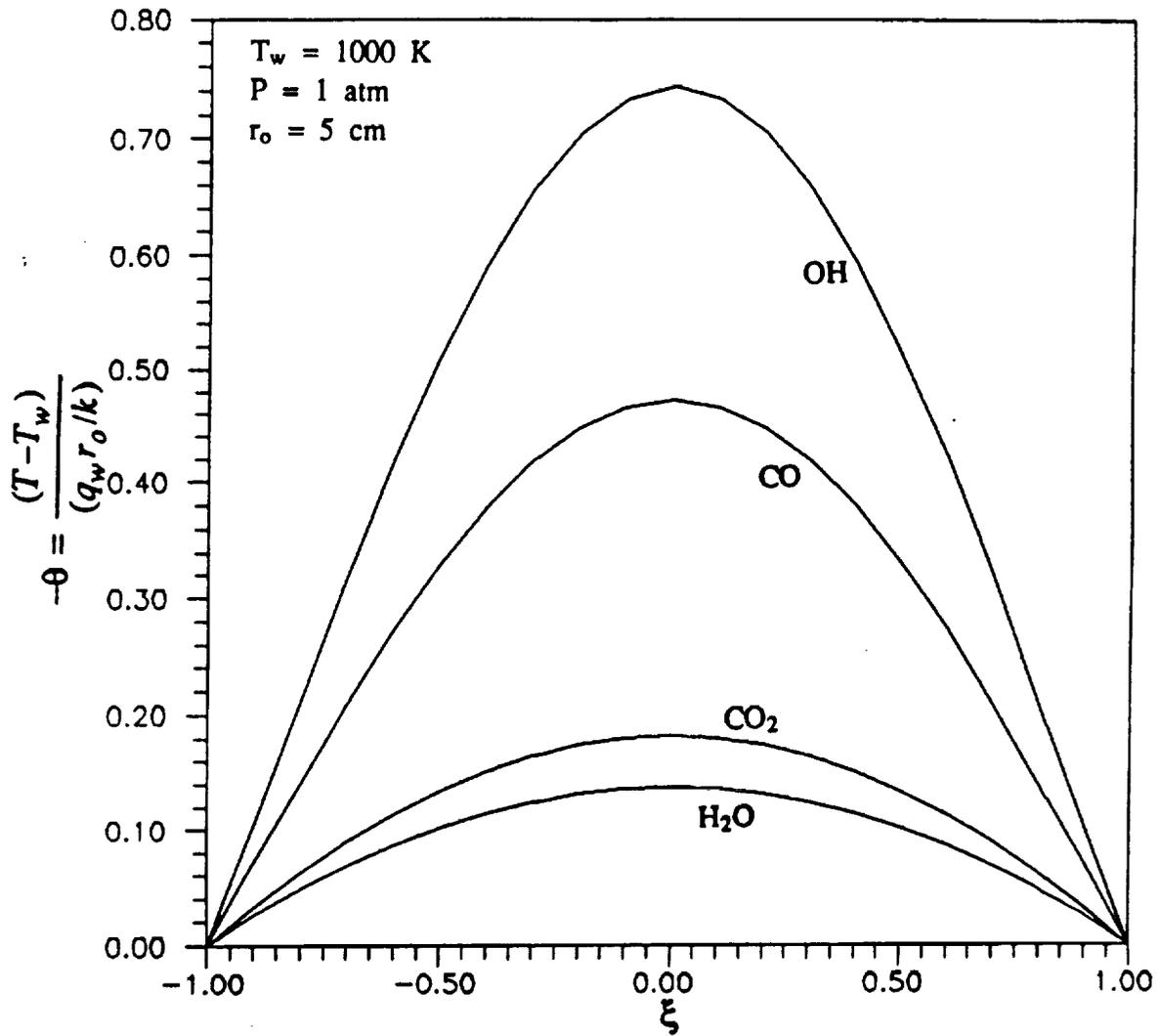
$T_w = 1000$ K and $r_o = 5$ cm.

Figure 6.15 Comparison of temperature variations across the duct for various species; $T_w = 1000$ K, $P = 1$ atm and $r_o = 5$ cm.
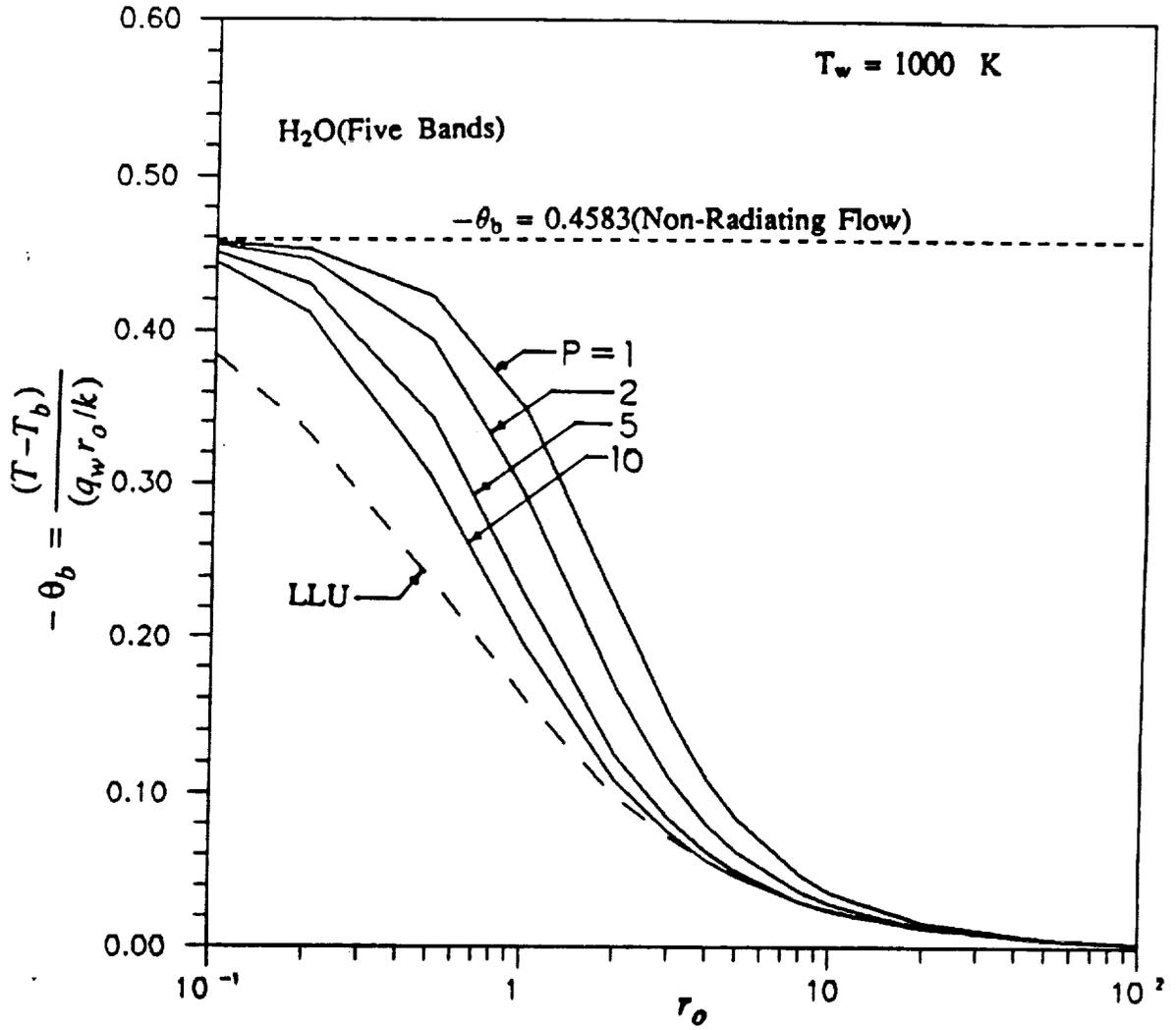
Figure 6.16 Variation of bulk temperature with radius for H_2O;

$T_w = 1000$ K.
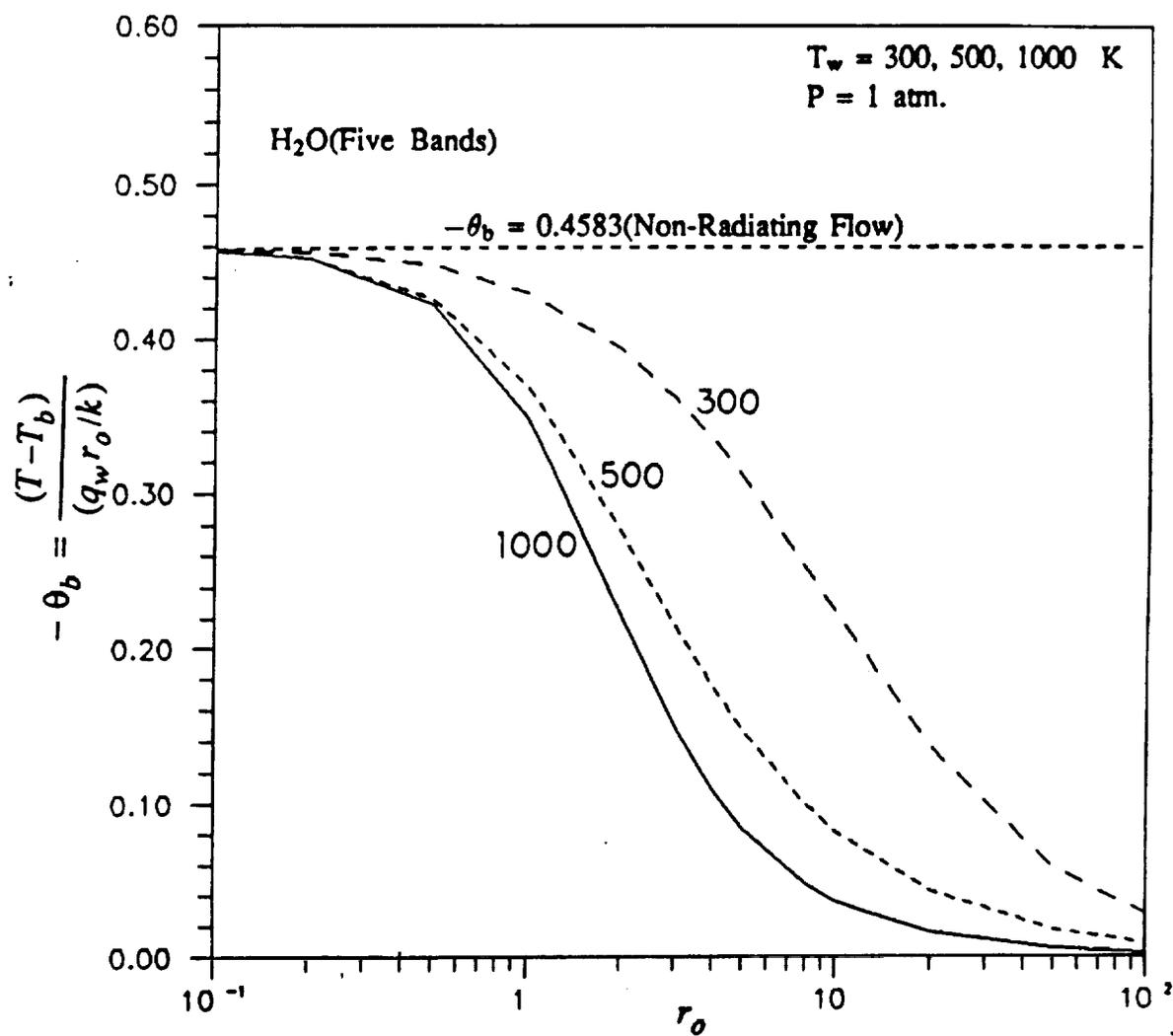
Figure 6.17 Variation of bulk temperature with radius for H_2O;

$P = 1$ atm.
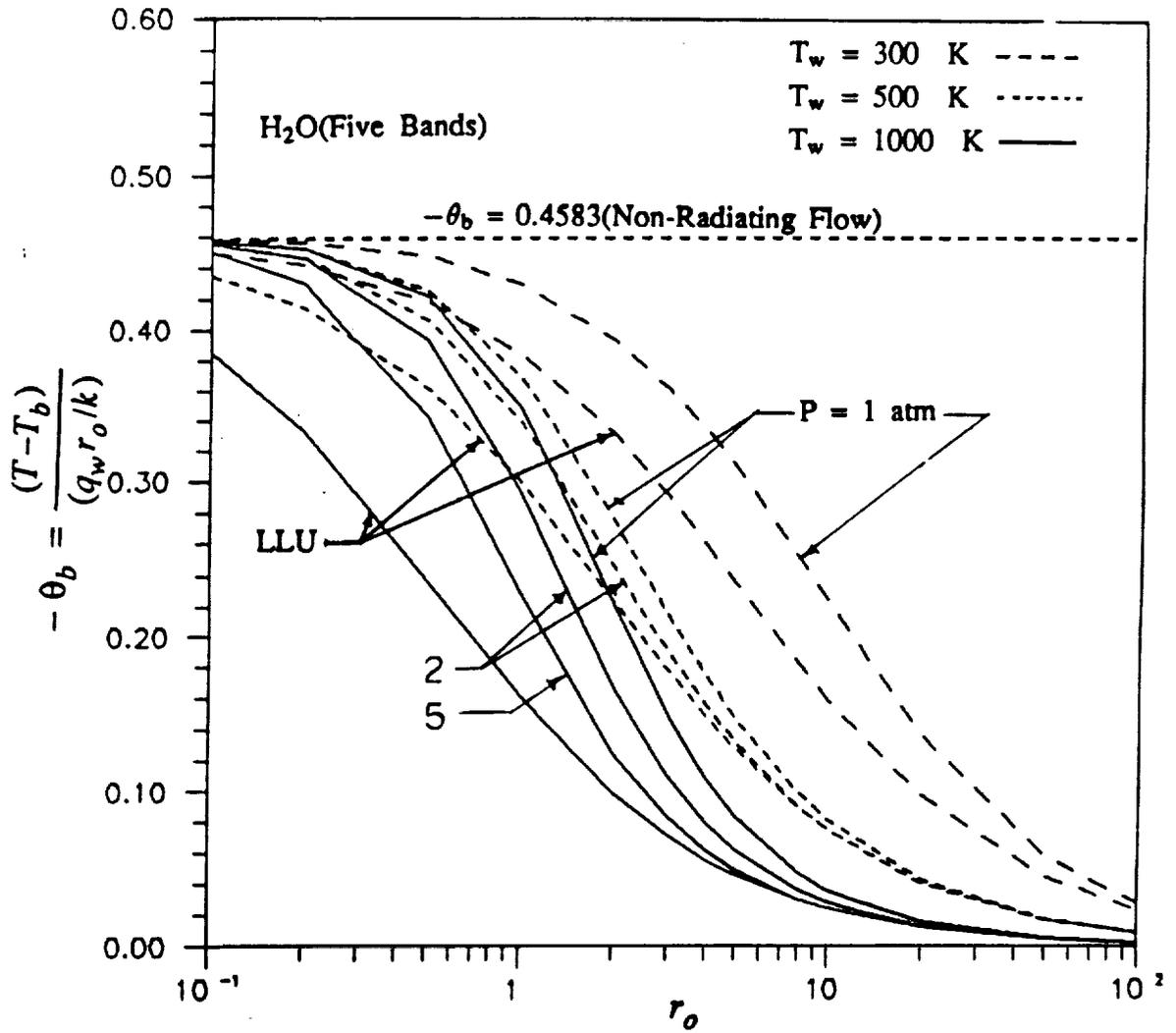
Figure 6.18 Variation of bulk temperature with radius for H_2O.
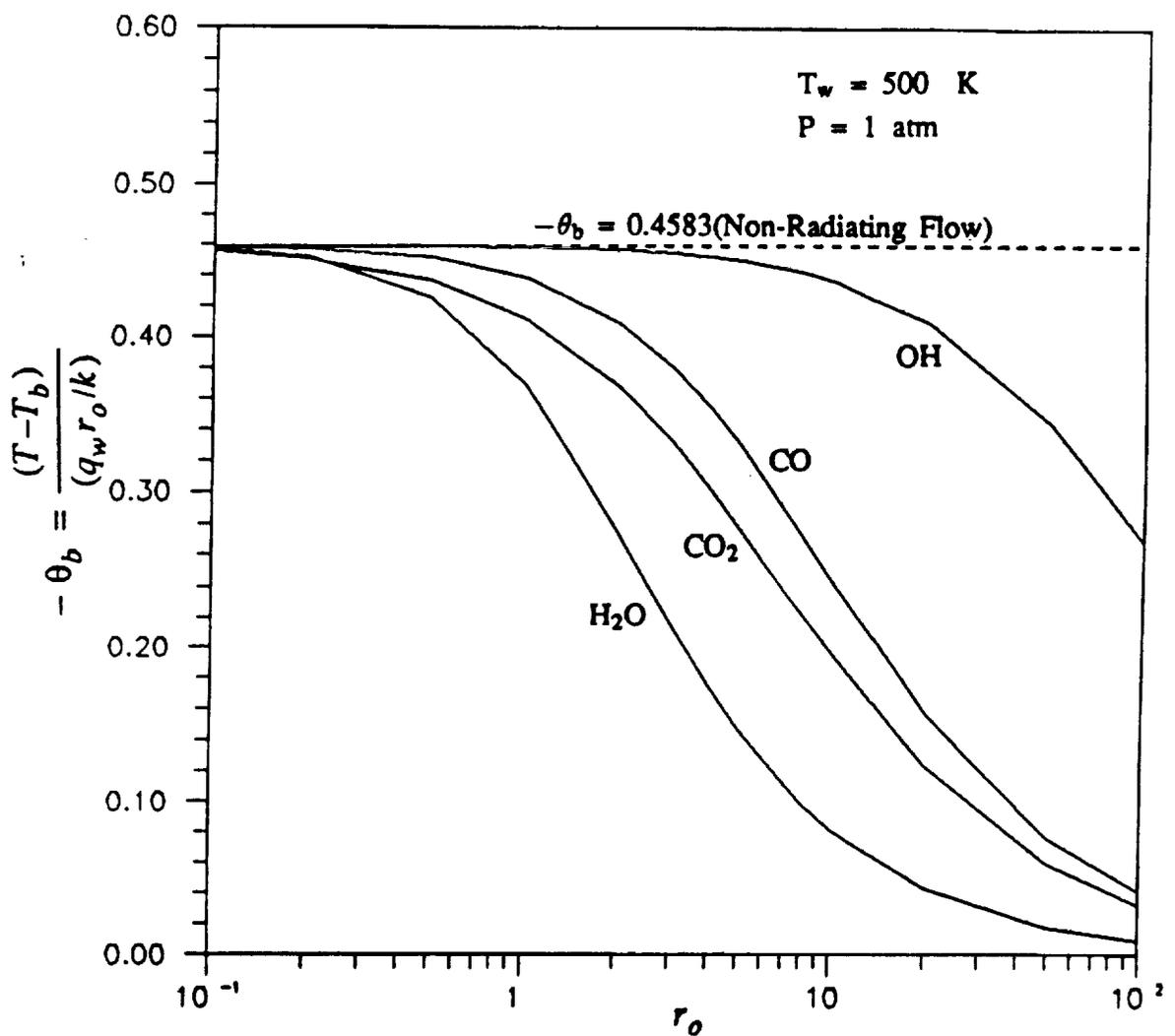
Figure 6.19 Variation of bulk temperature with radius for various species;
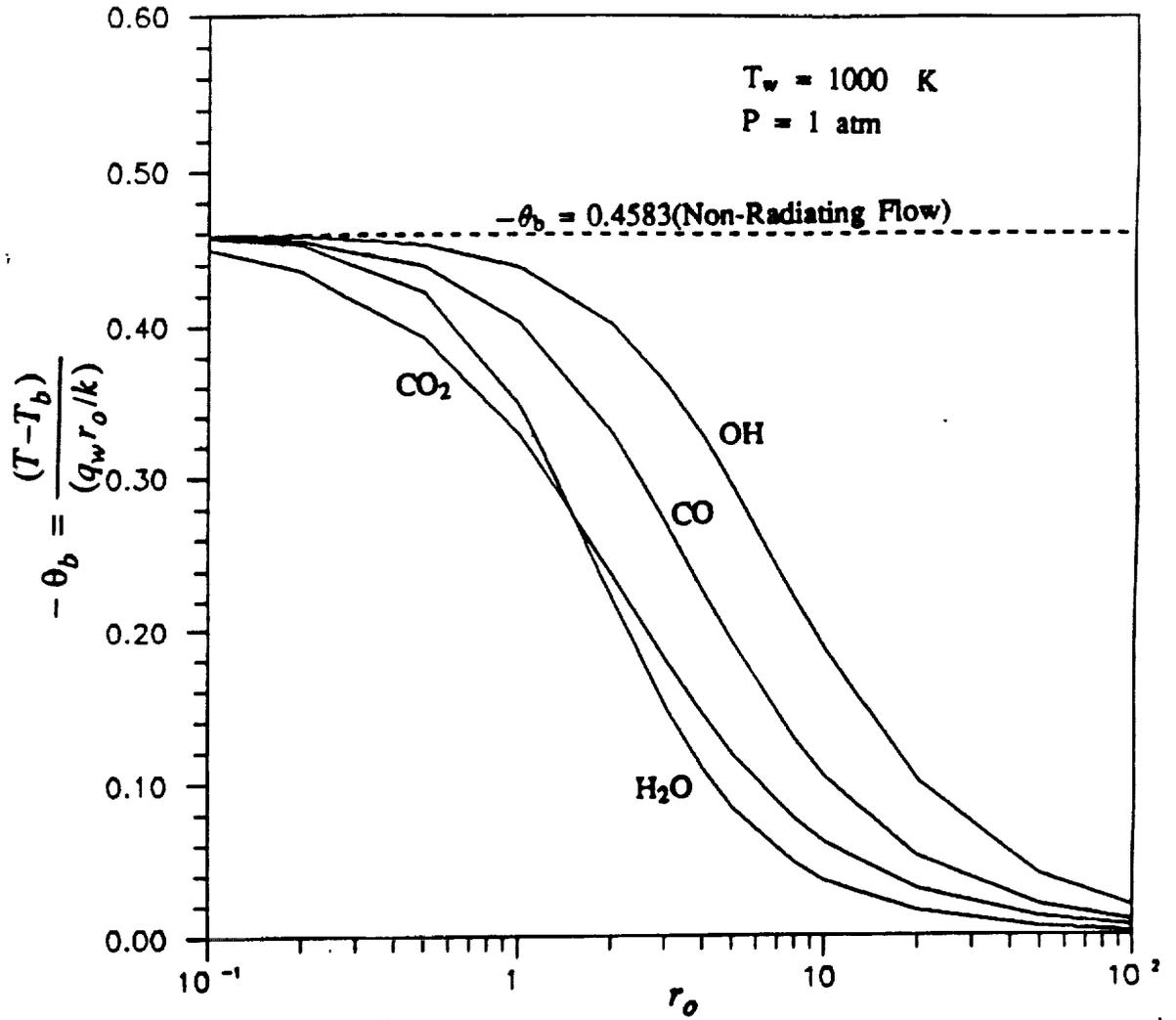
$T_w = 500$ K and P = 1 atm.

Figure 6.20 Variation of bulk temperature with radius for various species;

$T_w = 1000$ K and P = 1 atm.
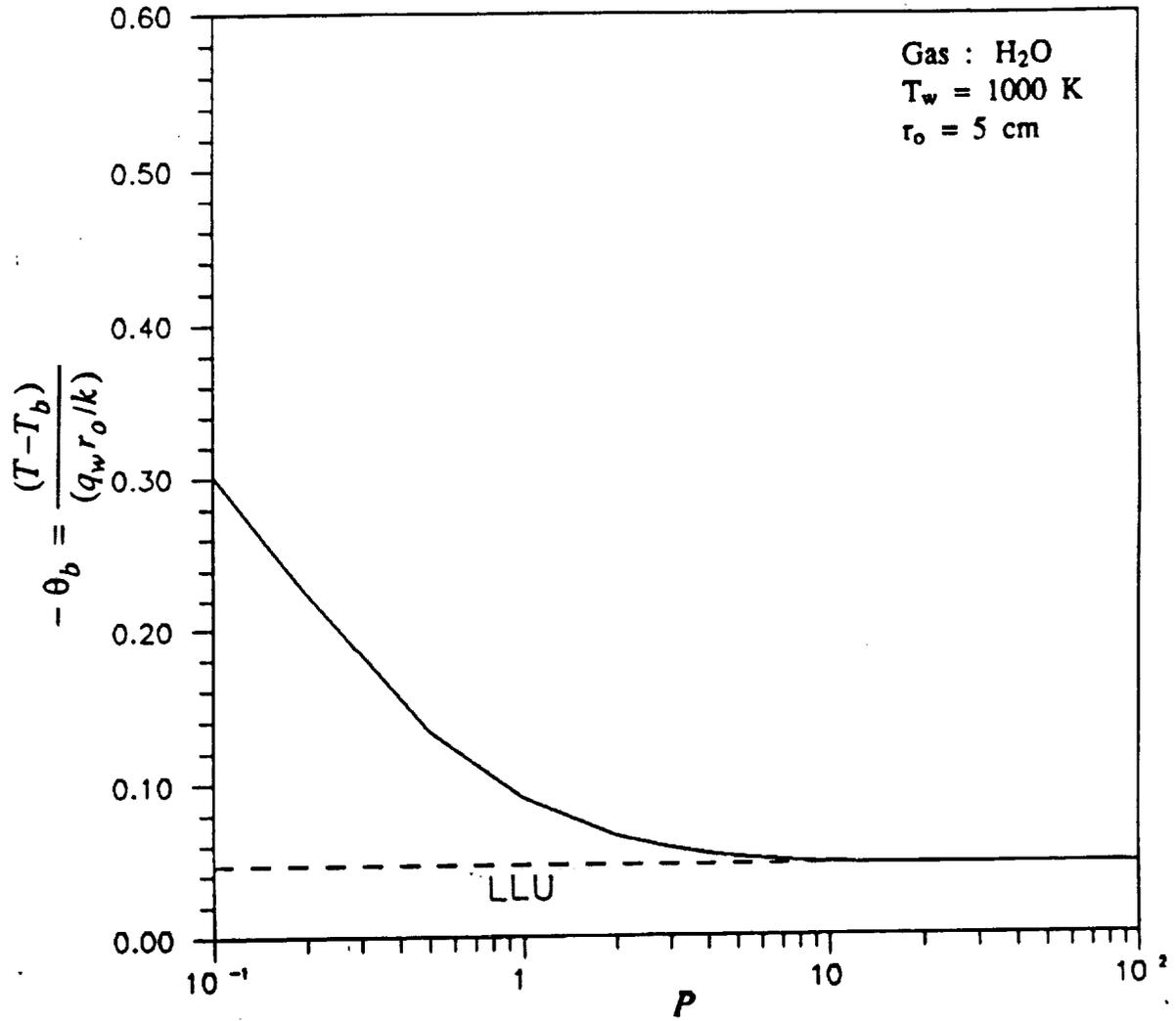
Figure 6.21 Variation of bulk temperature with pressure for H_2O;
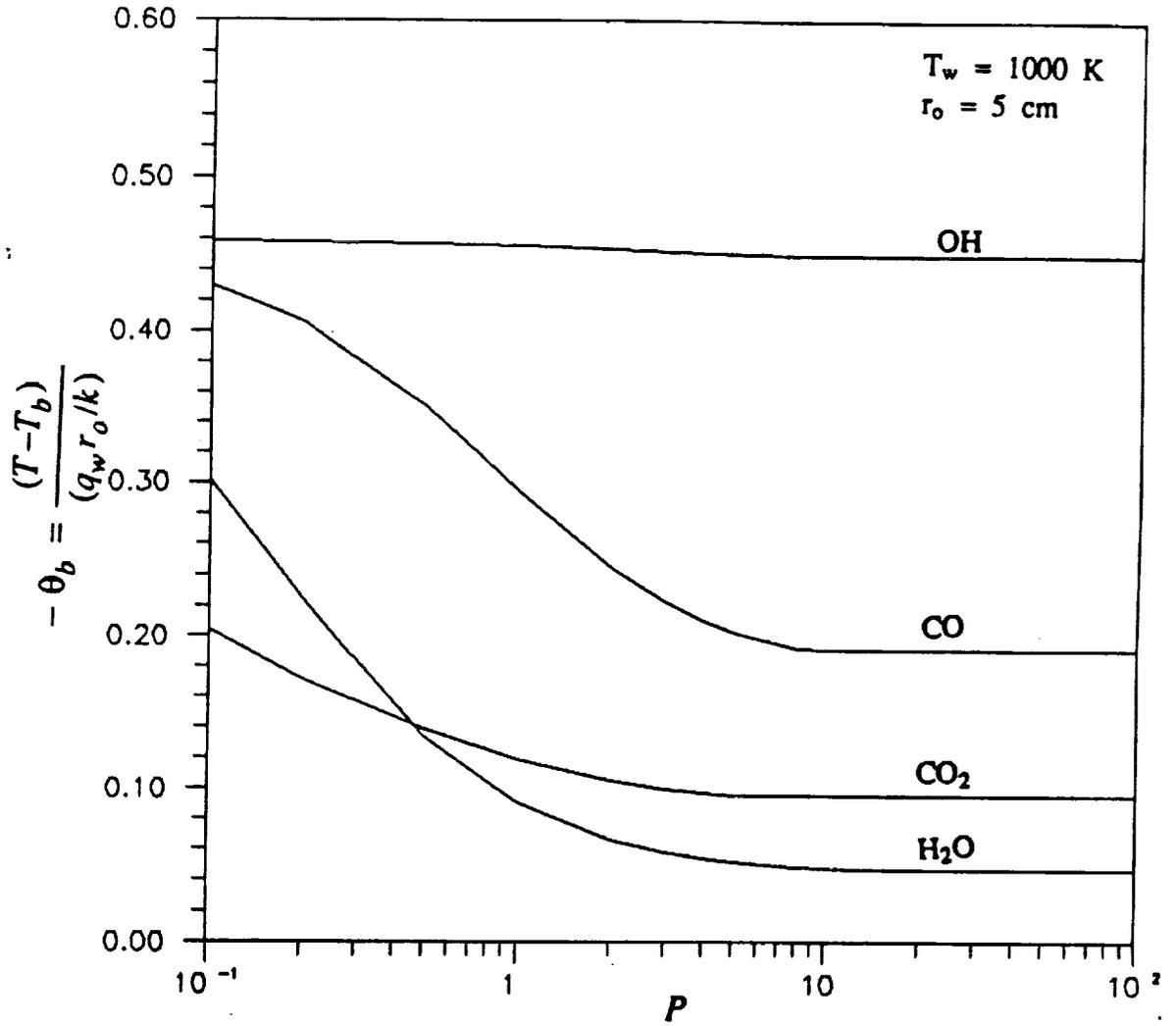
$T_w = 1000$ K and $r_o = 5$ cm.

Figure 6.22 Variation of bulk temperature with pressure for various species;

T_w = 1000 K and r_o = 5 cm.

Chapter 7

SUMMARY AND CONCLUSIONS

A brief review is presented on various band models and band model correlations that are useful in nongray radiative transfer analyses. Different formulations for one-dimensional radiative flux are provided. These are used to develop the basic governing equations for energy transfer in gaseous systems.

Analytical formulations and numerical procedures have been developed to investigate the radiative interaction of absorbing-emitting species in laminar fully developed flows between parallel plates and through a circular duct. Extensive results have been obtained for OH, CO, CO_2, and H_2O for different physical conditions. Illustrative results for the temperature distribution and bulk temperature are presented for different pressures and wall temperatures. The general nongray results for the circular duct have been obtained for the first time. In these results, a lower value of temperature implies a higher ability of the gas to transfer radiative energy.

The gray and nongray formulations for circular duct has been derived in local thermodynamic equilibrium. This formulation involves four integrals of which two are angular, one is spatial, and one is spectral. One angular integral is taken care of by using exponential kernal approximation [27, 32, 37]. Furthermore, the spectral integration for nongray formulation is represented by using a total band absorptance. The remaining two integrals, one angular and one spatial, are computed numerically by multidimensional quadrature method using Gauss-Kronrod rule [41]. The resulting equations are either integral or integro-differential and cannot be solved analytically. They are therefore solved numerically using the method of variation of parameter [1, 35].

67

The results, in general, demonstrate that the effect of radiation increases with increasing plate spacing/radius, and the radiative transfer is more pronounced at higher wall temperature and pressure. One important fact is that, for all species, the general solution approaches the correct limiting solution for large u_{oi}. Of all the species, H_2O is a highly radiation participating species (as compared to CO_2, CO and OH). The extent of radiative interactions is higher in circular duct, because it provides additional degrees of freedom.

The present study provides different kinds of limiting solutions for both the geometries. These limiting solutions are in closed form and therefore computationally less expensive to obtain. In many practical and realistic problems the limiting solutions are very useful to demonstrate the importance of radiative interaction. Finally it is important to note that any kind of extensive radiation model (line-by-line or narrow band model) can be easily used in the nongray formulation provided in this study.

REFERENCES

1. Sparrow, E.M. and Cess, R.D., _Radiantion Heat Transfer_, Brooks/Cole, Belmont, Calif., 1966 and 1970. New Augmented Edition, Hemisphere Publishing Corp., Washington, D.C., 1978.

2. Hottel, H.C. and Sarofim, A.F., _Radiantive Transfer_, McGraw-Hill Book Co., New York, 1967.

3. Siegel, R. and Howell, J.R., _Thermal Radiantion Heat Transfer_, Mcgraw-Hill Book Co., New York, 1971; Second Edition, 1981.

4. Ozisik, M.N., _Radiantive Transfer and Interaction with Conduction and Convection_, John Wiley & Sons, Inc., New York, 1973.

5. Edwards, D.K., _Radiantion Heat Transfer Notes_, Hemisphere Publishing Corporation, Washington, D.C., 1981.

6. Cess, R.D., "The Interaction of Thermal Radiantion with Conduction and Convection Heat Transfer", _Advances in Heat Transfer_, Vol. 1, Academic Press, New York, 1964.

7. Sparrow, E.M., " Radiantion Heat Transfer between Surfaces",_Advances in Heat Transfer_, Vol. 2, Academic Press, New York, 1965.

8. Viskanta, R., " Radiantion Transfer and Interaction of Convection with Radiantion Heat Transfer", _Advances in Heat Transfer_, Vol. 3, Academic Press, New York, 1966.

9. Tien, C.L., "Thermal Radiantion Properties of Gases", _Advances in Heat Transfer_, Vol. 5, Academic Press, New York, 1968.

10. Cess, R.D. and Tiwari, S.N., "Infrared Radiantive Energy Transfer in Gases", _Advances in Heat Transfer_, Vol. 8, Academic Press, New York, 1972.

11. Edwards, D.K., "Molecular Gas Band Radiantion", Advances in Heat Transfer, Vol. 12, Academic Press, New York, 1976.

12. Tiwari, S.N., "Band Models and Correlations for Infrared Radiantion", Radiantive Transfer and Thermal Control (Progress in Astronautics and Aeronautics), Vol. 49, American Institute of Aeronautics and Asrtonautics, New York, 1976.

13. Tiwari, S.N., "Models for Infrared Atmospheric Radiantion", Advances in Geophysics, Vol. 20, Academic Press, New York, 1978.

14. Tiwari, S.N., "Models for Infrared Atmospheric Radiantion", Advances in Geophysics, Vol. 20, Academic Press, New York, 1978.

15. Plass, G.N., "Models for Spectral Band Absorption", Journal of the Optical Society of America, Vol. 8, No. 10, October 1958, pp. 690–703.

16. Plass, G.N., "Useful Representation for Measurments of Spectral Band Absorption", Journal of the Optical Society of America, Vol. 50, No. 9, September 1960, pp. 868–875.

17. Wyatt, P.J., Stull, V.R., and Plass, G.N., "Quasi-Random Model of Band Absorption", Journal of the Optical Society of America, Vol. 52, No. 11, November 1962, pp. 1209–1217.

18. Edwards, D.K. and Menard, W.A., "Comparison of Methods for Correlation of Total Band Absorption", Applied Optics, Vol. 3, No. 5, May 1964, pp. 621–625.

19. Edwards, D.K., Glassen, L.K., Hauser, W.C., and Tucher, J.S., " Radiation Heat Transfer in Nonisothermal Nongray Gases", Journal of Heat Transfer, Vol. 89C, No. 3, 1967, pp. 219–229.

20. Edwards, D.K. and Balakrishnan, A., "Slab Band Absorptance for Molecular Gas Radiantion", Journal of the Quantitative Spectroscopy and Radiative Transfer, Vol. 12, 1972, pp. 1379–1387.

21. Edwards, D.K. and Balakrishnan, A., "Thermal Radiantion by Combustion Gases", <u>International Journal of Heat and mass Transfer</u>, Vol. 17, No. 1, January 1974, pp. 155–158.

22. Goody, R.M. and Belton, M.J.S., " Radiantive Relaxation Times for Mars(A Discussion of Martian Atmospheric Dynamics)", <u>Planetary and Space Science</u>, Vol. 1r, No. 2, 1967, pp. 247–256.

23. Tien, C.L. and Ling, G.R., "On a Simple Correlation for Total Band Absorptance of Radianting Gases", <u>International Journal of Heat and mass Transfer</u>, Vol. 12, No. 9, September 1969, pp. 1179–1181.

24. Tiwari, S.N., "Applications of Infrared Band Model Correlations to Nongray Radiantion", <u>International Journal of Heat and mass Transfer</u>, Vol. 20, No. 7, July 1977, pp. 741–751.

25. Ussikin, C. and Sparrow, E.M., "Thermal Radiantion Between Parallel Plates Separated by an Absorbing-Emitting Non-Isothermal Gas", <u>International Journal of Heat and mass Transfer</u>, Vol. 1, 1960, pp. 28–36.

26. Sparrow, E.M., Ussikin, C.M., and Hubbard, H.A., " Radiantion Heat Transfer in a spherical Enclosure Containing a Participating, Heat-Generating Gas", <u>Journal of Heat Transfer</u>, Vol. 82 C, 1961, pp. 197–206.

27. Viskanta, R., "Interaction of Heat Transfer by Conduction, Convection, and Radiantion in Radianting Fluids", <u>Journal of Heat Transfer</u>, Vol. 85 C, 1963, pp. 318–328.

28. Cess, R.D. and Tiwari, S.N., "Heat Transfer to Laminar Flow of an Absorbing-Emitting Gas between Parallel Plates", <u>Heat and Mass Transfer-USSR</u>, Vol. 1, May 1968, pp. 229–283.

29. Tiwari, S.N., " Radiantive Interaction in Transient Energy Transfer in Gaseous System", Dept. of Mechanical Engineering and Mechanics, Old Dominion University, Norfolk, Virginia, Progress Report NAG-1–423, December 1985; also NASA-CR-176644 NAS 1.26:176644, December 1985.

30. Tiwari, S.N. and Singh, D.J., "Interaction of Transient Radiantion in Fully Developed Laminar Flows", AIAA Paper 87–1521, June 1987; also in Applied Scientific Research, December 1989.

31. Einstein, T.H., "Radiant Heat Transfer in Absorbing Gases enclosed in a Circular Pipe with Conduction, Gas Flow and Internal Heat Generation", NASA TR R-156, 1963.

32. Nichols, L.D., " Temperature Profile in the Entrance Region of an Annular Passage Considering the Effects of Turbulent Convection and Radiantion", International Journal of Heat and mass Transfer, Vol. 8, 1965, pp. 589–607.

33. deSoto, S. and Edwards, D.K., " Radiantive Emission and Absorption in Nonisothermal Nongray Gases in Tubes", Proceedings 1965 Heat Transfer and Fluid Mechanics Institute, Stanford University Press, Stanford, Calif., 1965, pp. 358–372.

34. deSoto, S., "Coupled Radiantion, Conduction and Convection in Entrance Region Flow", International Journal of Heat and mass Transfer, Vol. 11, 1968, pp. 39–53.

35. Pearce, B.E. and Emery, A.F., "Heat Transfer by Thermal Radiantion and Laminar Forced Convection to an Absorbing Fluid in the Entry Region of a Pipe", Journal of Heat Transfer, Vol. 92, 1970, pp. 221–230

APPENDICES

APPENDIX A

DERIVATION OF CONSTANTS FOR CIRCULAR DUCT

To determine constants in Eq.(5.6), Eq.(5.8) is evaluated at any two convinient ξ locations. To avoid excessive writing, the following notations are used

$$b_i = bu_{oi}$$

$$c_i = \frac{1}{b_i} = \frac{1}{bu_{oi}} \tag{A.1}$$

where

$$b = \tfrac{5}{4}$$

Rewriting governing Equation for circular duct using the quantities defined in (A.1)

$$\frac{d\theta}{d\xi} + \xi^3 - 2\xi = \frac{4r_o}{\pi k} \sum_{i=1}^{n} H_i u_{oi} \int_0^{\frac{\pi}{2}} \Bigg\{$$

$$\int_{\xi \sin\gamma}^{\xi} \theta(\xi') \, \bar{A}_i' \left[\frac{b_i}{\cos\gamma} (\xi - \xi') \right] d\xi'$$

$$- \int_{\xi}^{1} \theta(\xi') \, \bar{A}_i' \left[\frac{b_i}{\cos\gamma} (\xi' - \xi) \right] d\xi'$$

$$+ \int_{\xi \sin\gamma}^{1} \theta(\xi') \, \bar{A}_i' \left[\frac{b_i}{\cos\gamma} (\xi + \xi' - 2\xi \sin\gamma) \right] d\xi' \Bigg\} \, d\gamma \tag{A.2}$$

Assuming solution of the form (A quartic solution in ξ)

$$\theta(\xi) = A_1 (\xi^2 - 1) + A_2 (\xi^4 - 1)$$

$$\theta'(\xi) = 2A_1\xi + 4A_2\xi^3 \tag{A.3}$$

74

By defining $u = \frac{b_i}{\cos \gamma} (\xi - \xi')$ for the first and the fourth integrals, $u = \frac{b_i}{\cos \gamma} (\xi' - \xi)$ for the second and the fifth integrals, and $u = \frac{b_i}{\cos \gamma} (\xi + \xi' - 2\xi \sin \gamma)$ for the third and the sixth integrals in Eq.(A.4) and changing the limits respectively. And substituting for $\theta\left(\xi\right)$ from (A.3) into Eq.(A.2) and rearranging, equation in terms of changed variables is obtained. The integrals with the changed variables are solved individually and then added up as defined in Eqs. (5.9) and (5.10). The procedure adopted to evaluate constants a_1 and a_2 is similar to one applied in Ref. 39.

APPENDIX B

ADDITIONAL RESULTS FOR LAMINAR FLOW OF NONGRAY
GAS THROUGH PARALLEL PLATE PLATE GEOMETRY

Extensive results obtained for laminar flow of nongray gas between two parallel black plates are presented here for reference purposes. The results are for species CO, OH, CO_2. Results for temprature variations across the duct as well as variation of bulk temprature with plate spacing and pressure are presented. All the results show similar trend as discussed for Figs. 6.1–6.12.
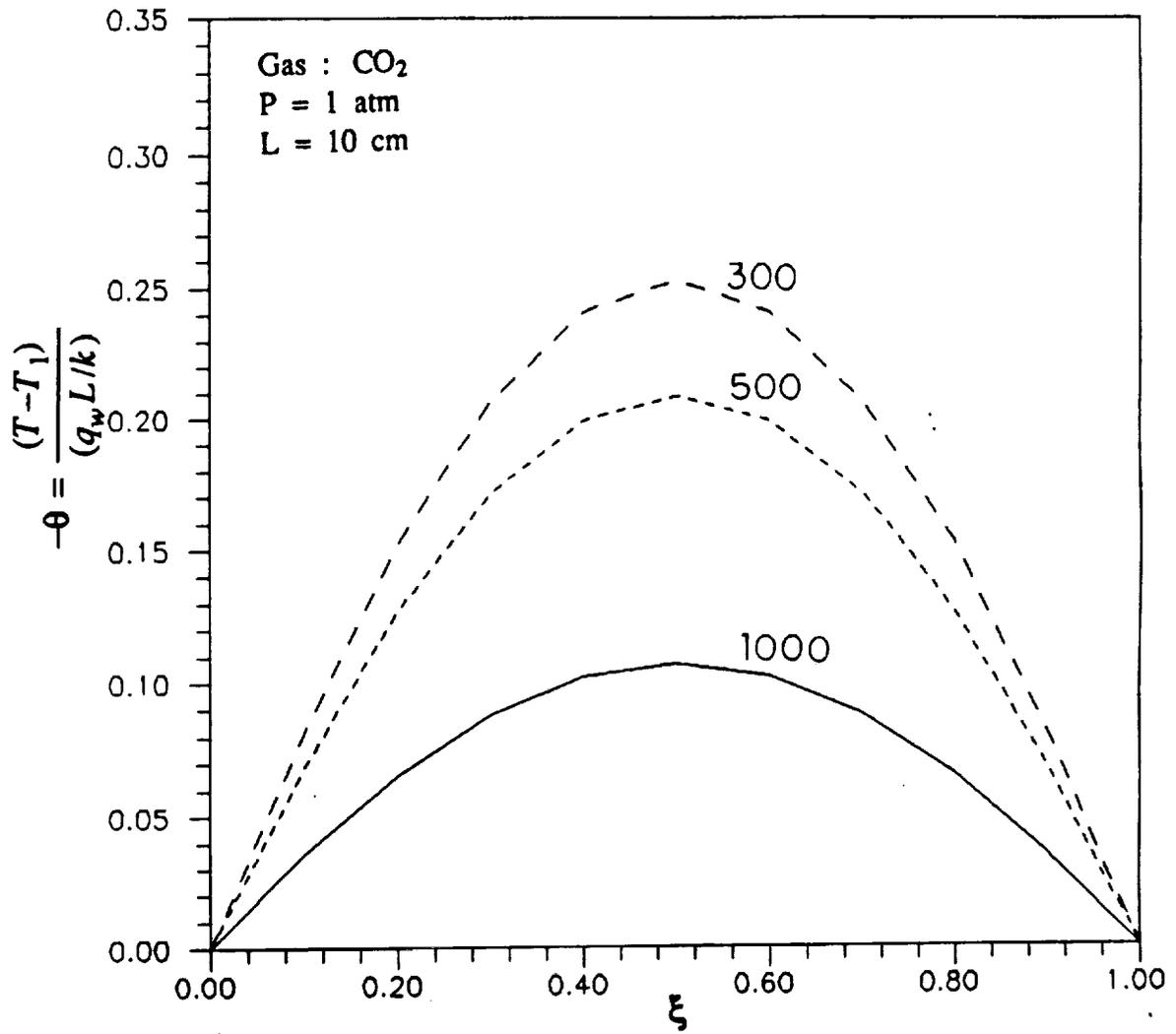
Figure B.1 Comparison of temperature variation across the duct for CO_2;

$T_w = 300, 500, 1000$ K, $P = 1$ atm and $L = 10$ cm.
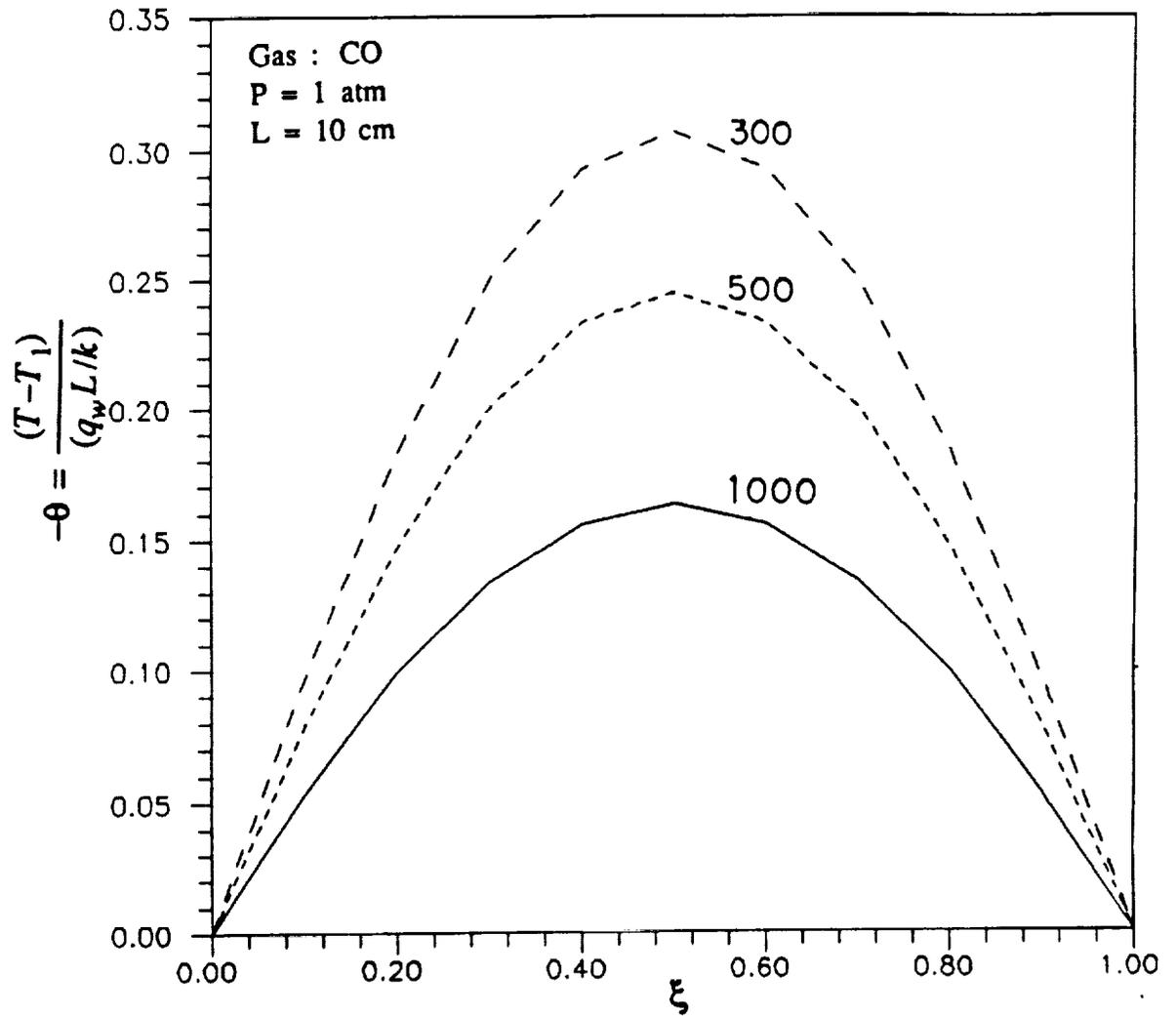
Figure B.2 Comparison of temperature variation across the duct for CO;

$T_w = 300,\ 500,\ 1000\ K,\ P = 1\ atm\ and\ L = 10\ cm.$
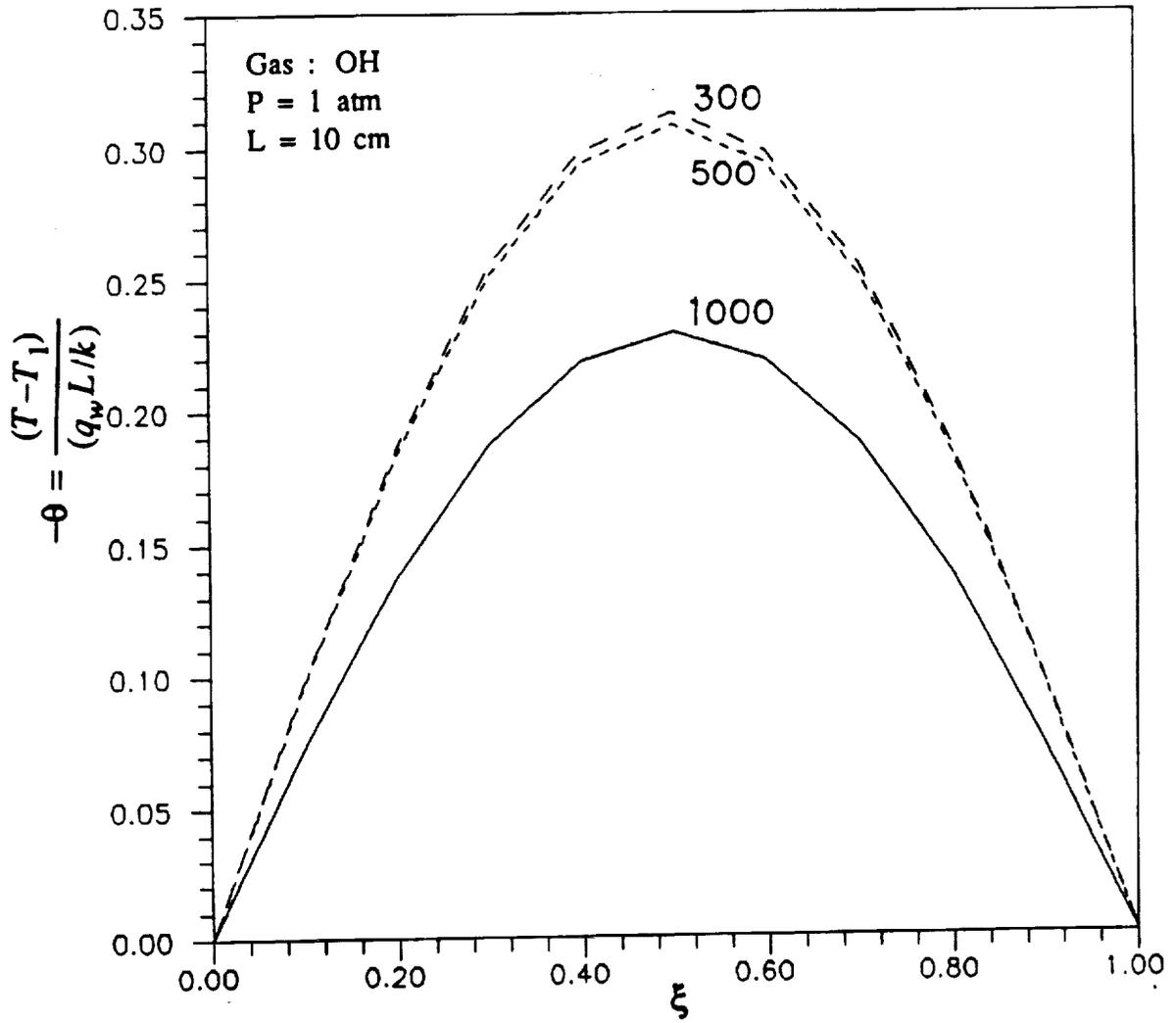
Figure B.3 Comparison of temperature variation across the duct for OH;

T_w = 300, 500, 1000 K, P = 1 atm and L = 10 cm.
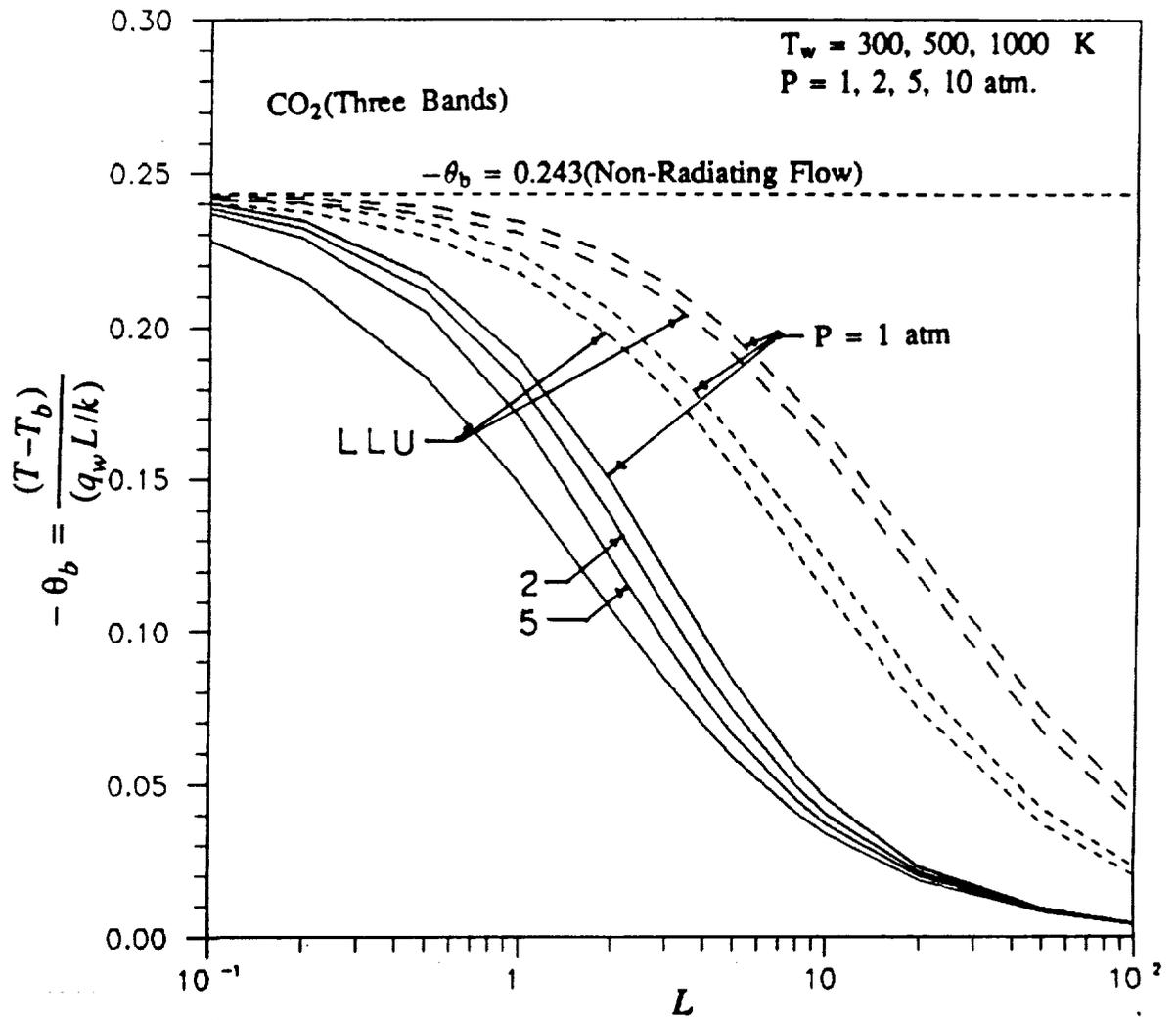
Figure B.4 Variation of bulk temperature with plate spacing for CO_2.
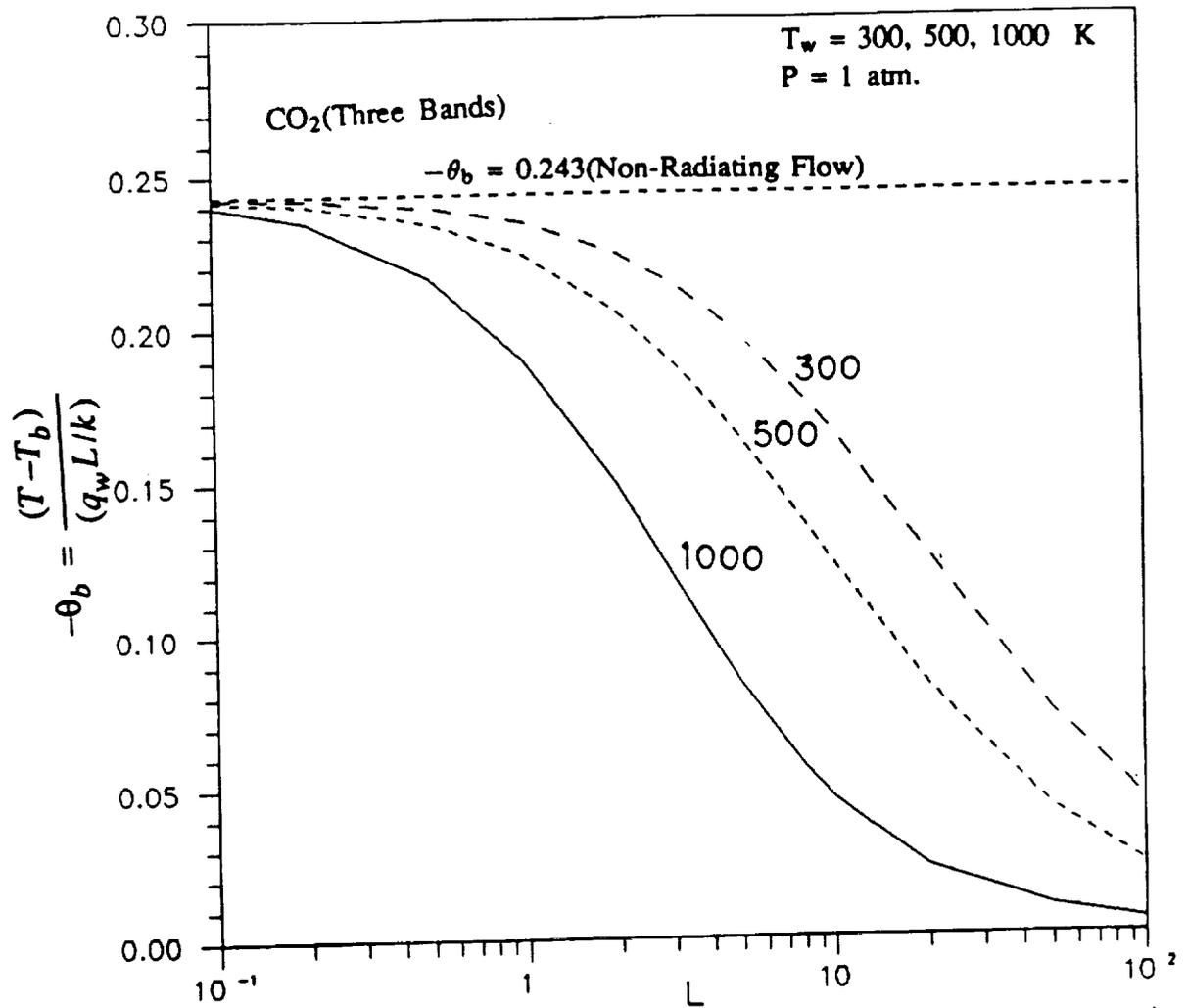
Figure B.5 Variation of bulk temperature with plate spacing for CO_2;

P = 1 atm.
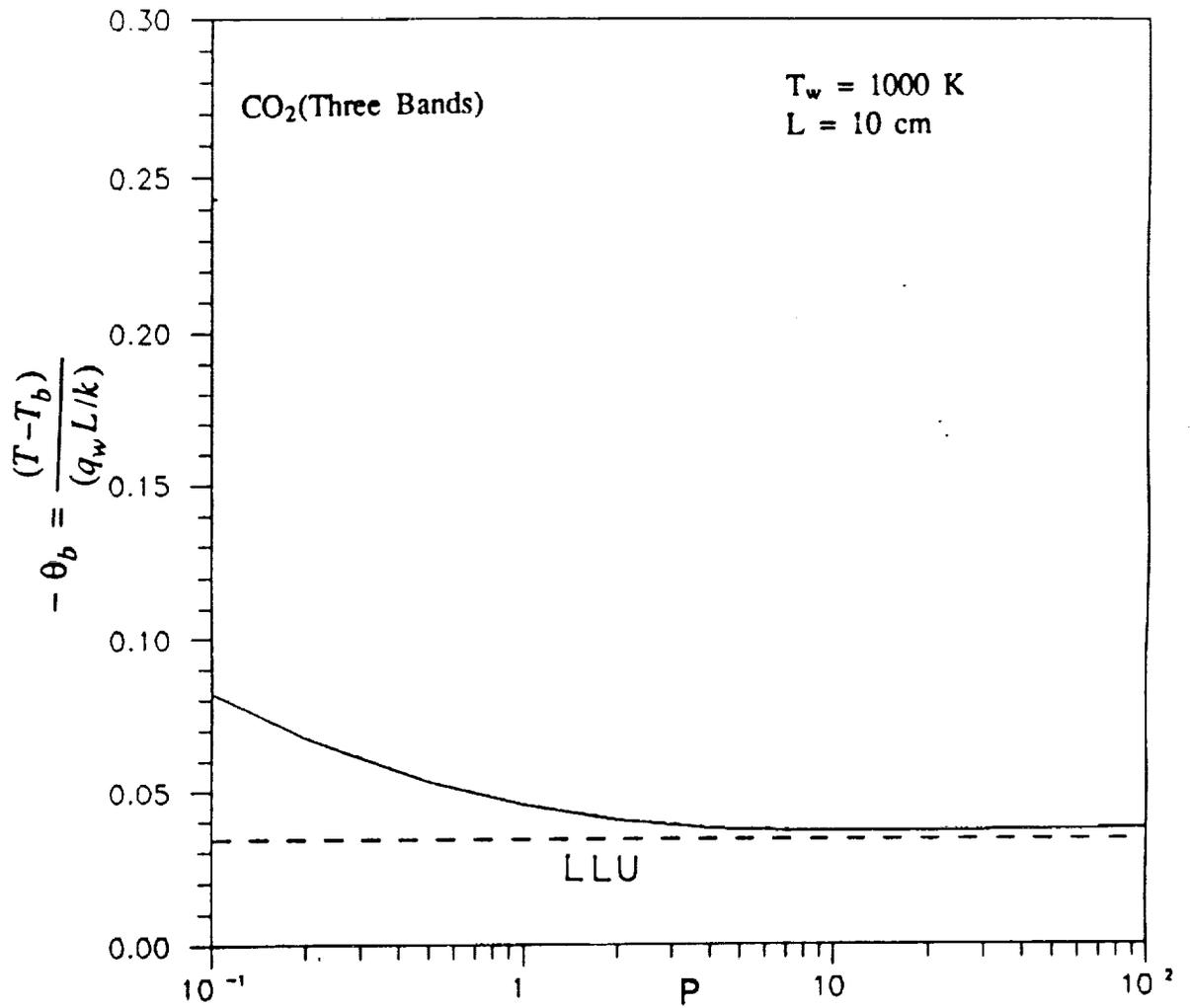
Figure B.6 Variation of bulk temperature with pressure for CO_2;

$T_w = 1000$ K and L = 10 cm.
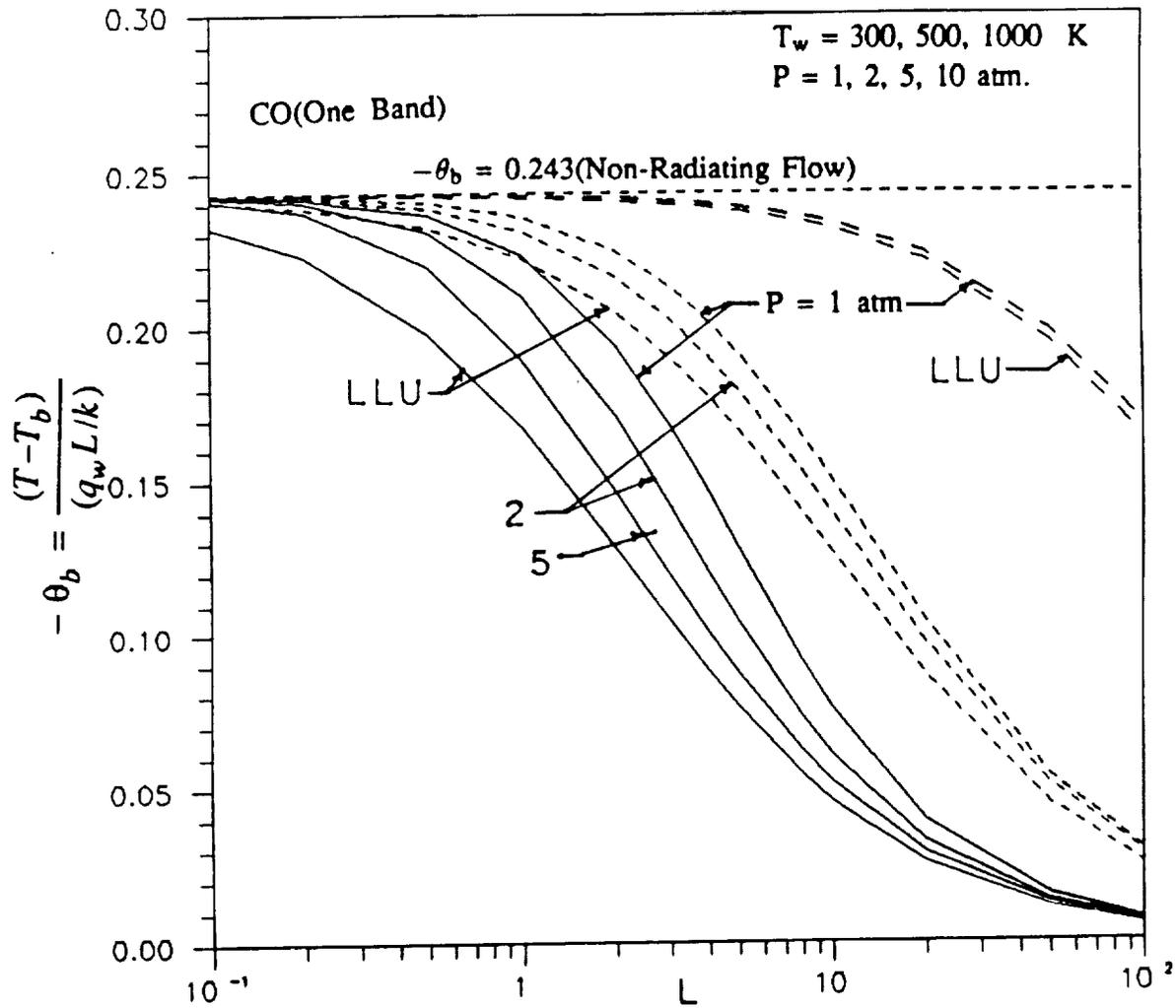
Figure B.7 Variation of bulk temperature with plate spacing for CO.
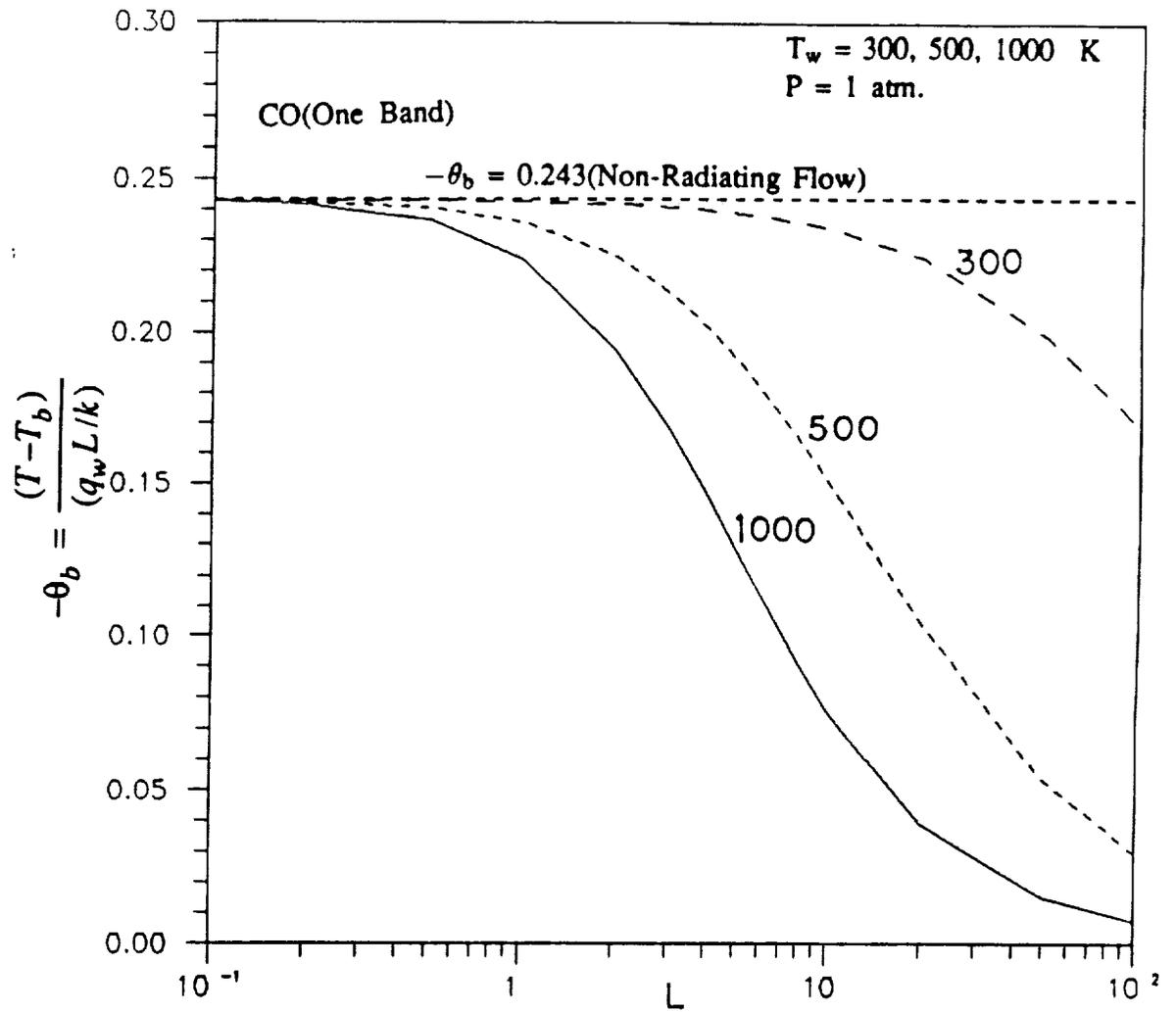
Figure B.8 Variation of bulk temperature with plate spacing for CO;

P = 1 atm.
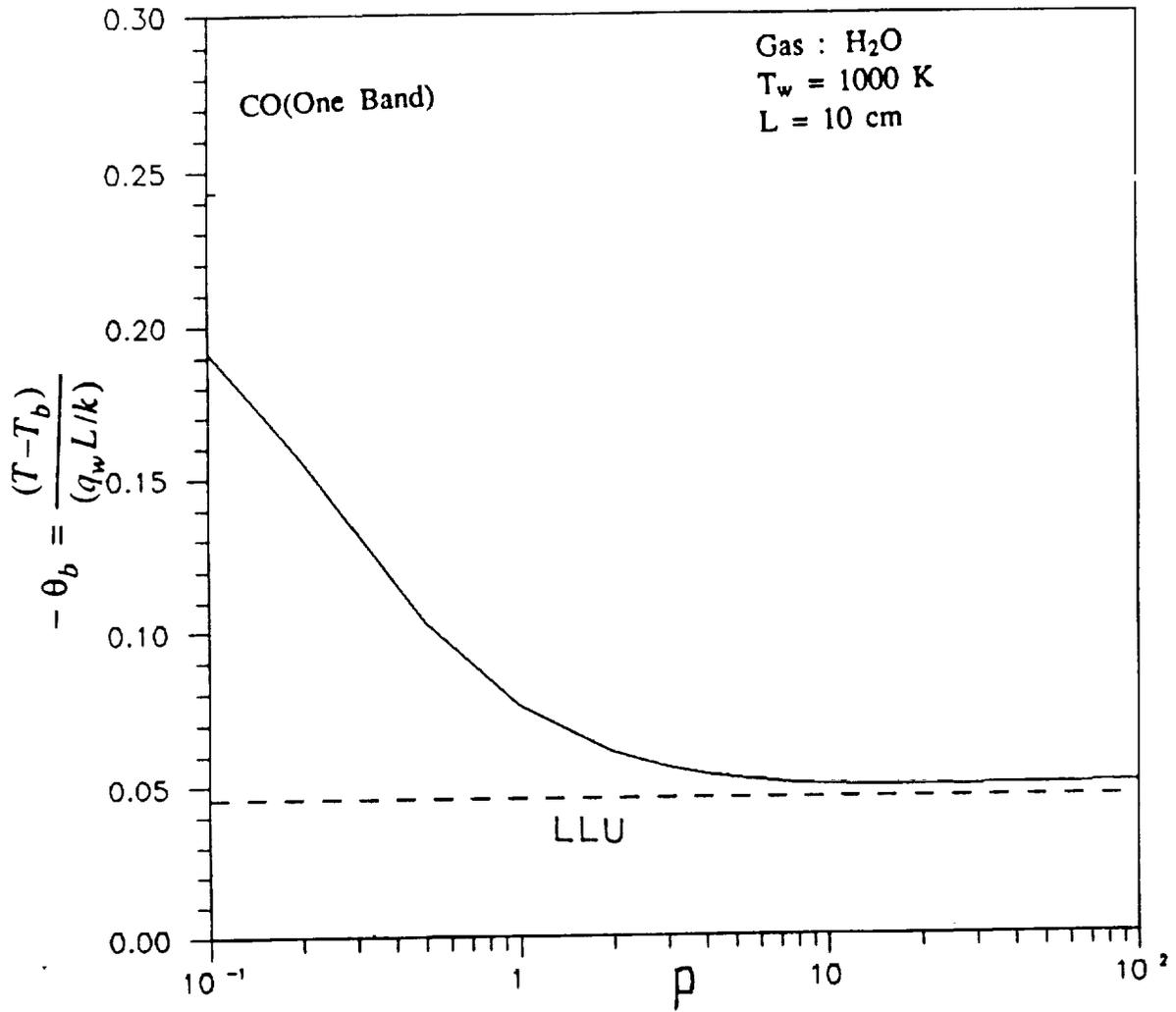
Figure B.9 Variation of bulk temperature with pressure for CO;

$T_w = 1000$ K and L = 10 cm.
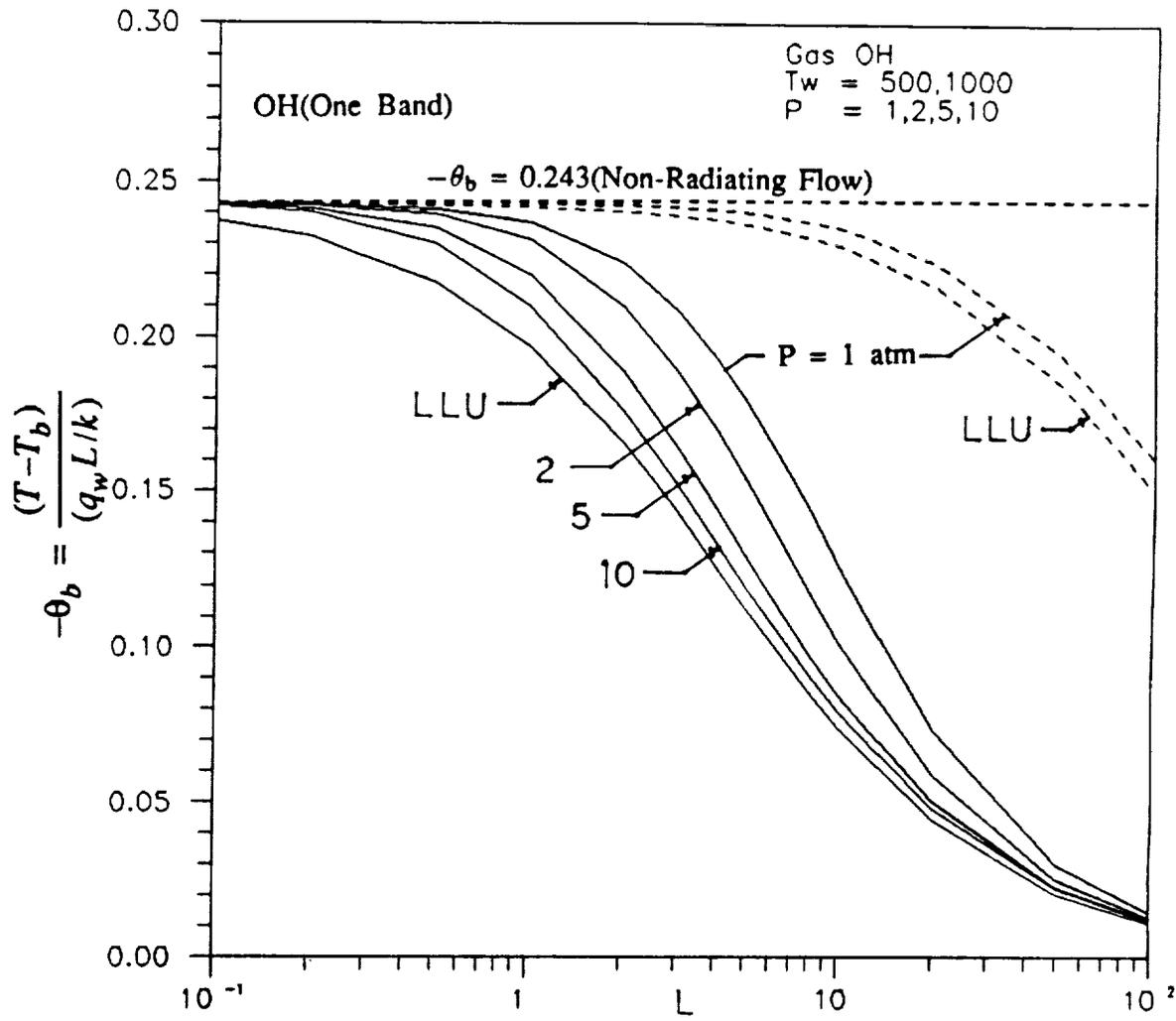
Figure B.10 Variation of bulk temperature with plate spacing for OH.
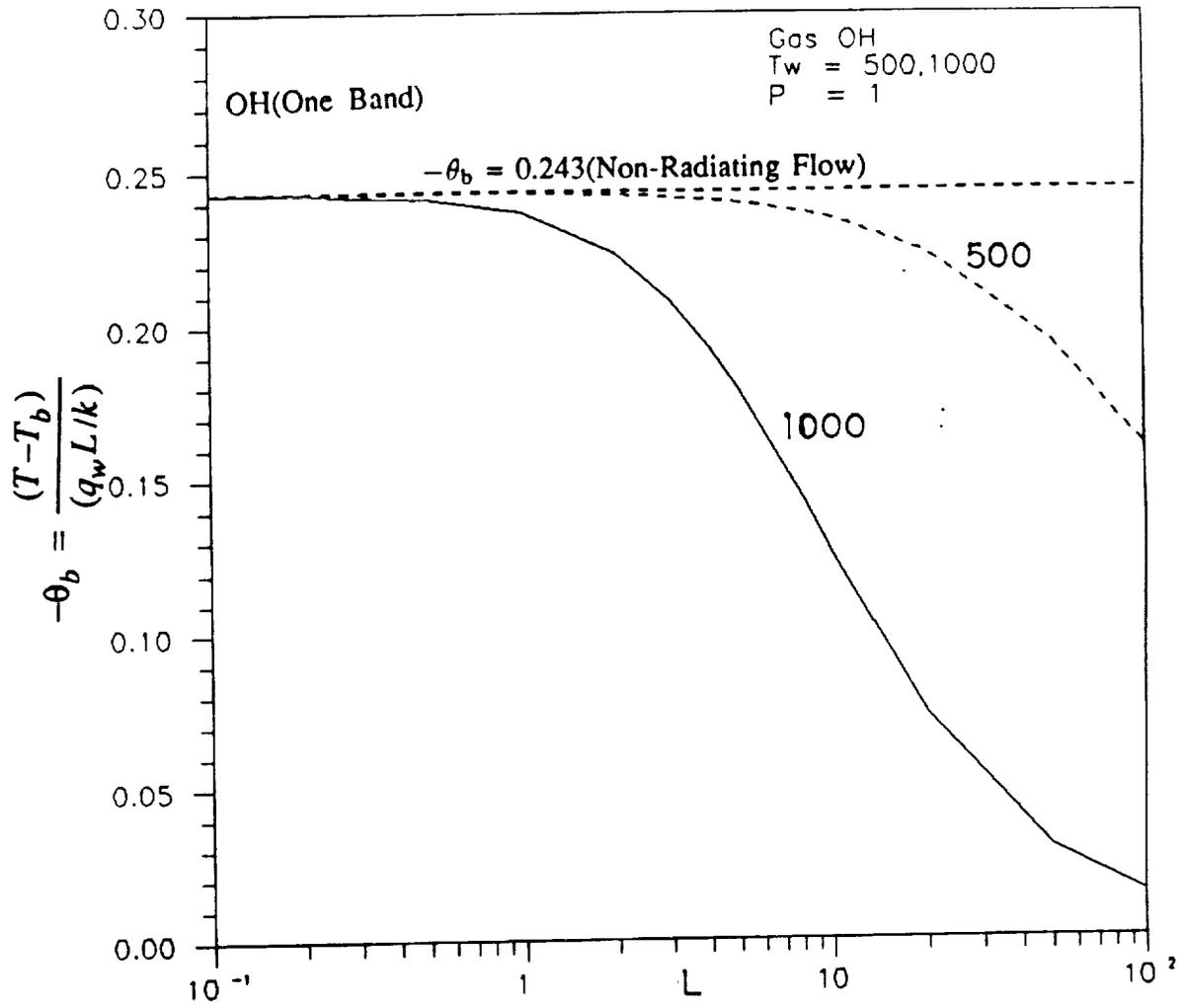
Figure B.11 Variation of bulk temperature with plate spacing for OH;

P = 1 atm.
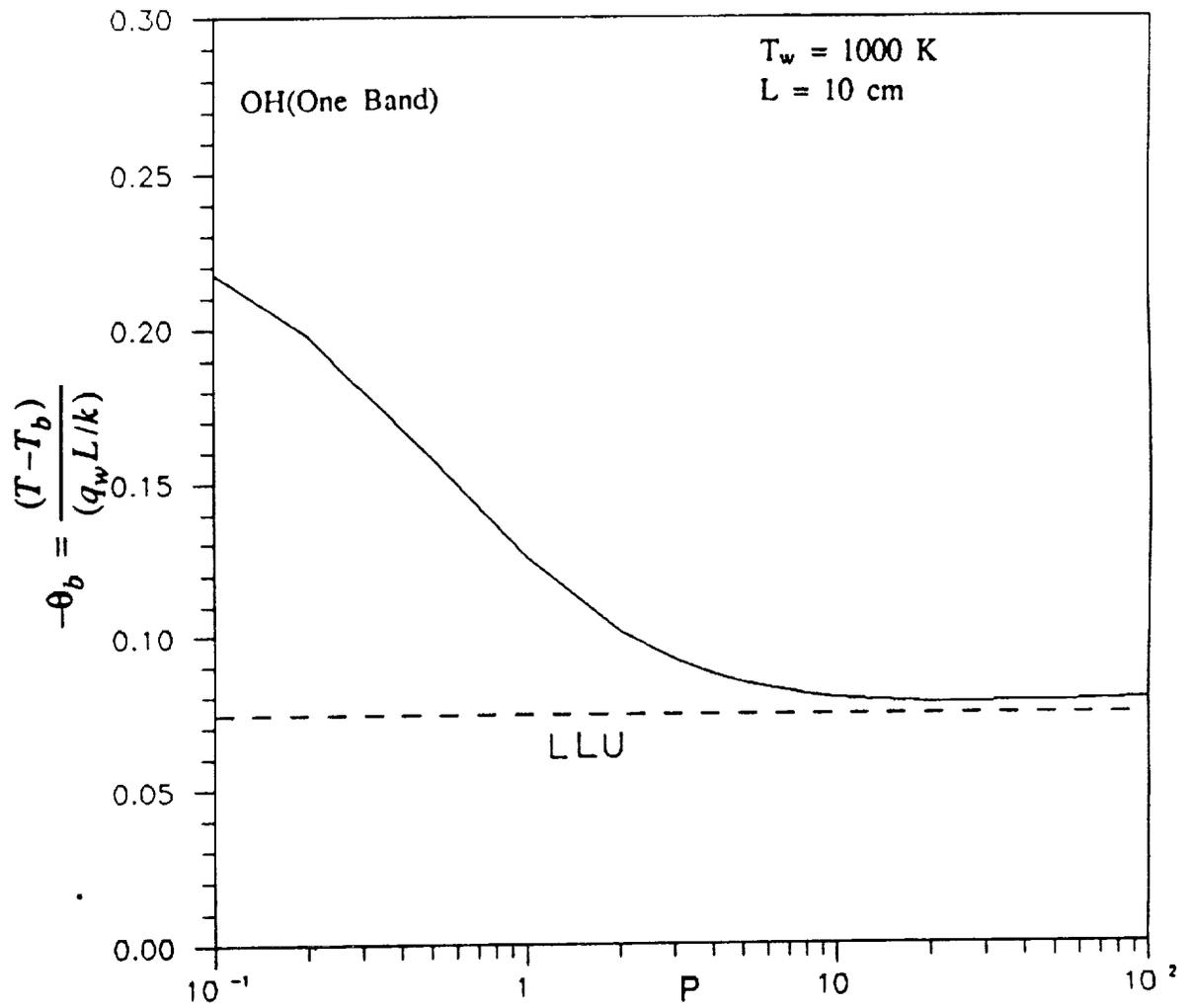
Figure B.12 Variation of bulk temperature with pressure for OH;

T_w = 1000 °K and L = 10 cm.

APPENDIX C

ADDITIONAL RESULTS FOR LAMINAR FLOW
OF NONGRAY GAS THROUGH CIRCULAR DUCT

Extensive results obtained for laminar flow of nongray gas black circular duct are presented here for reference purposes. The results are for species CO, OH, CO_2. Results for temprature variations across the duct as well as variation of bulk temprature with plate spacing and pressure are presented. All the results show similar trend as discussed for Figs. 6.13–6.22.
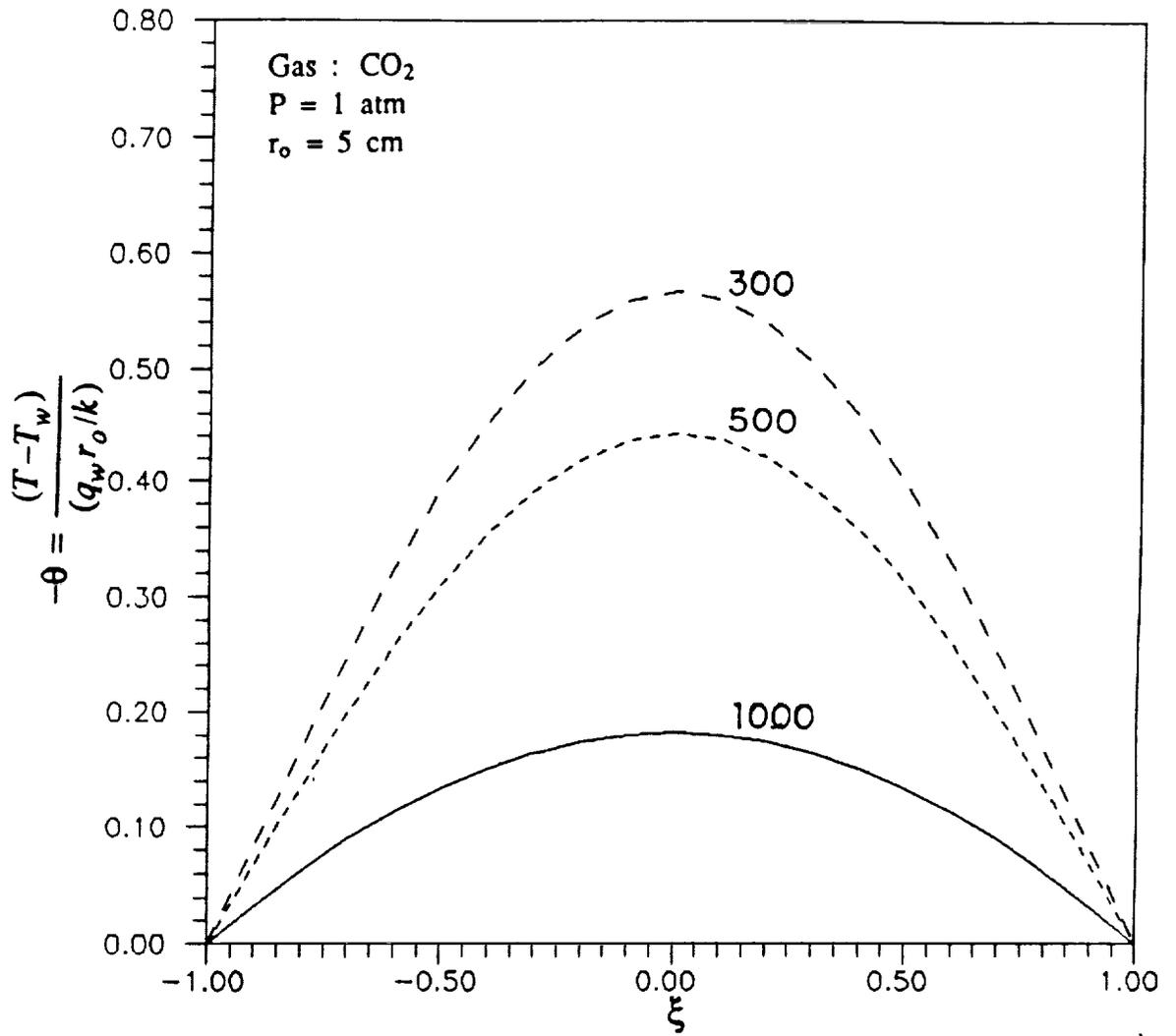
Figure C.1 Comparison of temperature variation across the duct for CO_2;

T_w = 300, 500, 1000 K, P = 1 atm and r_o = 5 cm.
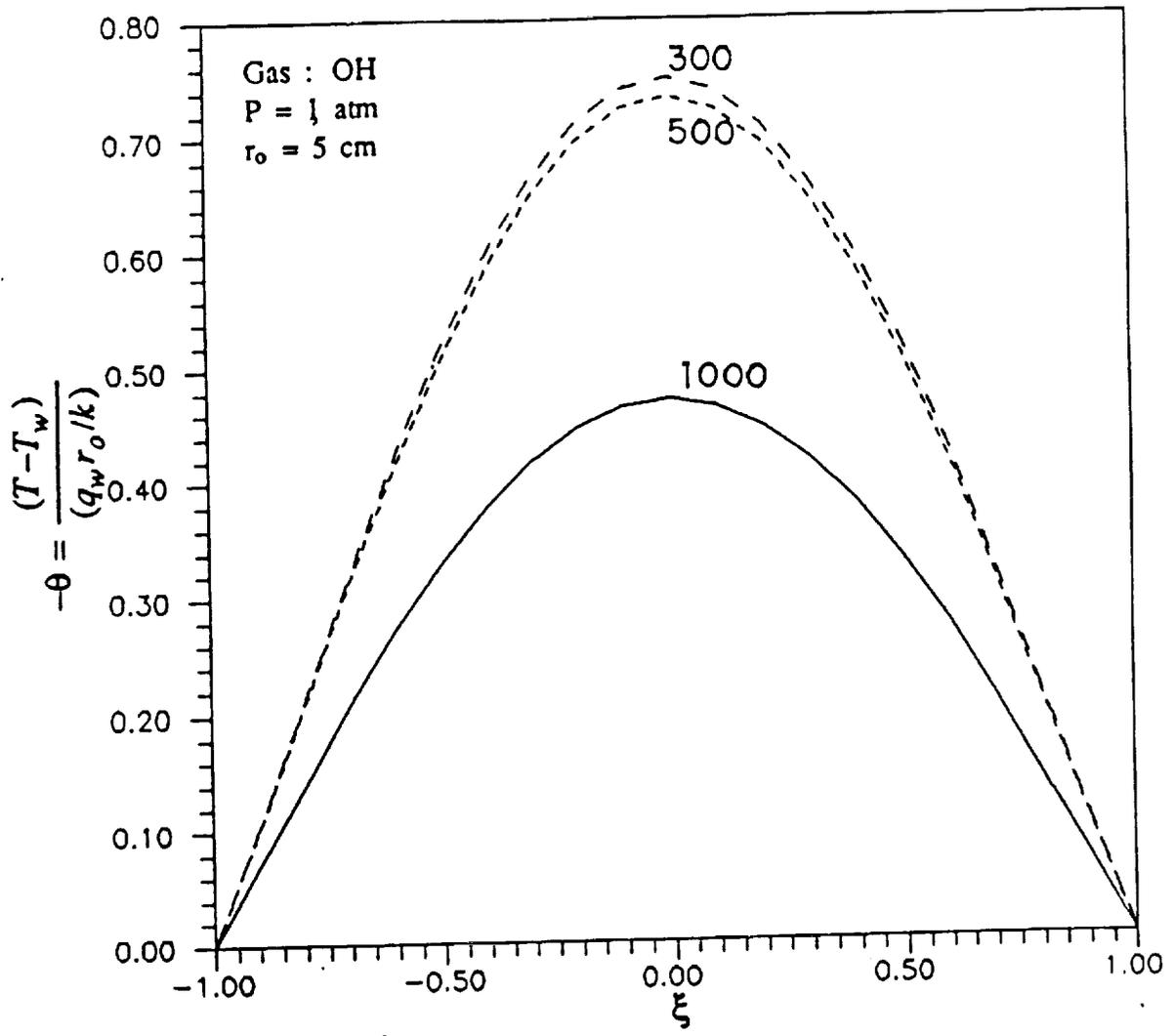
Figure C.2 Comparison of temperature variation across the duct for OH;

T_w = 300, 500, 1000 K, P = 1 atm and r_o = 5 cm.
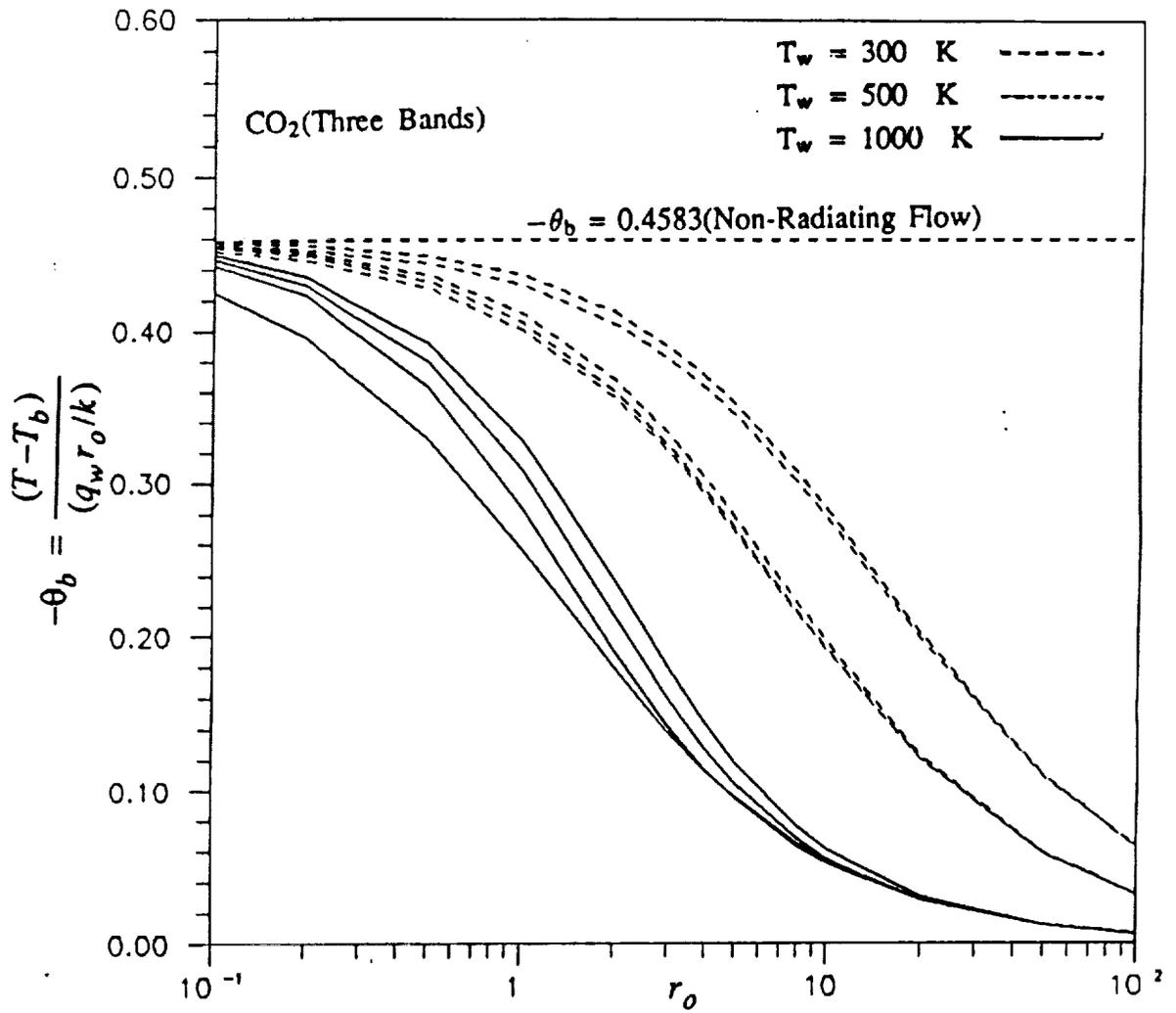
Figure C.3 Variation of bulk temperature with radius for CO_2.
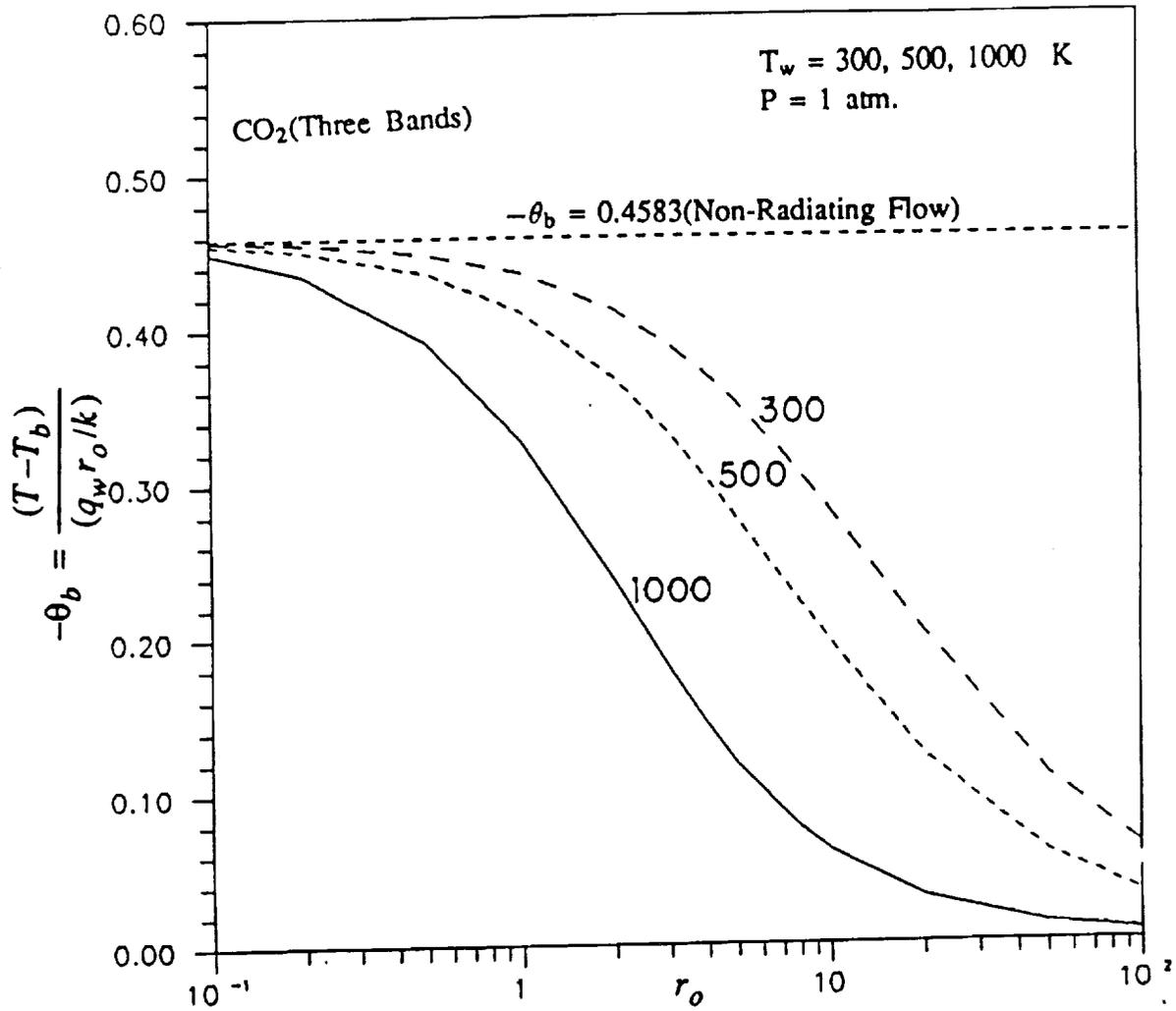
Figure C.4 Variation of bulk temperature with radius for CO_2;

P = 1 atm.
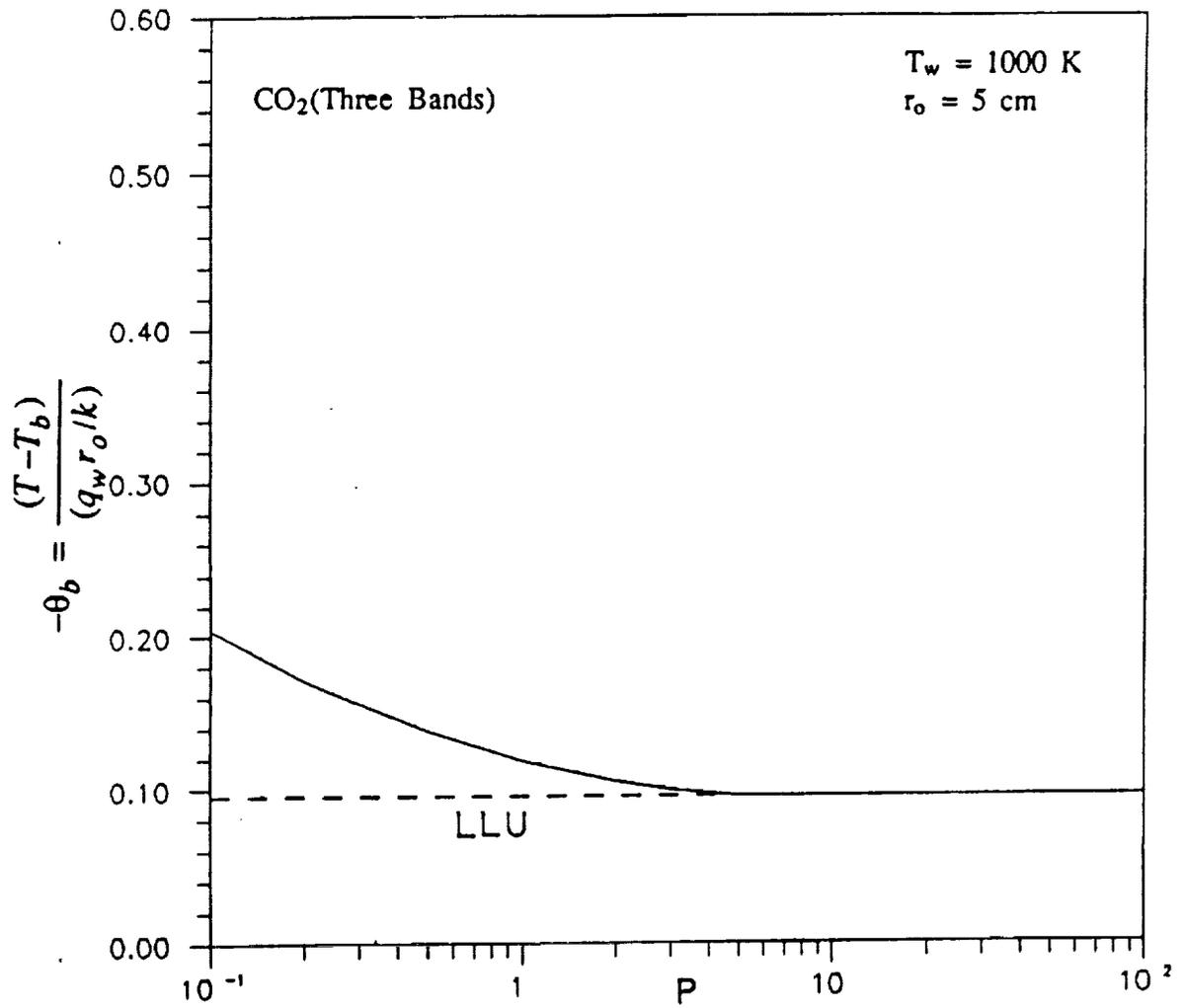
Figure C.5 Variation of bulk temperature with pressure for CO_2;

$T_w = 1000$ K and $r_o = 5$ cm.
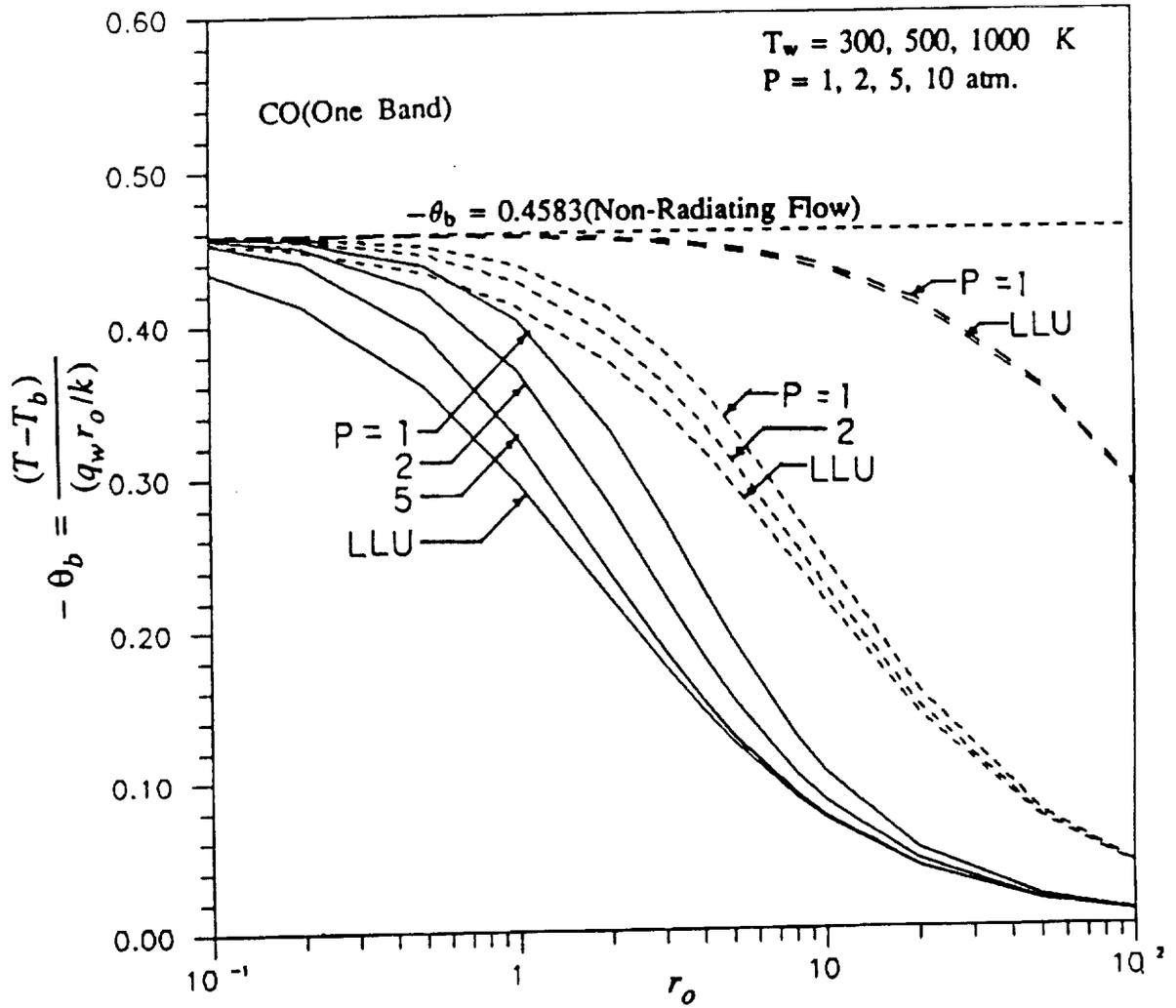
Figure C.6 Variation of bulk temperature with radius for CO.
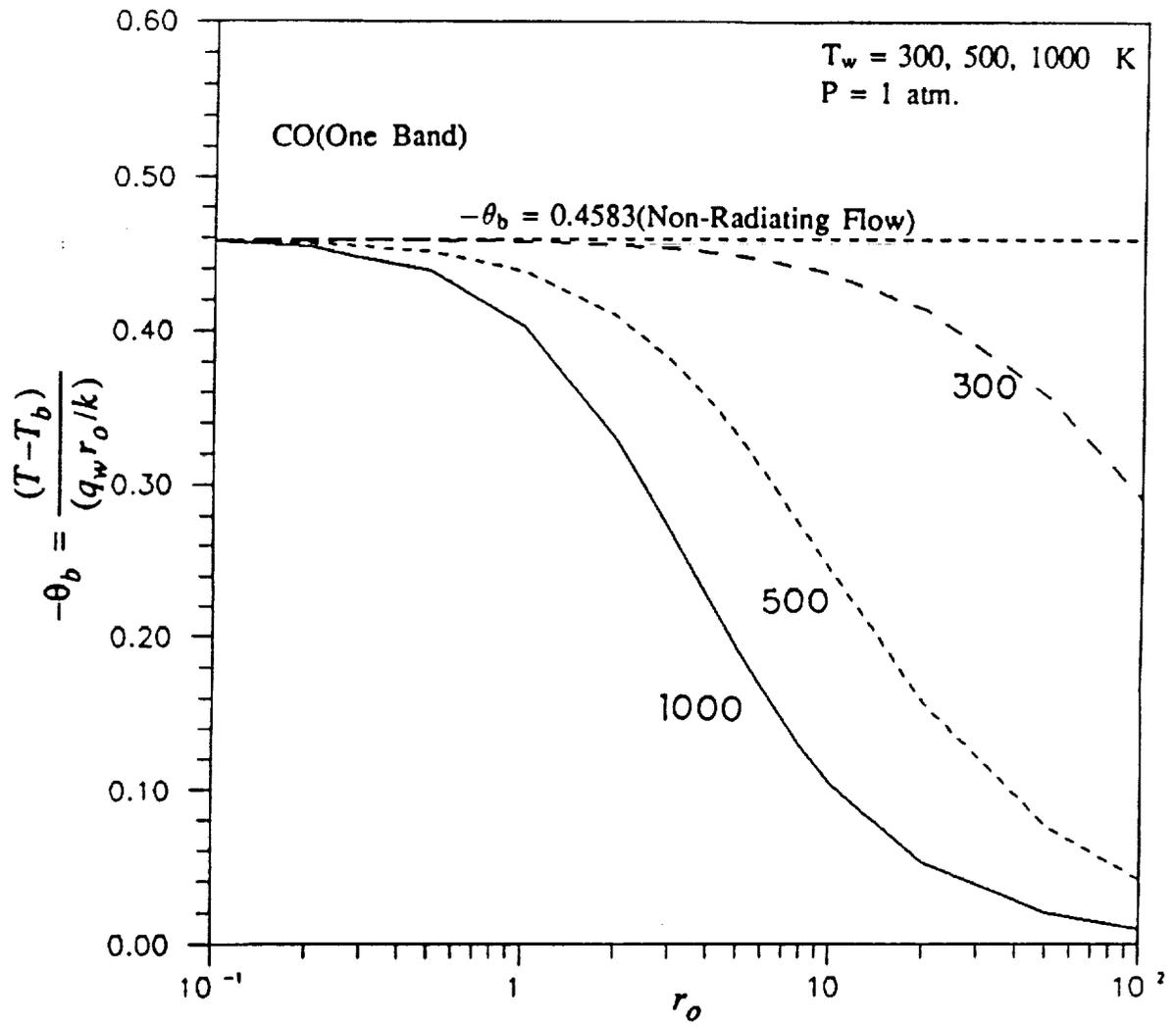
Figure C.7 Variation of bulk temperature with radius for CO;

P = 1 atm.
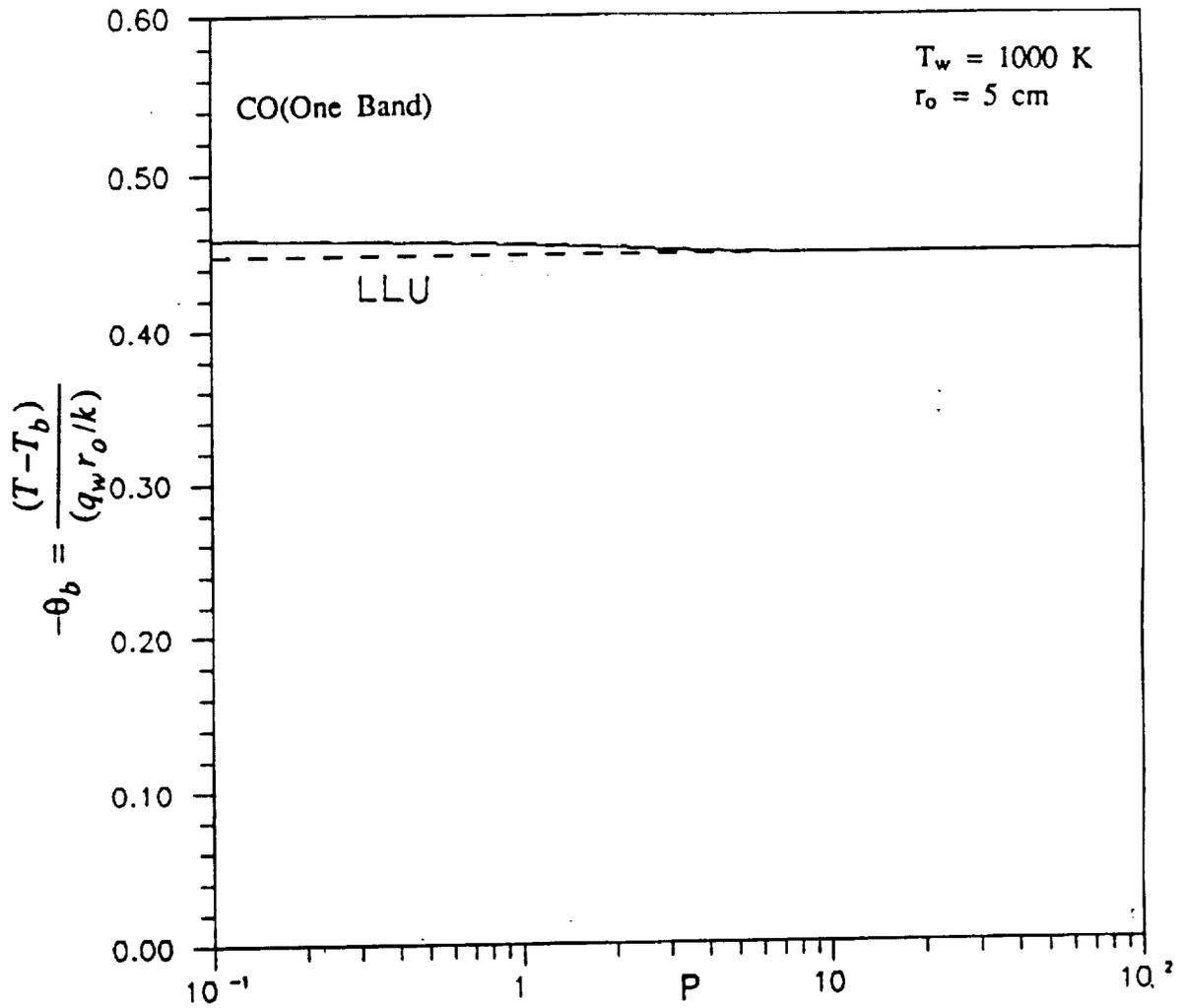
Figure C.8 Variation of bulk temperature with pressure for CO;

$T_w = 1000$ K and $r_o = 5$ cm.
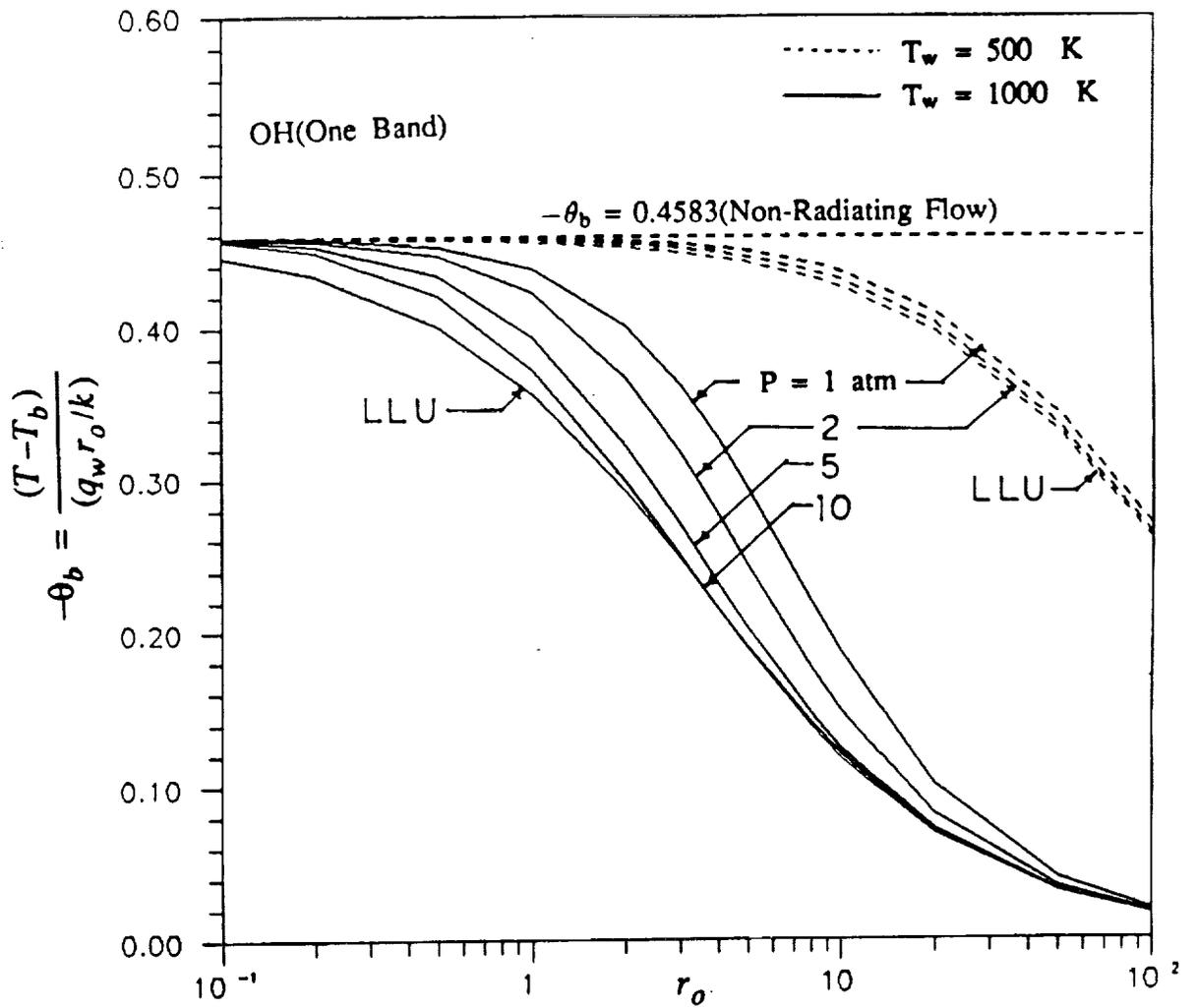
Figure C.9 Variation of bulk temperature with radius for OH.
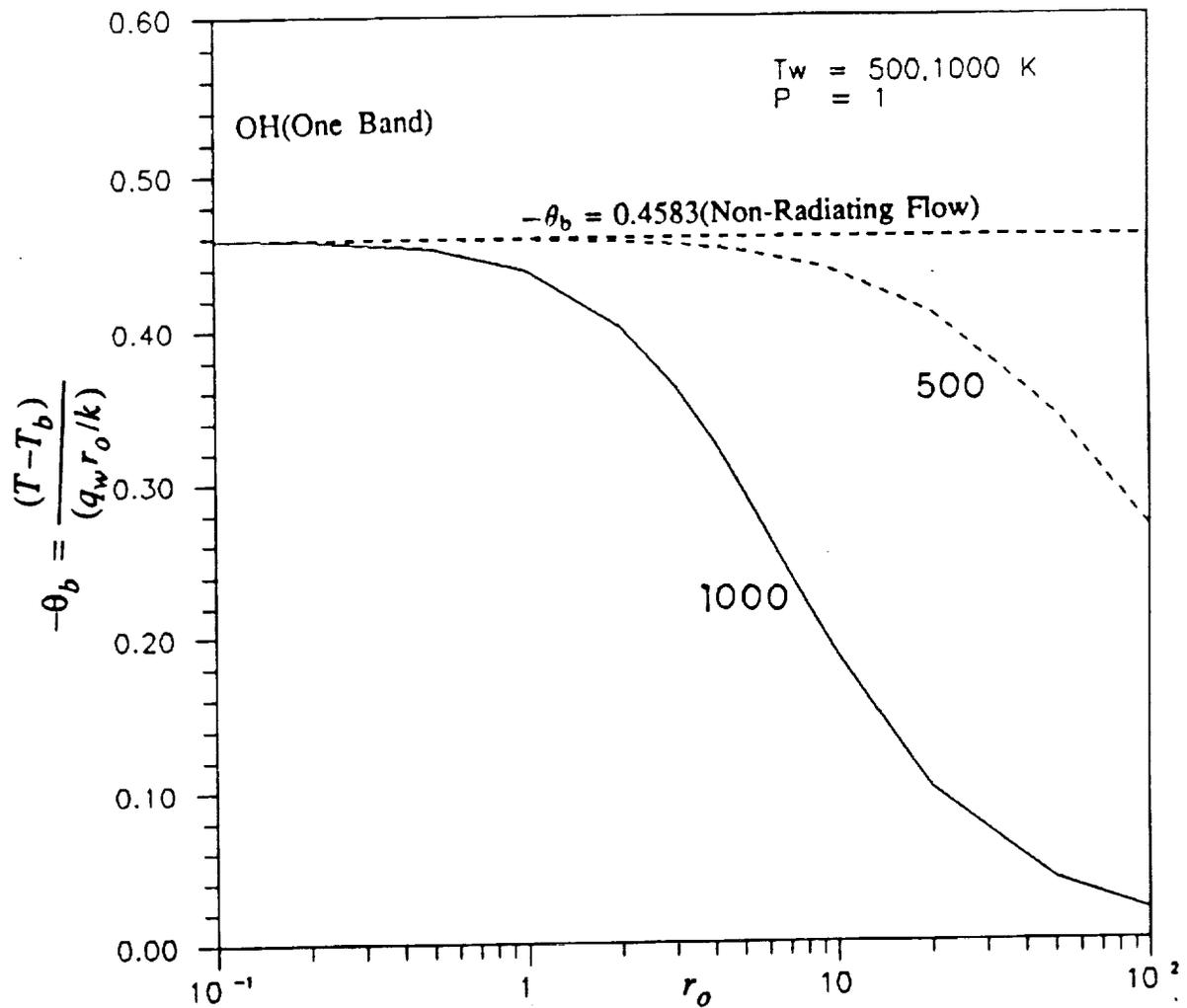
Figure C.10 Variation of bulk temperature with radius for OH;

P = 1 atm.
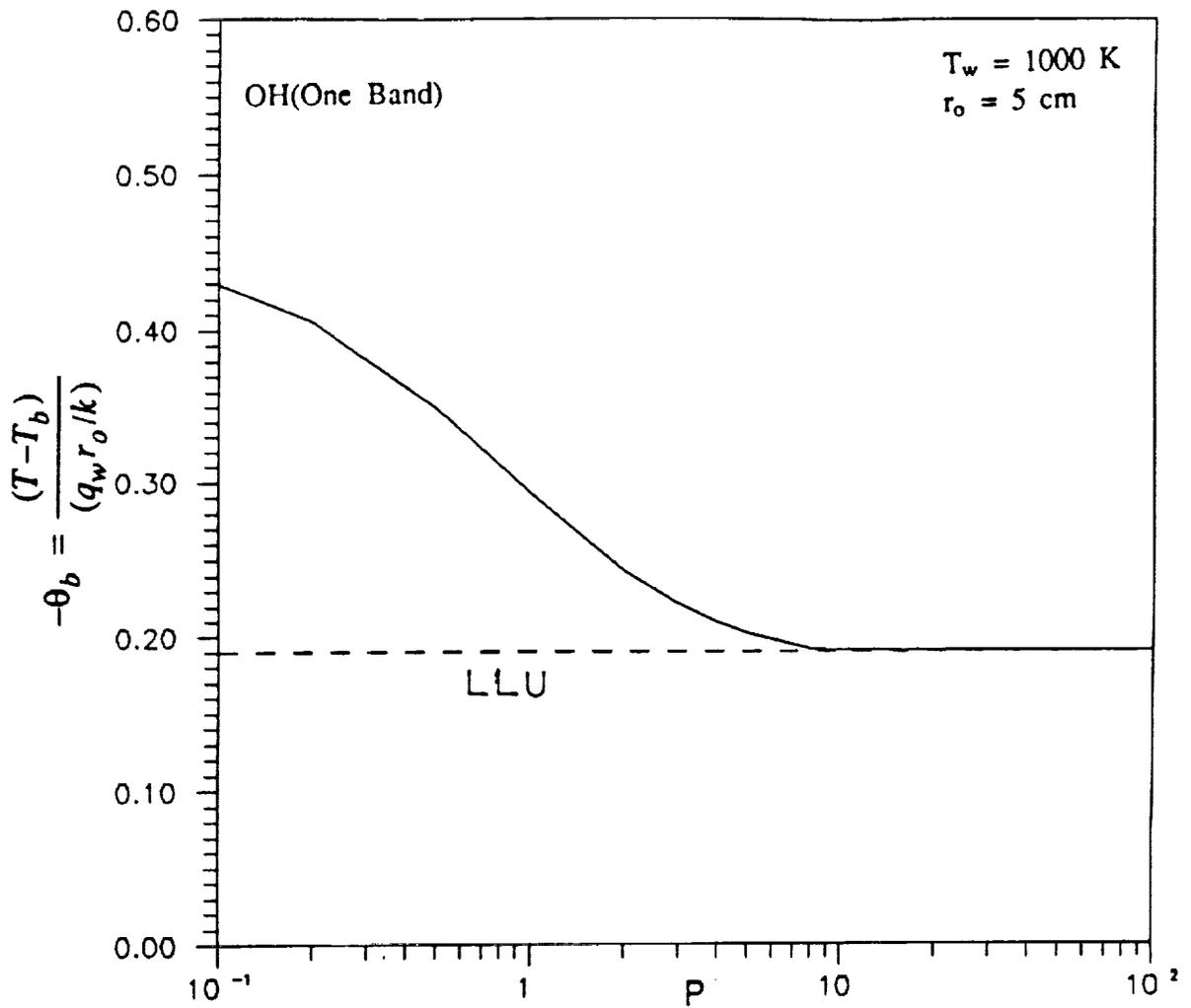
Figure C.11 Variation of bulk temperature with pressure for OH;

$T_w = 1000$ K and $r_o = 5$ cm.

APPENDIX D

PROGRAM LISTING FOR LAMINAR FLOW OF
NONGRAY GAS THROUGH PARALLEL PLATE DUCT

The listing of the FORTRAN program used for numerical procedure is given here. The program is coded on UNIX based SUN 386i. Input file consists of all the band parameters for different species[29]. The program uses romberg cautious integration routine for numerical integration purposes. The listing of romberg integration is not given here, but is available in IMSL libraries.

```
      program PLATE
C------kfb Thermal Conductivity of any Gas
      real l,kfb
C------n No. of Bands for the Gas
      parameter(n=2)
      external fpk0,fpk1,fpk2,fpk3,fpk4
      dimension fi(n),bi(n),hi(n),eps(3)
      common /func/f,b
      open(5,file='INPUT')
      rewind(5)
      open(6,file='OUTPUT')
      rewind(6)
C------eps(1) Absolute Error Desired
C------eps(2) Relative Error Desired
      eps(1) = 1.0e-6
```

```fortran
      eps(2)  = 1.0e-6
      do 333 i = 1,656
      read(5,*)t,pr,l,(fi(k),k=1,n),(bi(k),k=1,n),
     + (hi(k),k=1,n),kfb
      am = 1/kfb
      hsum = 0.0
      sum1 = 0.0
      sum2 = 0.0
      sum3 = 0.0
      sum4 = 0.0
      do 111 k = 1,n
      f = fi(k)
      b = bi(k)
      h = hi(k)
      hsum= hsum+h
      cu   = 1./b
      cus = cu*cu
      cuc = cu*cus
      cuq = cu*cuc
        x = 0.0
C------Numerical Integration
C------Cautious Romberg Integration
        call cadre(x,b,fpk1,eps,0,rr1,ir1)
        call cadre(x,b,fpk2,eps,0,rr2,ir2)
        call cadre(x,b,fpk3,eps,0,rr3,ir3)
        call cadre(x,b,fpk4,eps,0,rr4,ir4)
        sum1 = sum1+(h*((cu*rr1)-(2.*cuc*rr3)+(cuq*rr4)))
```

```fortran
      sum2 = sum2+(h*((cus*rr2)-(2.*cuc*rr3)+(cuq*rr4)))
        p  = b/4.
        q  = (3./4.)*b
      call cadre(p,q,fpk0,eps,0,ss1,is1)
      call cadre(x,p,fpk1,eps,0,ss2,is2)
      call cadre(x,q,fpk1,eps,0,ss3,is3)
      call cadre(p,q,fpk2,eps,0,ss4,is4)
      call cadre(x,p,fpk3,eps,0,ss5,is5)
      call cadre(p,q,fpk3,eps,0,ss6,is6)
      call cadre(p,q,fpk4,eps,0,ss7,is7)
      brk1 = (57./256.)*ss1
      brk2 = (11./16.)*cu*(ss2+ss3)
      brk3 = (9./8.)*cus*ss4
      brk4 = cuc*(ss5+ss6)
      brk5 = cuq*ss7
      sum3 = sum3+(h*(brk1+brk2-brk3-brk4+brk5))
      brs1 = (9./256.)*ss1
      brs2 = (3./16.)*cu*(ss2+ss3)
      brs3 = (1./8.)*cus*ss4
      brs5 = cuq*ss7
      sum4 = sum4+(h*(brs1+brs2-brs3-brs4+brs5))
111   continue
      alpha1 = 1.0+(am*sum1)
      alpha2 = am*sum2
      alpha3 = (11./16.)+(am*sum3)
      alpha4 = (3./16.)+(am*sum4)
      constt = 16.*((alpha1*alpha4)-(alpha2*alpha3))
```

```fortran
      const1 = (11.*alpha2)-(16.*alpha4)
      const2 = (16.*alpha3)-(11.*alpha1)
        a1   = const1/constt
        a2   = const2/constt
       bulk  = -((17.*a1)+(3.*a2))/70.
      call lpl(am,hsum,con1,con2,bulkl)
      write(6,*)t,pr,l,bulk,bulkl
      else
      continue
      endif
333   continue
      end
      function fpk0(u)
      common /func/f,b
      den = (f*((u*u)+(2.*u)+2.)+u)*(u+(2.*f))
      aud = (f*((u*u)+(4.*u*f)+(4.*f)))/den
      fpk0= aud
      return
      end
      function fpk1(u)
      common /func/f,b
      den = (f*((u*u)+(2.*u)+2.)+u)*(u+(2.*f))
      aud = (f*((u*u)+(4.*u*f)+(4.*f)))/den
      fpk1= u*aud
      return
      end
      function fpk2(u)
```

104

```fortran
      common /func/f,b
      den = (f*((u*u)+(2.*u)+2.)+u)*(u+(2.*f))
      aud = (f*((u*u)+(4.*u*f)+(4.*f)))/den
      fpk2= u*u*aud
      return
      end
      function fpk3(u)
      common /func/f,b
      den = (f*((u*u)+(2.*u)+2.)+u)*(u+(2.*f))
      aud = (f*((u*u)+(4.*u*f)+(4.*f)))/den
      fpk3= u*u*u*aud
      return
      end
      function fpk4(u)
      common /func/f,b
      den = (f*((u*u)+(2.*u)+2.)+u)*(u+(2.*f))
      aud = (f*((u*u)+(4.*u*f)+(4.*f)))/den
      fpk4= u*u*u*u*aud
      return
      end
      subroutine lpl(am,ht,con1,con2,bulkl)
      em = am*ht
      eta1 = 1.+((7./12.)*em)
      eta2 = (1./12.)*em
      eta3 = (11./16.)+(0.583154559*em)
      eta4 = (3./16.)+(0.127164755*em)
      phic = 16.*((eta1*eta4)-(eta2*eta3))
```

```
phi1 = (11.*eta2)-(16.*eta4)

phi2 = (16.*eta3)-(11.*eta1)

con1 = phi1/phic

con2 = phi2/phic

bulk1= -((17.*con1)+(3.*con2))/70.

return

end
```

APPENDIX E

PROGRAM LISTING FOR LAMINAR FLOW OF
NONGRAY GAS THROUGH CIRCULAR DUCT

The listing of the FORTRAN program used for numerical procedure is given here. The program is coded on UNIX based SUN 386i. Input file consists of all the band parameters for different species[29]. The program uses Multidimensional quadrature integration routine using Gauss-Kronrod rule (TWODQ), for numerical integration purposes. The subroutine is available in IMSL library (Chap. 4, Vol. 2.).

```
      program TUBE
      real kfb
C------kfb Thermal Conductivity of the Gas
      parameter (n=1,pi=3.1415926535898)
C------n No. of Bands in any Gas
      external fr11,fr12,fr21,fr22,fr31,fr32
      external o,q,r,s
      dimension fi(n),bi(n),hi(n),zi(2)
      dimension zz(2),gama1(2),gama2(2)
      common /func/f,b,z
C------INPUT Input Data File with All Properties for
C------      the Gas under consideration.
      open(5,file='INPUT')
      rewind(5)
      open(6,file='OUTPUT')
```

```fortran
      rewind(6)
C------ea Absolute Error Desired
C------er Relative Error Desired
      ea = 1.0e-4
      er = 1.0e-4
C------x Lower Limit of Integration for Outer Integral
C------y Upper Limit of Integration for Outer Integral
      x = 0.0
      y = (pi/2.0)
C------zi(1) & zi(2) Two Values of xi.
      zi(1) = 0.5
      zi(2) = 1.0
      do 333 i = 1,imax
      read(5,*)t,p,l,(fi(k),k=1,n),(bi(k),k=1,n),
     +  (hi(k),k=1,n),kfb
      am = (3.2*l)/(pi*kfb)
      do 222 k = 1,2
      z  = zi(k)
      xz = 2.*z
      yz = 4.*(z**3.)
      zz(k) = (z**3.)-(2.*z)
      brk1 = 0.0
      brk2 = 0.0
      hsum = 0.0
      do 111 j = 1,n
      f = fi(j)
      b = bi(j)
```

```fortran
      h  = hi(j)

      hsum= hsum+h

C------Numerical Integration

C------Multidimensional Quadrature Technique using

C------Gauss-Kronrod rule.

      call twodq(fr11,x,y,o,q,ea,er,1,rr11,er11)

      call twodq(fr12,x,y,o,q,ea,er,1,rr12,er12)

      call twodq(fr21,x,y,o,r,ea,er,1,rr21,er21)

      call twodq(fr22,x,y,o,r,ea,er,1,rr22,er22)

      call twodq(fr31,x,y,q,s,ea,er,1,rr31,er31)

      call twodq(fr32,x,y,q,s,ea,er,1,rr32,er32)

      brk1 = brk1+(h*(rr11-rr21+rr31))

      brk2 = brk2+(h*(rr12-rr22+rr32))

111   continue

      gama1(k)  = (am*brk1)-xz

      gama2(k)  = (am*brk2)-yz

222   continue

      alph1 = ((zz(1)*gama2(2))-(zz(2)*gama2(1)))

      alph2 = ((zz(2)*gama1(1))-(zz(1)*gama1(2)))

      alphc = ((gama1(1)*gama2(2))-(gama2(1)*gama1(2)))

       a1  = alph1/alphc

       a2  = alph2/alphc

       em  = hsum*am

      call lpl(em,con1,con2,bulkl)

      bulk  = -(((-2./3.)*a1)+((-5./6.)*a2))

      bulkl = -(((-2./3.)*con1)+((-5./6.)*con2))

      write(6,*)t,p,r,bulk,bulkl
```

109

```fortran
      if(r.eq.5.0)then
      do 11 ii = 1,11
      xi = 0.1*float(ii-1)
      theta = -(a1*((xi**2.)-1.)+a2*((xi**4.)-1.))
      theta1= -(con1*((xi**2.)-1.)+con2*((xi**4.)-1.))
      write(6,*)t,p,xi,theta,theta1
11    continue
      else .
      continue
      endif
333   continue
      end
      function fr11(x,u)
      common /func/f,b,z
      den = (f*((u*u)+(2.*u)+2.)+u)*(u+(2.*f))
      aud = (f*((u*u)+(4.*u*f)+(4.*f)))/den
      fr11= ((z-(cos(x)*u/b))**2.-1.)*cos(x)*aud
      return
      end
      function fr12(x,u)
      common /func/f,b,z
      den = (f*((u*u)+(2.*u)+2.)+u)*(u+(2.*f))
      aud = (f*((u*u)+(4.*u*f)+(4.*f)))/den
      fr12= ((z-(cos(x)*u/b))**4.-1.)*cos(x)*aud
      return
      end
      function fr21(x,u)
```

110

```fortran
      common /func/f,b,z
      den = (f*((u*u)+(2.*u)+2.)+u)*(u+(2.*f))
      aud = (f*((u*u)+(4.*u*f)+(4.*f)))/den
      fr21= ((z+(cos(x)*u/b))**2.-1.)*cos(x)*aud
      return
      end
      function fr22(x,u)
      common /func/f,b,z
      den = (f*((u*u)+(2.*u)+2.)+u)*(u+(2.*f))
      aud = (f*((u*u)+(4.*u*f)+(4.*f)))/den
      fr22= ((z+(cos(x)*u/b))**4.-1.)*cos(x)*aud
      return
      end
      function fr31(x,u)
      common /func/f,b,z
      den = (f*((u*u)+(2.*u)+2.)+u)*(u+(2.*f))
      aud = (f*((u*u)+(4.*u*f)+(4.*f)))/den
      fr31= ((z*(2.*sin(x)-1.)+(cos(x)*u/b))**2.-1.)*cos(x)*aud
      return
      end
      function fr32(x,u)
      common /func/f,b,z
      den = (f*((u*u)+(2.*u)+2.)+u)*(u+(2.*f))
      aud = (f*((u*u)+(4.*u*f)+(4.*f)))/den
      fr32= ((z*(2.*sin(x)-1.)+(cos(x)*u/b))**4.-1.)*cos(x)*aud
      return
      end
```

111

```fortran
function o(x)
common /func/f,b,z
o = 0.0
return
end
function q(x)
common /func/f,b,z
q = b*z*(1.-sin(x))/cos(x)
return
end
function r(x)
common /func/f,b,z
r = b*(1.-z)/cos(x)
return
end
function s(x)
common /func/f,b,z
s = b*(1.+z-(2.*z*sin(x)))/cos(x)
return
end
```